Advances in Phillips Polymerisation Catalysis: In-situ Synthesis of Light Linear Alpha Olefins

DIMITRIJE CICMIL

Advances in Phillips Polymerisation Catalysis: In-situ Synthesis of Light Linear Alpha Olefins

Vooruitgang in Phillips Polymerisatie Katalyse: In-situ Synthese van Korte Lineaire Alpha Olefines

(met een samenvatting in het Nederlands)

Proefschrift

ter verkrijging van de graad van doctor aan de Universiteit Utrecht
op gezag van de rector magnificus, prof. dr. G. J. van der Zwaan,
ingevolge het besluit van het college voor promoties
in het openbaar te verdedigen op woensdag 2 maart 2016
des ochtends te 10:30 uur

door **Dimitrije Cicmil**
geboren op 28 juni 1986 te Smederevo, Servië

Promotor: **Prof. dr. ir. B. M. Weckhuysen**

This PhD thesis is accomplished with financial support from
the Total Research and Technology Feluy and Total SA.

Безъ муке се пѣсна неиспоя!
Безъ муке се сабля несакова.

Горскій віенацъ
П. П. Негош

Ч. О. О. Мехитаристи
Беч, 1847

Apart from suffering never can be song,
Apart from sweat of brow no sword is forged!

The Mountain Wreath
P. P. Njegoš

Translated by James W. Wiles
George Allen & Unwin, Ltd.
London, 1930

Cicmil, Dimitrije

Title: Advances in Phillips Polymerisation Catalysis:
In-situ Synthesis of Light Linear Alpha Olefins

ISBN: 978-90-393-6486-4

Printed by: Gildeprint - The Netherlands

Circulation: 200 copies

Cover design: Dimitrije Cicmil

The work described in this Thesis was carried out in the Group of Inorganic Chemistry and Catalysis, Debye Institute for Nanomaterials Science, Faculty of Science, Utrecht University, The Netherlands.

Table of Contents

TOTAL RESEARCH & TECHNOLOGY
Feluy, Belgium

I

General Introduction

Many years have passed since the discovery of ethylene polymerisation with a silica-supported chromium catalyst. Industrial processes have been established and many different polyethylene grades have been produced ever since. But still, much research is required in order to tailor the production processes, with respect to catalyst formulation, polymerisation and application technologies, as the demand of various types of polyethylenes continue to rapidly grow. The topic of this ***PhD thesis*** is to focus on a specific part of chromium-based polymerisation catalysis in order to elucidate the *in-situ* generation of linear α-olefins during the polymerisation of ethylene. This ***Chapter*** introduces the reader to the topic, by giving an overview on different types of polyethylenes, olefin polymerisation catalysts and more specifically, the Phillips-type Cr/SiO_2 catalyst. Current views on the catalyst structure and modifications will be summarised, followed by a discussion of the literature-proposed oligo/-polymerisation mechanisms. Finally, the scope and outline of this dissertation will be presented.

1.1 FROM POLYMERS TO POLYETHYLENES

The first definition of a polymer dates back to 1833 when Jöns Jacob Berzelius coined the term from the Greek words *πολύς* (polys), meaning "many", and *μέρος* (meros), meaning "parts", in order to define organic compounds, which shared identical empirical formulas, but differed in molecular weight.[1,2] As the concept of chemical structures was not known at that time, many of the small compounds were mistakenly taken as monomers of bigger compounds. It took almost a century until 1920 and a decade of extensive research on rubber and cellulose, by the 1953 Nobel Prize winner Herman Staudinger, in order to confirm the correct, modern-day definition of polymer as "a molecule of high relative molecular mass, with the structure that essentially comprises of multiple repetitions of units derived, actually or conceptually, from molecules of low relative molecular mass".[3,4]

Polymers range from natural bio-polymers, DNA and proteins, to familiar synthetic plastics, which have already displaced many of the traditional materials *i.e.* wood, stone, leather, metal and glass, mainly in the packaging and building industry ***(Figure 1.1a)***.[5,6] The success of plastics as a material comes from their versatility and possibility of use in many different forms, such as natural polymers, thermoplastics, thermosetting plastics and biodegradable plastics. Plastics are of great interest in the industrial and scientific world, due to a broad range of unique properties, including toughness, strength, light and chemical resistance, viscoelasticity, and their tendency to form glasses and semi-crystalline structures rather than crystals. They can be used at a wide range of temperatures and easily processed as a hot melt.

Despite the variety of plastic materials that are commercially available, only six types account for approximately 80% of the total demand, including polyethylene (PE), polypropylene (PP), polyvinyl chloride (PVC), polystyrene (PS), polyurethane (PUR) and polyethylene terephthalate (PET), with their share presented in ***Figure 1.1b.*** Amongst all, PEs have been and still are by far the most widely used commodity polymer, owing to their excellent chemical resistance against acids, greases and oils, high impact strength and stiffness at low temperatures. PE is capable of being moulded, extruded and cast into many various shapes.

In the past 60 years, numerous PEs were produced with different and unique properties. There are several grades of PE based on the average density of the resin and polymer architecture: 0.925 $g\ cm^{-3}$ linear low density polyethylene (LLDPE), 0.915–0.935 $g\ cm^{-3}$ low density polyethylene (LDPE), 0.930–0.945 $g\ cm^{-3}$ medium density polyethylene (MDPE) and 0.945–0.975 $g\ cm^{-3}$ high density polyethylene (HDPE).[7] The properties of these PEs originate from different structures of the polymer chains. For example, HDPE consists of linear chains without any or only a few short branch-

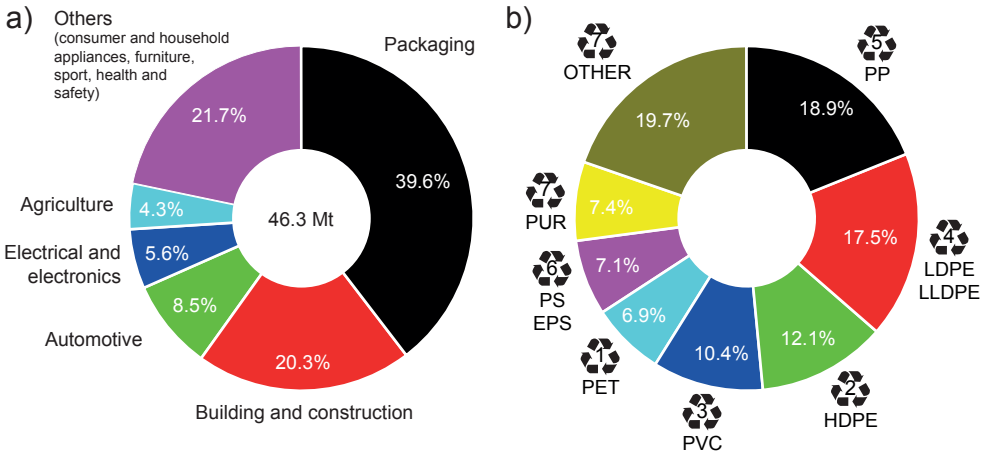

[FIGURE 1.1]
(a) Packaging applications are the largest application sector for the plastics industry and represent 39.6% of the total plastics demand in Europe, followed by the building and construction sector with 20.3% of the total EU demand in 2013. **(b)** Polyethylenes, including LLDPE, LDPE and HDPE, account for 29.6% of the demand by the polymer type.[6]

es. On the other hand, LLDPE consists of linear chains with short branches determined by the co-polymer composition. Finally, LDPE is composed of the chains with long side chains as well as short branches, giving it the lowest crystallinity ***(Table 1.1)***. The principal structural differences of these classes of PE are illustrated in ***Figure 1.2***, and are a consequence of the different polymerisation procedures, conditions and catalysts used.

[TABLE 1.1]
Overview of the properties and production conditions of different classes of commercial PE.[7]

	HDPE	LLDPE	LDPE
Branching amount	none to little	high	high
Branching type	short	short	short and long
Density (g cm^{-3})	0.945–0.975	0.915–0.935	0.915–0.935
Melt index (g $10min^{-1}$)	0–100	0.5–60	0.5–20
Pressure (bar)	20–50	20–50	690–2760
Manufacturing process	slurry, gas phase, solution phase	slurry, gas phase, solution phase	free radical
Catalyst	Phillips, Ziegler-Natta, metallocene	Phillips, Ziegler-Natta, metallocene	oxygen, peroxides

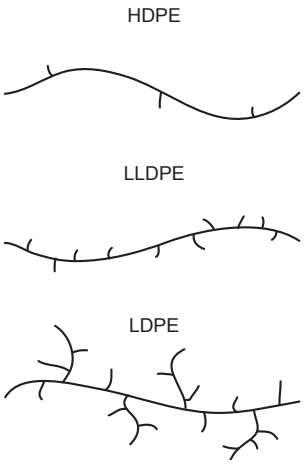

[FIGURE 1.2]
Illustration of the structural differences of different classes of commercial polyethylene.

The ethylene monomer is produced in the petrochemical industry by steam cracking of naphtha, and in a highly purified form, it is piped directly from the refinery to a separate polymerisation plant. Here, under the right conditions of temperature, pressure and catalysis, the double bond of ethylene monomer is activated while many monomers link up to form long PE chains. Today, PE manufacturing processes are usually categorised into "high-pressure" and "low-pressure" operations ***(Table 1.2)***.[7] The former are generally recognised as producing LDPE by free radical combination reactions at high temperature and high pressure of 523–573 *K* and > 50 *bar*, respectively, while the latter make high density HDPE, MDPE and LLDPE polyethylenes by using either homogeneous or heterogeneous catalysts under relatively milder conditions of 353–463 *K* and < 50 *bar*.[8]

The application of LDPE is in film wrap and

[TABLE 1.2]
Overview of commercial ethylene polymerisation operations.[7]

	"High-pressure"		"Low-pressure"			
	Autoclave	Tubular	Solution	Slurry	Slurry	Gas phase
PE type	LDPE	LDPE	LDPE, HDPE	HDPE	LLDPE, HDPE	LLDPE, HDPE
PE architecture	branched	branched	linear	linear	linear	linear
Reactor type	CSTR	tube	CSTR	CSTR	loop	fluidised bed
Pressure (bar)	650–2750	650–2750	10–40	7–20	40–70	10–30
Temperature (K)	393–573	393–573	398–523	333–363	343–383	343–383
Medium	PE melt	PE melt	solvent	solvent	nonsolvent	gas
Medium composition	-	-	cyclohexane, isopar‡	hexane, pentane	isobutane, isopentane	nitrogen and ethylene
Catalyst	oxygen, peroxides	oxygen, peroxides	Phillips, Ziegler-Natta, metallocene	Ziegler-Natta	Phillips, Ziegler-Natta, metallocene	Phillips, Ziegler-Natta, metallocene
Residence time (min)	1–10	1–10	10–60	90–180	60	120–240

‡ Isopar fluids are high-purity synthetic isoparafins with consistent and uniform quality.

plastic bags because of its soft and waxy solid properties. HDPE, due to its rigid and translucent solid properties is used for electrical insulation, bottles and toys. LLDPE has in general the same applications as LDPE, but due to slightly different properties, *i.e.* higher tensile strength and flexibility, it is convenient for making even thinner films.

Even a slight change in the polymerisation conditions or in the catalyst formulation can lead to a new variety of PE, which might be interesting for a specific type of application. Therefore, a great challenge in order to rationalise and predict the outcome of an ethylene polymerisation reaction still remains a hot topic both in academia and in the polymer industry.

1.2 OLEFIN POLYMERISATION CATALYSTS

The discovery of John P. Hogan and Robert L. Banks at the Phillips Petroleum Company in 1951 that the silica-supported chromium catalyst was able to produce PP and HDPE at milder conditions,[9,10] compared to the high-pressure free radical ethylene polymerisation invented in 1937 by Imperial Chemical Industries,[11] represents a breakthrough in industrial catalysis. Together with the 1953 discovery of Karl Ziegler that a mixture of transition metal compounds and aluminium alkyls was able to polymerise ethylene[12–14] and one year later Giulio Natta's synthesis of isotactic PP and introduction of the concept of stereospecific olefin polymerisation,[15] these systems are among the most important industrial catalysts for PE production nowadays. Also, the recently commercialised single-site metallocene catalysts and other transitional metal complexes activated by methylaluminoxane (MAO) are becoming more relevant. These three families of polymerisation catalysts differ in chemical composition, reaction mechanisms and activation of the catalyst.

1.2.1 Ziegler-Natta-type catalysts

After the invention of the original catalyst of this type consisting of a mixture of triethylaluminium (TEAl) and $TiCl_4$, several improvements have been accomplished in order to enhance the activity and selectivity of propylene polymerisation. The first breakthrough in this field, *i.e.* the supporting of $TiCl_4$ on crystalline $MgCl_2$, lead to a significant simplification of industrial PE and isotactic PP production. With the second major discovery that the addition of a Lewis base (*e.g.* alcohol, amine, ester or ether) to the $TiCl_4$-$MgCl_2$ binary mixture can increase the selectivity towards the isotactic PP, modern-day heterogeneous Ziegler-Natta catalysts for olefin polymerisation have been established. In principle, these catalysts are ternary mixtures, Lewis base-$TiCl_4$/$MgCl_2$ which are activated with aluminium alkyl co-catalysts.[16–19]

1.2.2 Metallocene-type catalysts

Metallocenes are a more recent innovation in olefin catalysis research. They consist of bis-cyclopentadienyl derivatives of Zr, Hf or Ti in combination with MAO, *e.g.* Cp_2ZrCl_2-$[MAO]_n$.[8,20–22] These "single-site" catalysts show only one kind of active site and are used today mainly for the rapidly increasing production of LLDPE and some specialty co-polymers. Metallocenes show certain advantages over Ziegler-Natta catalysts as they exhibit higher activity in solution processes (mainly due to the MAO co-catalyst) and produce ethylene homo- and co-polymers with narrow molecular weight distribution (MWD). In the development of these catalysts, there are several challenges which have to be overcome, *i.e.* maintaining the single-site character of metallocenes upon heterogenisation, preventing catalyst leaching and eliminating the separate feed of the MAO co-catalyst.[23]

1.2.3 Phillips-type catalysts

This ***Dissertation*** will focus on the Phillips-type catalyst, which consists of a chromium oxide supported on an amorphous material, such as silica or silica-alumina.[7,8,24–26] The success of the Phillips polymerisation process originates from its diversity: these catalysts are responsible for the industrial production of over 50 different types of HDPE and LLDPE.[27] Since they do not require the intervention of any activators, crucial for the two previously described types of catalysts, the catalyst preparation and production process becomes more simplified. Although extensive research has been conducted over the past 60 years, there is not yet an univocal agreement on the mechanism of the ethylene polymerisation initiation and the structure of the active sites, which still places this system under both academic and industrial spotlights.

Another interesting feature of the Phillips catalyst is the possibility of the oligomerisation of olefins, if used with metal alkyl co-catalysts.[7,28] Currently, olefins are introduced *via* a separate feed of co-monomer. If the oligomerisation process within a single reactor can take place and be influenced, there would be no need for a separate feed of co-monomers during the production of LLDPE or problems regarding the compatibility with another oligomerisation catalyst in the case of tandem catalysis.[29] This *in-situ* generation of olefins and the subsequent co-polymerisation with ethylene would reduce the chances of contamination *via* the feed of co-monomer, simplify production procedures and reduce costs. With the recent drop in ethylene price of ~40% within just four months ***(Figure 1.3)***, elimination of co-monomer feed and cheap PE production becomes even more interesting.[30]

[FIGURE 1.3]
Global ethylene prices expressed as monthly averages according to Platts Global Petrochemical Index.[30]

1.3 PREPARATION OF THE PHILLIPS-TYPE CATALYST

The preparation of the Phillips catalysts is relatively simple and is usually performed by an aqueous impregnation of a preferably chromium(III) compound (*e.g.* chromic acetate, nitrate, acetylacetonate) onto a porous support material, most commonly a wide pore silica, which would allow the fragmentation of the catalyst particle by the growing PE.[26] The material is subsequently calcined in oxygen or dry air at temperatures between 573 *K* and 1173 *K*. At around 423–623 *K*, the chromium compound decomposes and becomes oxidised to CrO_3, which reacts with the surface hydroxyl groups of the support and becomes well dispersed and anchored as surface hexavalent chromate, dichromate or polychromate species, giving a yellow/orange colour to the catalyst ***(Scheme 1.1)***.[24,31,32] Increasing the temperature causes the condensation of surface hydroxyl groups, leaving a highly dehydroxylated catalyst surface, which

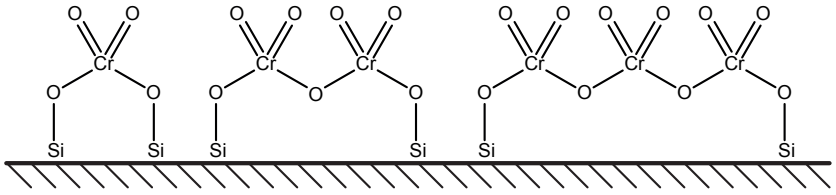

[SCHEME 1.1]
Possible hexavalent chromate species of the activated Cr/SiO_2 Phillips-type catalyst anchored on a silica surface. The presence and ratio of these three species is determined by the choice of the support, Cr loading and calcination procedure.[26]

enhances the polymerisation activity and especially the termination rate, but only up to 1173 *K* at which temperature sintering of the material starts.[33] Respectable polymerisation activity occurs if the catalyst is activated above 823 *K*. Finally, the catalyst is flushed with an inert gas, cooled to room temperature and stored in a glove box under an inert atmosphere due to its high sensitivity to moisture and air. Commercial catalysts usually contain between 0.5–1.0 *wt.%* of chromium. Higher concentrations convert Cr^{6+} species to a bulk Cr_2O_3 phase, which is inactive for the polymerisation of ethylene.

In order to decrease the polymerisation induction time, Cr^{6+} species of the activated catalyst can be pre-reduced by successive reductive treatments with H_2, CO, aluminium alkyl co-catalyst or other reducing agents[34–36] to Cr in lower oxidation state(s), which are considered to be the polymerisation-active species. Pre-reduction is rarely performed on an industrial scale, since ethylene itself acts as a reducing agent during the induction time.

1.3.1 Titanation of the Phillips-type catalyst

Titania itself is not a good carrier for Cr^{6+} species as it does not possess the porosity necessary for ethylene polymerisation and the adequate chemical environment.[7] However, it can be a useful promotor. Its presence inside the Cr/SiO_2 catalyst, in a quantity of no more than 6 *wt.%*, can be beneficial as it increases the activity of the catalyst. Firstly, by shortening the induction time and secondly by allowing higher polymerisation rates.[7] It also shows a promotional effect on the termination rate. Overall, titanation leads to the production of PE with a lower molecular weight and broader MWD than the pure Cr/SiO_2 catalyst. These effects probably arise from the change in the electronic environment on the chromium and the formation of Si-O-Ti-O-Cr-O-Si linkages.[37,38] However, too high titania loading may cause the sintering of the active phase of the catalyst. Titanation can be performed in two ways; either by a co-precipitation with the silica gel, when titania becomes highly dispersed in the bulk catalyst material,[39] or by a reaction of a titanium compound with the hydroxyl groups of the support, therefore coating the silica surface with a layer of titania.[40–43]

1.4 OLIGO/-POLYMERISATION MECHANISMS

Although studied extensively during the last 60 years, some questions still remain unanswered. ***(a)*** What is the molecular structure and oxidation state of the Cr active site? ***(b)*** What is the exact initiation and ethylene polymerisation mechanism? ***(c)*** How do the co-catalysts react with the active site and influence the polymerisation?

[TABLE 1.3]
Most commonly used spectroscopic techniques for the characterisation of the Phillips-type Cr catalyst. Adapted from Weckhuysen *et al.*[24]

Technique	Signature	Origin	Cr specie	Ref.
UV-Vis diffuse reflectance spectroscopy (DRS) (cm^{-1})	27 000–30 000 36 000–41 000	charge transfer	chromate	[44-49]
	21 000–23 000 27 000–30 000 36 000–41 000	charge transfer	polychromate	
	15 000–17 000	d-d transfer	distorted Cr^{3+}_{Oh}	
	10 000–13 000	d-d transfer	distorted Cr^{2+}_{Oh}	
	7 000–10 000	d-d transfer	distorted Cr^{2+}_{Td}	
Infrared spectroscopy (FT-IR) (cm^{-1})	900–950	ν(Cr=O)	Cr^{6+}	[36,50,51]
	1800–1900	2ν(Cr=O)	Cr^{6+}	
	2191	ν(CO), RT	Cr^{2+}_{B} (CN = 3)	
	2178; 2184	$\nu_{as,s}$(CO), RT	Cr^{2+}_{A} (CN = 2)	
	2200	ν(CO), 77 K	Cr^{2+}_{C} (CN = 4)	
Raman spectroscopy (RS) (cm^{-1})	865	Cr=O vibrations	hyd. chromate	[48,50,52–58]
	900; 942	Cr=O vibrations	hyd. dichromate	
	907; 956; 987	Cr=O vibrations	hyd. trichromate	
	980–990	Cr=O vibrations	dehyd. chromate	
	850–880; 1000–1100	Cr=O vibrations	dehyd. polychromate	
	550	Cr=O vibrations	Cr^{3+}_{Oh}	
Electron paramagnetic resonance (EPR) (g-factor)	1.9–2.0	e spin excitation	isolated axially symmetric/rhombic Cr^{5+} (γ-signal)	[59,60]
	1.9–2.4	e spin excitation	Cr_2O_3 clusters (β-signal)	
	4	e spin excitation	isolated rhombic Cr^{3+}_{Oh} (δ-signal)	
X-ray photoelectron spectroscopy (XPS) (eV)	580	2p binding energy	Cr^{6+}	[61–65]
	579	2p binding energy	C^{5+}	
	577	2p binding energy	Cr^{3+}	
	576	2p binding energy	Cr^{2+}	

The reason for this arises from the complex nature of the Phillips catalyst:

I. As only a small fraction of Cr species are considered to be active, *i.e.* 0.01–20% of total Cr, it is hard to relate characterisation results only to the active sites. Furthermore, the already low Cr loading makes it difficult to surpass the detection limitation of certain characterisation techniques.
II. High activity of the catalyst and the incorporation of the catalyst particle inside the PE matrix complicate the research on the initial stages of polymerisation. Many *in-situ* studies have been performed on model catalysts and under conditions, which are often far away from the real industrial conditions.
III. Sensitivity of the catalyst to moisture, oxygen and organic contaminants requires special care and handling under inert conditions, often impossible for some characterisation methods.
IV. Besides the intrinsic heterogeneity of Cr sites and multiple valences, the catalyst structure is extremely sensitive to different preparation routes and the results from different research groups can be difficult to correlate.

Therefore, the study of the Phillips catalyst system and answering these questions requires a multi-technique approach, often combining the most common spectroscopic characterisation techniques, as summarised in ***Table 1.3***, but also many other methods, *e.g.* XAS,[48,66,67] SIMS,[68–70] ssNMR,[38,71] XRD,[72] SEM/EDX,[73–76] EPMA,[64] AFM,[77] RBS,[78] TPR,[72] TPD-MS,[79] TGA,[65] PIXE,[65] LA-MS[70] and LDI-MS[70] and DFT modelling.[67]

1.4.1 Nature of active sites

The ability of the Phillips catalyst to polymerise ethylene without the intervention of any activator that would introduce an initial alkyl ligand, from which the PE chain could grow, makes it rather different from Ziegler-Natta and metallocene catalysts. In order for ethylene polymerisation to start, Cr^{6+} species of the activated catalyst need to be reduced to Cr species in lower oxidation states, and redox products (*i.e.* aldehydes and ketones)[80] should desorb from the coordination sphere of Cr ***(Scheme 1.2)***. Subsequently, hydride or an alkyl ligand has to be formed where a monomer can be inserted. Without the presence of any alkylation agents, these roles have to be performed by the ethylene monomer and are the cause of the reported induction period before the start of the polymerisation.

Many studies have been performed in determining the active sites of the Phillips-type catalyst.[8,25] Most of the spectroscopic studies, especially XAS techniques, show that the major number of Cr sites are in the form of isolated surface Cr^{2+} species. *In-situ* CO adsorption FT-IR measurements by Groppo *et al.* show that it is possible

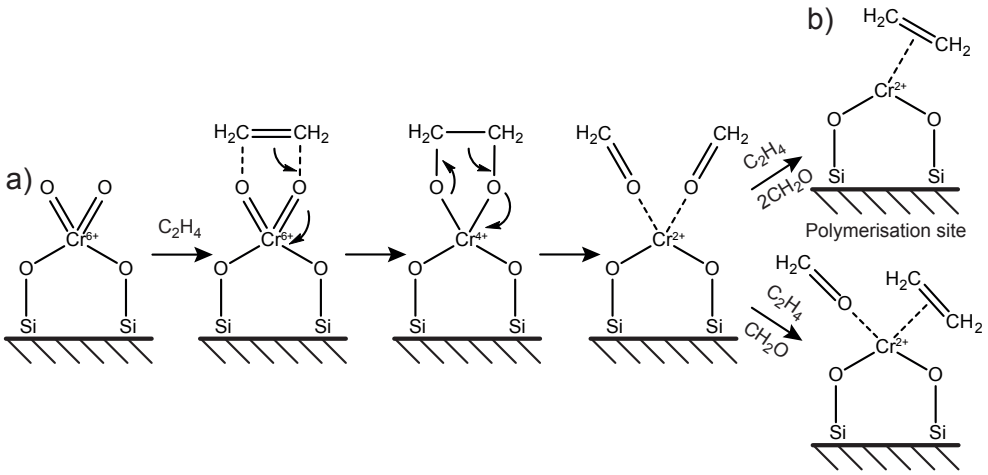

[SCHEME 1.2]
Proposed mechanism of the reduction of Cr^{6+} species **(a)** with the ethylene monomer to the polymerisation active Cr^{2+} site **(b)** during the induction period and coordination of an ethylene molecule. Adapted from Cheng *et al.*[26]

to discriminate three different families of surface Cr^{2+} species, *i.e.* Cr_A^{2+}, Cr_B^{2+} and Cr_C^{2+}, which differ in their degree of coordinative unsaturation (A < B < C) and consequently in their propensity to react (A > B > C).[8,31,51,81–83] After the reduction by the ethylene monomer, CO or other reducing agents, these Cr^{2+} species are considered to be the polymerisation active sites.

Even though Cr^{2+} species are the most abundant in the CO reduced catalyst, other studies suggest that the polymerisation active site is actually comprised of Cr species in a higher oxidation state, *e.g.* Cr^{3+}, which could even give higher polymerisation activity.[84–90]

Despite all of these research efforts, the exact nature of the actual polymerisation active site is still unknown.

1.4.2 Pathways based on Cossee-Arlman linear insertion model

After the initiation phase and formation of the ethylene polymerisation site, the most generally accepted mechanism for chain propagation is the Cossee-Arlman linear insertion model.[91–93] In this case, the metal active site must possess one alkyl or hydride ligand and an available coordination site, as depicted by the black route in ***Scheme 1.3***. As soon as the monomer is inserted into the vacant site, chain propagation starts *via* a migratory insertion reaction, which is repeated numerous times to synthesise the polymer and terminates with a hydrogen β-elimination. The question of the initial alkylation is still problematic.

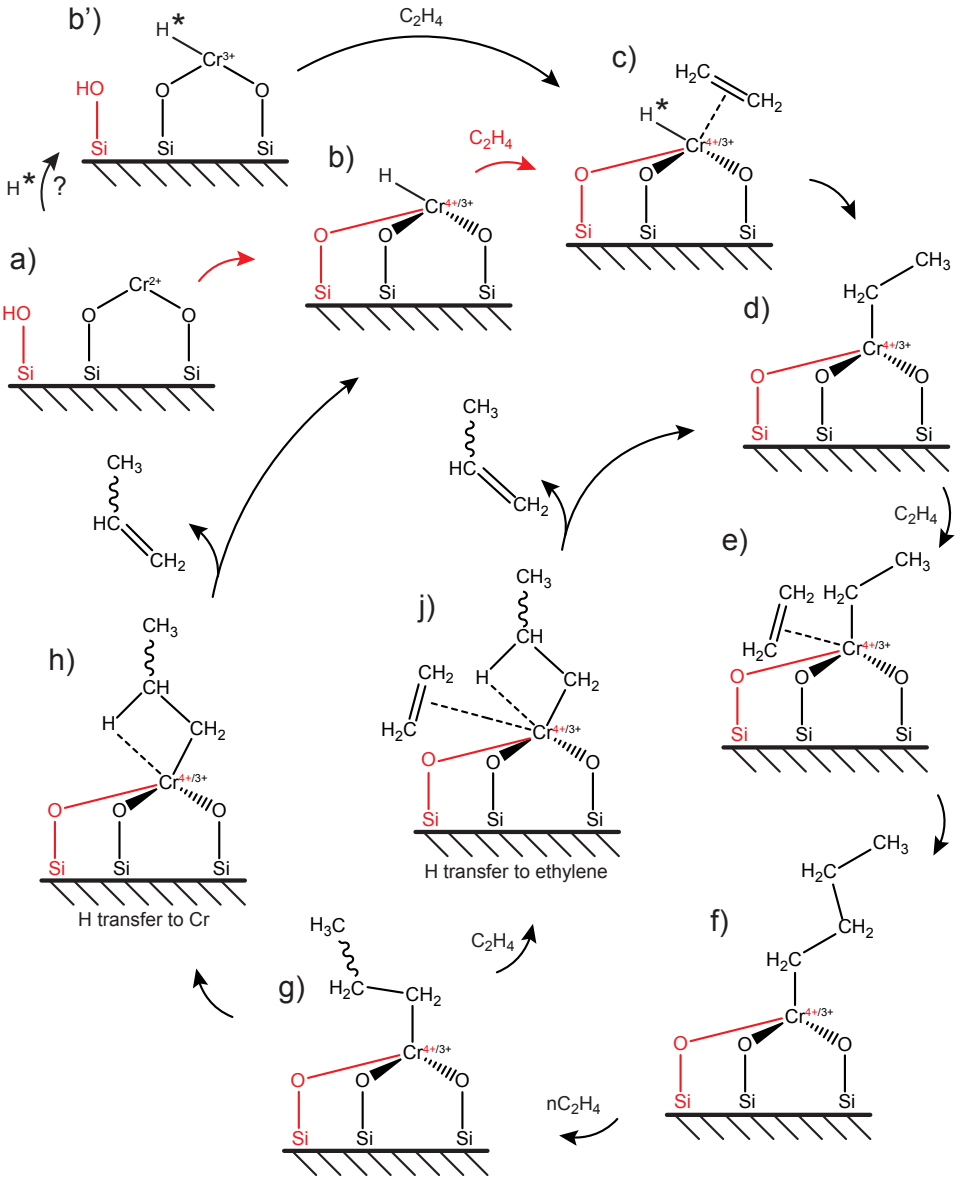

[SCHEME 1.3]

(Black and **red)** Proposed chain initiation on a Cr^{2+} site **(a-b-c-d)** by the hydrogen atom of an adjacent silanol group followed by subsequent chain propagation **(e-f-g)** and termination **(h-b and j-d)** *via* the Cossee-Arlman mechanism. This model cannot explain why the catalyst calcined at higher temperatures containing much less surface hydroxyl groups usually exhibits higher activity than after calcination at lower temperatures. **(Black)** In the case of pre-hydrogenated or pre-alkylated (when H is replaced by an R group) Cr^{2+} site **(b')** at position marked by *, chain initiation **(c-d)**, propagation **(e-f-g)** and termination follow the black route **(h-b** and **j-d)**. This route however does not explain the origin of the first *H or *R group. Adapted from McDaniel[7] and Cheng *et al.*[26]

Although ample research has been done in the past decades, the last alkylation step during the initiation phase of the polymerisation without an activator is still poorly understood. Several different pathways have been proposed. ***Scheme 1.3*** (black and red) shows the chain initiation on the divalent Cr site by the H atom of an adjacent silanol group, subsequent chain propagation and termination *via* Cossee-Arlman mechanism. The group of Copéret have proposed Cr^{3+} as the polymerisation active site and the chain initiation by H-transfer of the first ethylene monomer to one of the oxygens bonded to the Cr site ***(Scheme 1.4)***.[88,94]

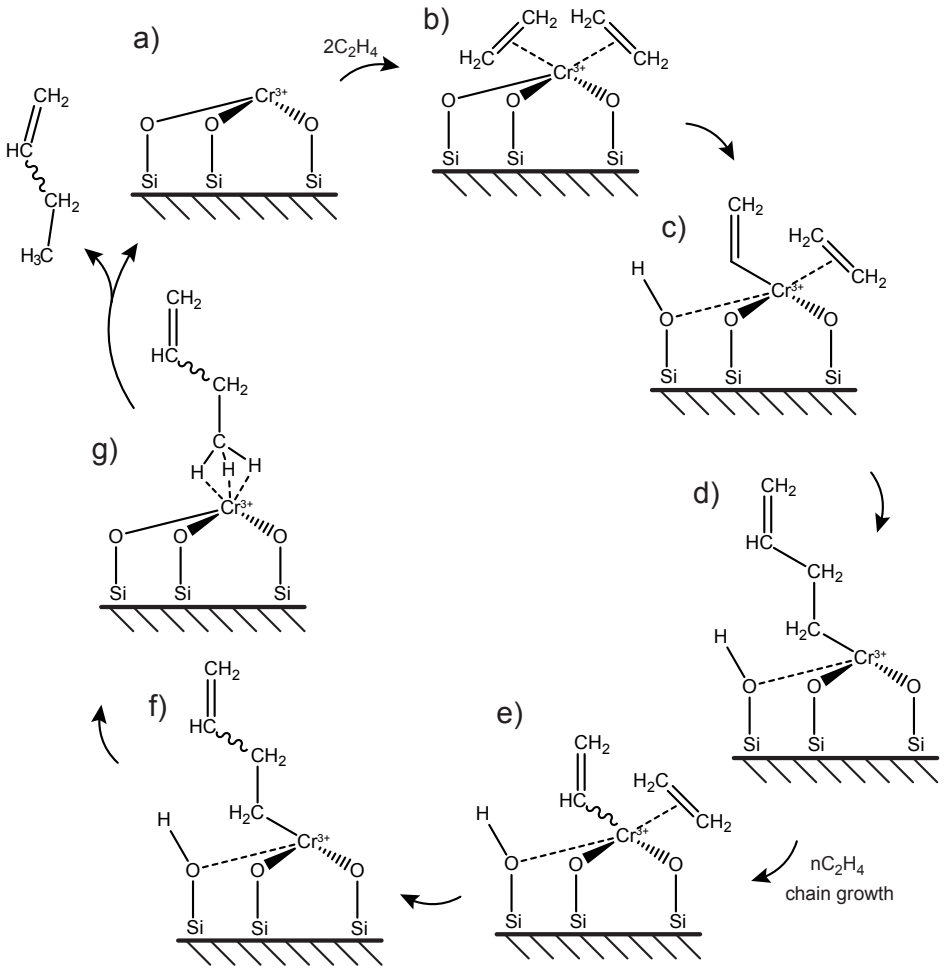

[SCHEME 1.4]
Proposed initial activation of the catalyst and ethylene polymerisation mechanism on a Cr^{3+} polymerisation site **(a)**. C-H bond is activated by H-transfer to O of the Cr-O bond **(b-c)**. Chain propagation further occurs by successive coordination and insertion of monomers **(c-d-e-f)**, until the hydrogen is transferred to the *a* carbon of the PE, chain growth terminated and polymer released **(g)**. Adapted from Conley *et al.*[94] and Fong *et al.*[95]

1.4.3 Alternative pathways: Ivin-Rooney-Green and metallacycle model

A couple of other possible pathways, which do not require the initially alkylated Cr polymerisation sites, have been also proposed. In the case of the ***Ivin-Rooney-Green carbene model (Scheme 1.5)***, only one ethylene molecule is coordinated at the time.[96] *Via* the formation of a Cr^{4+}-ethylidene species through a metal-catalysed H-transfer between the C atoms in ethylene, the first chain is initialised. Chain propagation further occurs by a repeated insertion of monomers in a metathesis-like step *via* 1,3 H-shift. Another competitive process can also occur, *i.e.* 2,3 H-transfer, which leads to the termination of the reaction and release of an ethylene oligo-/polymer. This model however failed to exhibit any hydrogen scrambling between normal and deuterated ethylene[97] and is not backed-up with kinetic investigations.[95]

In the ***Metallacycle model***, the need of an additional hydrogen or an alkyl group is avoided by the formation of a chromacyclopentane intermediate by coordination of two ethylene molecules to a chromium site. Larger metallacycles may be formed

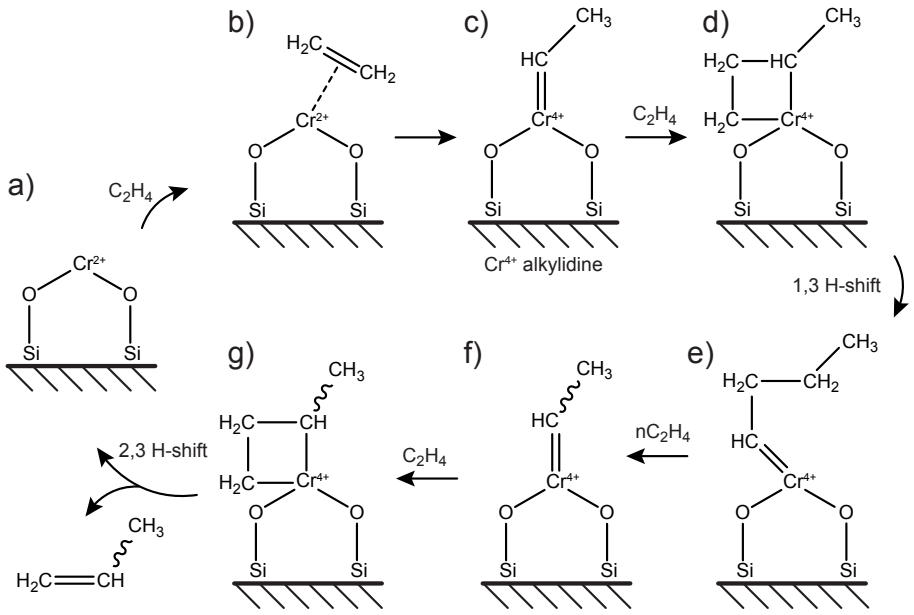

[SCHEME 1.5]
The initiation step is performed by two-electron oxidation of Cr^{2+} species (**a**) by ethylene monomer (**b**) to form Cr^{4+}-alkylidene intermediate (**c**). Chain propagation is established by insertion of ethylene monomers *via* 1,3 H-shift in a metathesis step (**d-e-f**). If 2,3 H-transfer occurs, chain growth terminates and PE molecule released (**g**). Adapted from Ivin *et al.*[96]

by further insertions at one of the two chromium-carbon single bonds. The metallacyclic species may propagate as such, until termination occurs by H-transfer from one of the β-methylene groups to the opposite α-carbon, thus forming linear polymer chains with one methyl and one vinyl end group ***(Scheme 1.6)***. The initiation mechanism *via* this route was the conclusion of many studies in the group of Zecchina,[98–101] although in the research of McGuinness *et al.* the metallacyclic path was ruled out as the main chain propagation process in favour of the Cossee-Arlman model.[102]

1.5 CO-CATALYSTS AND *IN-SITU* BRANCHING

The activity of the Cr/SiO_2 Phillips-type catalyst can be significantly changed with the addition of small amounts of co-catalyst, which include compounds, such as metal alkyls, metal hydrides, π-bonded allyls or metal cyclopentadienyl complexes. The first two require at least one M-R or M-H bond, while the rest of the groups can include other unreactive groups. These compounds can perform several different roles, *i.e.* ***(a)*** reduce Cr^{6+} species, ***(b)*** alkylate Cr sites to induce the formation of the first chain, ***(c)*** scavenge poisons, ***(d)*** modify the Cr sites and neighbouring silanol and siloxane groups, ***(e)*** attack the Cr-support bond, ***(f)*** destroy the active sites, ***(g)*** exchange alkyl groups with the active site and ***(h)*** promote oligomerisation of ethylene to shorter olefins.[7]

The consequences of employing co-catalysts are the shortening of the induction time, accelerating the development and raising of the highest achievable polymerisation rate.[27] The highest activity is mostly obtained for the Cr to metal ratio of ~1 or less, as at higher co-catalyst concentrations the activity becomes diminished by the attack on Cr-support bonds, which leads to the formation of inactive species. Furthermore, the change in the distribution of active sites with co-catalyst can provide means of tailoring the final PE properties, especially with the variety of available compounds.

1.5.1 *α*-Olefin co-production

It has been reported that the addition of metal alkyl co-catalysts, such as BEt_3 or $AlEt_3$, changes the PE product, which leads to the production of LLDPE. In this case, the polymer density is decreased and branching is introduced as the result of co-polymerisation with the *in-situ* produced light α-olefins from newly formed sites responsible for ethylene oligomerisation.[7,103] It has been proposed that these sites are created only on ligand-free Cr species after the initial reduction of Cr^{6+} when they become alkylated and one of the Cr-O bonds is attacked by the co-catalyst. The analy-

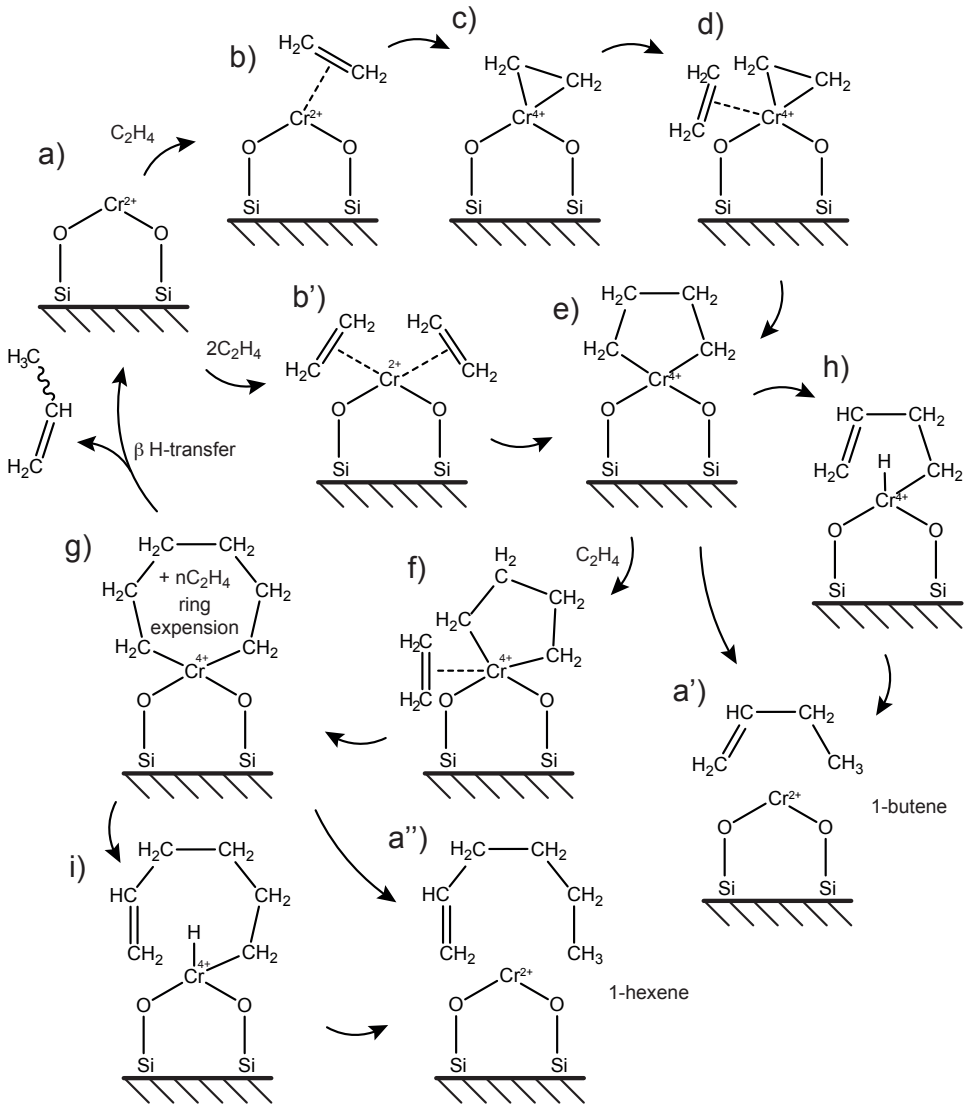

[SCHEME 1.6]
Oxidative coupling of two ethylene monomers leads to the oxidation of Cr^{2+} species **(a)** and initiation and formation of a chromacyclopentane intermediate **(e)**. By coordination and insertion of another monomer, the chromacyclic ring is able to grow **(f-g)**. *Via* a *β*-H-transfer step, ethylene oligomers can be released and the Cr species can be converted back to the Cr^{2+} site **(g-a, e-a'** and **g-a'')**. Adapted from Cheng *et al.*[26]

sis of the branching content of the PE formed led to the conclusion of two superimposed olefin distributions, namely a Schulz-Flory distribution of even-numbered linear α-olefins (LAO) and a spike of 1-hexene indicating a variety of *in-situ* olefin generation sites and oligomerisation mechanisms.[7] Furthermore, the *in-situ* produced α-olefins are incorporated more efficiently than in normal co-polymerisation with externally added 1-hexene.[104]

Most of the research has been performed on the analysis of the final PE product by means of ^{13}C NMR and GPC-IR analyses. On the other hand, spectroscopic data of the *in-situ* oligomerisation sites are rather scarce. Barzan *et al*. have shown that by using temperature- and pressure-resolved FT-IR spectroscopy, it is possible to detect α-olefin species under *operando* conditions in a polymerisation reaction using a CO-reduced Cr^{2+}/SiO_2 catalyst modified with SiH_4. The research group of Terano have systematically studied the activation of the Phillips catalyst by aluminium alkyl co-catalyst with XPS and ssNMR. Besides the identification of multiple oxidation states of Cr, *i.e.* +2, +3, +5 and +6, they have named $Cr^{2+}{\cdot}2Cr^{6+}$ as the cluster of species responsible for polymerisation activity.[63,105] These clusters may also be involved in the *in-situ* oligomerisation activity of the catalyst.

1.6 SCOPE AND OUTLINE OF THIS PHD THESIS

Linear PEs account for about one third of the global PE market. Cr/SiO_2 Phillips-type catalysts are responsible for the production of about half of all HDPE sold worldwide and also hold a large share in the production of LLDPE.[7] Co-monomers, such as 1-hexene, are used to control the density of the produced PE and have a beneficial effect on the impact properties of the polymer resin. Usually, they are separately fed into the reactor, which demands additional infrastructure and increases the probability of introducing impurities, increasing the risk of catalyst poisoning and decreasing the productivity. This problem can be solved with the concept of tandem catalysis,[29] but a single-reactor single-catalyst "one-pot" setup could be a more ingenuitive approach, as vulnerability to poisoning from different reactant feeders and the interference between the two catalysts could be eliminated. Furthermore, a significantly lower price of ethylene compared to the price of 1-hexene makes the concept of the *in-situ* generation of the co-monomer inside the polymerisation reactor, when 1-hexene is produced alongside polymerisation, highly desirable from a practical and an economical point of view ***(Figure 1.4)***.

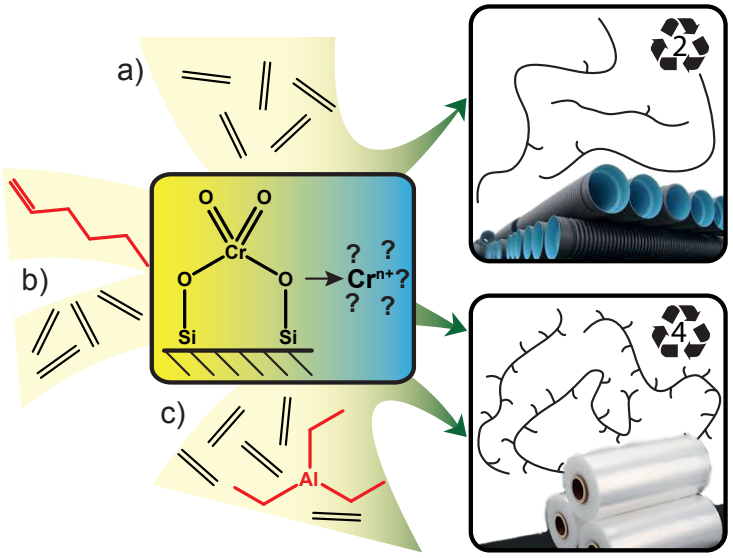

[FIGURE 1.4]
(a) Polymerisation of ethylene to HDPE using the Cr^{6+}/SiO_2 Phillips-type catalyst. **(b)** Production of LLDPE involves co-polymerisation of ethylene with 1-hexene, separately fed into the reactor. **(c)** Alternative method for the production of LLDPE *via* co-polymerisation of ethylene with the *in-situ* produced LAOs. Selective oligomerisation of ethylene could be induced by a modification of the catalyst with metal alkyl compounds.

In this ***PhD thesis*** the investigation of the oligomerisation properties of Phillips-type Cr/SiO_2 catalysts has been described.

Chapter 2 presents the development of a triethylaluminium(TEAl)-modified Phillips ethylene polymerisation $Cr/Ti/SiO_2$ catalyst, specifically titanated in the catalyst shell. With the multi-technique characterisation approach in hand, involving traditional and advanced characterisation methods, such as STXM, different active sites have been discovered with respect to their ability to oligomerise ethylene and to incorporate *in-situ* produced oligomers into the growing PE chain. This chapter explains the "reverse" co-monomer incorporation by relating microscale properties of the catalyst/PE particle with the macroscopic characteristics of the polymer.

Chapter 3 presents a DRIFT spectroscopy study of the Phillips system providing a comparison of the performance of Cr/SiO_2 and $Cr/Ti/SiO_2$ catalysts, with the catalysts modified with TEAl, offering further insights into the role of this co-catalyst and the effect of the titanium loading. The titanation increases the acidity of the catalyst support, as testified by the appearance of an additional 3719 cm^{-1} hydroxyl stretching vibration. These acid sites are able to pull electrons from the Cr species away, enabling an easier coordination of the ethylene monomer. This results in the shortening

of the induction time and an increase of the polymerisation rate. Modification of the catalysts with TEAl as co-catalyst is highly promoting the polymerisation activity in comparison to the pristine catalysts. TEAl is able to increase the number of active sites by scavenging poisons and ethylene oxidation products created during the initiation step, but also to increase the activity of part of the active sites by modifying their molecular structure. However, under the applied conditions, *in-situ* ethylene oligomerisation products could not be detected. Finally, from the comparison of the DRIFT spectra of the titanated and non-titanated Phillips-type catalysts, the spectral assignment of the OH stretching region was reinterpreted, attributing the 3610 cm^{-1} to the stretching vibration of bridging titanol group.

Chapter 4 investigates further the influence of the catalyst structure and reactant mixture compositions. A TEAl-modified $Cr/Ti/SiO_2$ catalyst with different amounts of titanation, and activated at different temperatures, were tested in ethylene polymerisation reactions in a specially designed *operando* setup, which combined UV-Vis-NIR diffuse reflectance spectroscopy, mass spectrometry and gas chromatography. Different distributions of light α-olefins have been detected due to the change in the oligomerisation mechanism, which is highly influenced by the titanation degree of the catalyst. It was found that TEAl is able to modify Cr sites, producing oligomerisation sites with higher selectivity towards the production of 1-hexene, which can be explained with the metallacyclic oligomerisation mechanism. Changing the chemical environment of Cr by titanation promotes β-H-transfer and significantly decreases the oligomer yield, while shifting the selectivity towards 1-butene.

Chapter 5 summarises the main findings and conclusions of the preceding chapters. In addition, some future perspectives are presented.

1.7 REFERENCES

[1] J. Gribbin, Ed., *The Britannica Guide to the 100 Most Influential Scientists*, Encyclopaedia Britannica, Inc, Chicago, **2008**, pp. 154–157.

[2] "Jöns Jacob Berzelius," can be found under https://en.wikipedia.org/wiki/J%C3%B6ns_Jacob_Berzelius, accessed July **2015**.

[3] A. D. Jenkins, P. Kratochvil, R. F. T. Stepto, U. W. Suter, *Pure Appl. Chem.* **1996**, *68*, 2287–2311.

[4] W. Reusch, "Polymers," can be found under https://www2.chemistry.msu.edu/faculty/reusch/VirtTxtJml/polymers.htm, accessed July **2015**.

[5] A. L. Andrady, M. A. Neal, *Philos. Trans. R. Soc. B* **2009**, *364*, 1977–1984.

[6] PlasticsEurope, *Plastics - the Facts 2014/2015. An Analysis of European Plastics Production, Demand and Waste Data,* digital booklet, **2015**, pp. 1–34.

[7] M. P. McDaniel, *Adv. Catal.* **2010**, *53*, 123–606.

[8] B. M. Weckhuysen, R. A. Schoonheydt, *Catal. Today* **1999,** *51*, 215–221.

[9] J. P. Hogan, R. L. Banks, US2825721, **1958**.

[10] J. P. Hogan, R. L. Banks, US2951816, **1960**.

[11] E. W. Fawcett, R. O. Gibson, M. W. Perrin, J. G. Patton, E. G. Williams, BP472590, **1937**.

[12] K. Ziegler, H. Breil, H. Martin, E. Holzkamp, DE973626, **1953**.

[13] K. Ziegler, H. Breil, H. Martin, US3257332A, **1954**.

[14] K. Ziegler, BE533362, **1954**.

[15] V. Busico, *Adv. Polym. Sci.* **2013**, *257*, 37–58.

[16] G. Wilke, *Angew. Chem. Int. Ed.* **2003**, *42,* 5000–5008.

[17] L. L. Böhm, V. Busico, R. Cheng, M. S. Eisen, G. Fink, X. He, B. Liu, B. Monrabal, L. A. Novokshonova, P. Qiu, S. L. Scott, T. Taniike, M. Terano, V. A. Zakharov, L. Zhong, *Polyolefins: 50 Years after Ziegler and Natta I*, Springer, Berlin, **2013**, pp. 1–58.

[18] L. A. Novokshonova, V. A. Zakharov, *Adv. Polym. Sci.* **2013**, *257*, 99–134.

[19] L. L. Böhm, *Angew. Chem. Int. Ed.* **2003**, *42,* 5010–5030.

[20] H. Sinn, W. Kaminsky, H.-J. Vollmer, R. Woldt, *Angew. Chem. Int. Ed.* **1980**, *19,* 390–392.

[21] H. H. Brintzinger, D. Fischer, R. Mülhaupt, B. Rieger, R. M. Waymouth, *Angew. Chem. Int. Ed.* **1995**, *34*, 1143–1170.

[22] W. Kaminsky, *Macromolecules* **2012**, *45,* 3289–3297.

[23] M. Atiqullah, S. Anantawaraskul, A.-H. M. Emwas, M. A. Al-Harthi, I. Hussain, A. Ul-Hamid, A. Hossaen, *Polym. Int.* **2014**, *63,* 955–972.

[24] B. M. Weckhuysen, I. E. Wachs, R. A. Schoonheydt, *Chem. Rev.* **1996**, *96*, 3327–3350.

[25] E. Groppo, C. Lamberti, S. Bordiga, G. Spoto, A. Zecchina, *Chem. Rev.* **2005**, *105*, 115–184.

[26] R. Cheng, Z. Liu, L. Zhong, X. He, P. Qiu, M. Terano, M. S. Eisen, S. L. Scott, B. Liu, *Adv. Polym. Sci*. **2013**, *257*, 135–202.

[27] M. P. McDaniel, *Adv. Catal.* **1985**, *33*, 47–98.

[28] C. Barzan, E. Groppo, E. A. Quadrelli, V. Monteil, S. Bordiga, *Phys. Chem. Chem. Phys.* **2012**, *14*, 2239–2245.

[29] D. S. McGuinness, *Chem. Rev.* **2011**, 111, 2321–2341.

[30] "Platts Global Ethylene Price Index," can be found under a) www.platts.com/news-feature/2013/petrochemicals/pgpi/ethylene, b) www.platts.com/news-feature/2014/petrochemicals/pgpi/ethylene, c) www.platts.com/news-feature/2015/petrochemicals/pgpi/ethylene, accessed July **2015**.

[31] A. Zecchina, E. Groppo, A. Damin, C. Prestipino, in *Top. Organomet. Chem.* (Eds.: C. Copéret, B. Chaudret), Springer, Berlin, **2005**, pp. 1–35.

[32] W. K. Jóźwiak, I. G. Dalla Lana, R. Fiedorow, *J. Catal.* **1990**, *121*, 183–195.

[33] M. P. McDaniel, M. B. Welch, *J. Catal.* **1983**, *82*, 98–109.

[34] E. D. Schwerdtfeger, R. Buck, M. P. McDaniel, *Appl. Catal. A Gen.* **2012**, *423–424*, 91–99.

[35] M. B. Welch, M. P. McDaniel, *J. Catal.* **1983**, *82*, 110–117.

[36] A. Zecchina, E. Garrone, G. Ghiotti, C. Morterra, E. Borello, *J. Phys. Chem.* **1975**, *79*, 966–972.

[37] M. P. McDaniel, M. B. Welch, M. J. Dreiling, *J. Catal.* **1983**, *82*, 118–126.

[38] R. Cheng, C. Xu, Z. Liu, Q. Dong, X. He, Y. Fang, M. Terano, Y. Hu, T. J. Pullukat, B. Liu, *J. Catal.* **2010**, *273*, 103–115.

[39] R. E. Dietz, US3887494, **1975**.

[40] G. Debras, J.-P. Dath, EP0882743 B1, **1998**.

[41] T. J. Pullukat, D. Plaines, M. Shida, US3780011, **1973**.

[42] J. P. Hogan, D. R. Witt, US3622521, **1971**.

[43] B. Horvath, US3625864, **1971**.

[44] B. M. Weckhuysen, L. M. De Ridder, R. A. Schoonheydt, *J. Phys. Chem.* **1993**, *97*, 4756–4763.

[45] R. A. Schoonheydt, *Chem. Soc. Rev.* **2010,** *39*, 5051–5066.

[46] B. M. Weckhuysen, A. A. Verberckmoes, A. R. de Baets, R. A. Schoonheydt, *J. Catal.* **1997**, *166*, 160–171.

[47] A. Bensalem, B. M. Weckhuysen, R. A. Schoonheydt, J. *Phys. Chem. B* **1997**, *101*, 2824–2829.

[48] B. M. Weckhuysen, R. A. Schoonheydt, J.-M. Jehng, I. E. Wachs, S. J. Cho, R. Ryoo, S. Kijlstra, E. Poels, *J. Chem. Soc. Faraday Trans.* **1995**, *91*, 3245–3253.

[49] B. M. Weckhuysen, R. A. Schoonheydt, *Catal. Today* **1999**, *49*, 441–451.

[50] I. E. Wachs, *Catal. Today* **1996**, *27*, 437–455.

[51] C. Lamberti, A. Zecchina, E. Groppo, S. Bordiga, Chem. *Soc. Rev.* **2010**, *39*, 4951–5001.

[52] B. M. Weckhuysen, I. E. Wachs, *J. Chem. Soc. Faraday Trans.* **1996**, *92*, 1969–1973.

[53] I. E. Wachs, C. A. Roberts, *Chem. Soc. Rev.* **2010**, *39*, 5002–5017.

[54] B. M. Weckhuysen, I. E. Wachs, *J. Phys. Chem.* **1996**, 14437–14442.

[55] T. J. Dines, S. Inglis, *Phys. Chem. Chem. Phys.* **2003**, *5*, 1320–1328.

[56] G. Ghiotti, E. Garrone, A. Zecchina, *J. Mol. Catal.* **1988**, *46*, 61–77.

[57] E. Groppo, A. Damin, F. Bonino, A. Zecchina, S. Bordiga, C. Lamberti, *Chem. Mater.* **2005**, *17*, 2019–2027.

[58] A. Damin, F. Bonino, S. Bordiga, E. Groppo, C. Lamberti, A. Zecchina, *ChemPhysChem* **2006**, *7*, 342–344.

[59] B. M. Weckhuysen, L. M. De Ridder, P. J. Grobet, R. A. Schoonheydt, *J. Phys. Chem.* **1995**, *99*, 320–326.

[60] B. M. Weckhuysen, R. A. Schoonheydt, F. E. Mabbs, D. Collison, *J. Chem. Soc. Faraday Trans.* **1996**, *92*, 2431–2436.

[61] R. Merryfield, M. P. McDaniel, G. Parks, *J. Catal.* **1982**, *77*, 348–359.

[62] P. C. Thüne, C. P. J. Verhagen, M. J. G. van den Boer, J. W. Niemantsverdriet, *J. Phys. Chem. B* **1997**, *101*, 8559–8563.

[63] B. Liu, P. Šindelář, Y. Fang, K. Hasebe, M. Terano, *J. Mol. Catal. A Chem.* **2005**, *238*, 142–150.

[64] B. Liu, M. Terano, J. *Mol. Catal. A Chem.* **2001**, *172*, 227–240.

[65] A. Rahman, M. H. Mohamed, M. Ahmed, A. M. Aitani, *Appl. Catal. A Gen.* **1995**, *121*, 203–216.

[66] L. Zhong, M.-Y. Lee, Z. Liu, Y.-J. Wanglee, B. Liu, S. L. Scott, *J. Catal.* **2012**, *293*, 1–12.

[67] C. A. Demmelmaier, R. E. White, J. A. van Bokhoven, S. L. Scott, *J. Catal.* **2009**, *262*, 44–56.

[68] P. C. Thüne, R. Linke, W. J. H. van Gennip, A. M. de Jong, J. W. Niemantsverdriet, *J. Phys. Chem. B* **2001**, *105*, 3073–3078.

[69] P. C. Thüne, J. Loos, D. Wouters, P. J. Lemstra, J. W. Niemantsverdriet, *Macromol. Symp.* **2001**, 37–52.

[70] F. Aubriet, J. F. Muller, C. Poleunis, P. Bertrand, P. G. Di Croce, P. Grange, *J. Am. Soc. Mass Spectrom.* **2006**, *17*, 406–414.

[71] W. Xia, B. Liu, Y. Fang, T. Fujitani, T. Taniike, M. Terano, *Appl. Catal. A Gen.* **2010**, *389*, 186–194.

[72] W. K. Jóźwiak, I. G. Dalla Lana, *J. Chem. Soc. Faraday Trans.* **1997**, *93*, 2583–2589.

[73] W. C. Conner, S. W. Webb, P. Spanne, K. W. Jones, *Macromolecules* **1990,** *23*, 4742–4747.

[74] K. W. Jones, P. Spanne, S. W. Webb, W. C. Conner, R. A. Beyerlein, W. J. Reagan, F. M. Dautzenberg, *Nucl. Instruments Methods Phys. Res.* **1991**, *B56/57*, 427–432.

[75] X. Zheng, M. Smit, J. C. Chadwick, J. Loos, *Macromolecules* **2005**, *38*, 4673–4678.

[76] H. Schmidt, W. Riederer, H. L. Krauss, *J. Prakt. Chem.* **1996**, *338*, 627–633.

[77] P. C. Thune, J. Loos, X. Chen, E. M. E. van Kimmenade, B. Kong, J. W. Niemantsverdriet, *Top. Catal.* **2007**, *46*, 239–245.

[78] E. M. E. van Kimmenade, A. E. T. Kuiper, Y. Tamminga, P. C. Thüne, J. W. Niemantsverdriet, *J. Catal.* **2004**, *223*, 134–141.

[79] B. Liu, H. Nakatani, M. Terano, *J. Mol. Catal. A Chem.* **2003**, *201*, 189–197.

[80] L. M. Baker, W. L. Carrick, *J. Org. Chem.* **1968**, *33*, 616–618.

[81] E. Groppo, K. Seenivasan, C. Barzan, C*atal. Sci. Technol.* **2013**, *3*, 858–878.

[82] A. Zecchina, E. Groppo, *Proc. R. Soc. A Math. Phys. Eng. Sci.* **2012**, *468*, 2087–2098.

[83] A. Zecchina, E. Garrone, G. Ghiotti, S. Coluccia, *J. Phys. Chem.* **1975**, *79*, 972–978.

[84] J. H. Lunsford, S.-L. Fu, D. L. Myers, *J. Catal.* **1988**, *111*, 231–234.

[85] B. Rebenstorf, *J. Mol. Catal.* **1989**, *56*, 170–182.

[86] D. L. Myers, J. H. Lunsford, *J. Catal.* **1986**, *99*, 140–148.

[87] D. L. Myers, J. H. Lunsford, *J. Catal.* **1985**, *92*, 260–271.

[88] (a) M. P. Conley, M. F. Delley, G. Siddiqi, G. Lapadula, S. Norsic, V. Monteil, O. V. Safonova, C. Copéret, *Angew. Chem. Int. Ed.* **2014**, *53*, 1872–1876. (b) M. P. Conley, M. F. Delley, G. Siddiqi, G. Lapadula, S. Norsic, V. Monteil, O. V. Safonova, C. Copéret, *Angew. Chem. Int. Ed.* **2015**, *53*, 6670–6670.

[89] M. F. Delley, M. P. Conley, C. Copéret, *Catal. Lett.* **2014**, *144*, 805–808.

[90] M. F. Delley, F. Núñez-Zarur, M. P. Conley, A. Comas-Vives, G. Siddiqi, S. Norsic, V. Monteil, O. V. Safonova, C. Copéret, *Proc. Natl. Acad. Sci. U. S. A.* **2014**, *111*, 11624–11629.

[91] P. Cossee, *J. Catal.* **1964**, *3*, 80–88.

[92] E. J. Arlman, *J. Catal.* **1964**, *3*, 89–98.

[93] E. J. Arlman, P. Cossee, *J. Catal.* **1964**, *3*, 99–104.

[94] M. P. Conley, M. F. Delley, F. Núñez-Zarur, A. Comas-Vives, C. Copéret, *Inorg. Chem.* **2015**, *54*, 5065–5078.

[95] A. Fong, Y. Yuan, S. L. Ivry, S. L. Scott, B. Peters, *ACS Catal.* **2015**, *5*, 3360–3374.

[96] K. J. Ivin, J. J. Rooney, C. D. Stewart, M. L. H. Green, R. Mahtab, *J. Chem. Soc. Chem. Commun.* **1978**, 604–606.

[97] M. P. McDaniel, D. M. Cantor, *J. Polym. Sci. Polym. Chem. Ed.* **1983**, *21*, 1217–1221.

[98] S. Bordiga, S. Bertarione, A. Damin, C. Prestipino, G. Spoto, C. Lamberti, A. Zecchina, *J. Mol. Catal. A Chem.* **2003**, *204–205*, 527–534.

[99] E. Groppo, C. Lamberti, S. Bordiga, G. Spoto, A. Damin, A. Zecchina, *J. Phys. Chem. B* **2005**, *109*, 15024–15031.

[100] E. Groppo, C. Lamberti, S. Bordiga, G. Spoto, A. Zecchina, *J. Catal.* **2006**, *240*, 172–181.

[101] E. Groppo, J. Estephane, C. Lamberti, G. Spoto, A. Zecchina, *Catal. Today* **2007**, *126*, 228–234.

[102] D. S. McGuinness, N. W. Davies, J. Horne, I. Ivanov, *Organometallics* **2010**, *29*, 6111–6116.

[103] M. P. McDaniel, D. D. Klendworth, D. D. Norwood, E. T. Hsieh, E. A. Boggs, US4735931A, **1988**.

[104] E. A. Benham, M. P. McDaniel, R. R. McElvain, R. O. Schneider, US5071927A, **1991**.

[105] W. Xia, B. Liu, Y. Fang, K. Hasebe, M. Terano, *J. Mol. Catal. A Chem.* **2006**, *256*, 301–308.

[This page is intentionally left blank]

CANADIAN LIGHT SOURCE
Saskatoon, Canada

II

Polyethylene with Reverse Co-monomer Incorporation:

From an Industrial Serendipitous Discovery to Fundamental Understanding

A triethylaluminium(TEAl)-modified Phillips ethylene polymerisation Cr/Ti/SiO_2 catalyst has been developed with two distinct active regions positioned respectively in the inner core and outer shell of the catalyst particle. DRIFTS, EPR, UV-Vis-NIR DRS, STXM, SEM-EDX and GPC-IR studies revealed that the catalyst produces simultaneously two different polymers, *i.e.* low molecular weight linear-chain polyethylene in the Ti-abundant catalyst particle shell and high molecular weight short-chain branched polyethylene in the Ti-scarce catalyst particle core. Co-monomers for the short-chain branched polymer were generated *in-situ* within the TEAl-impregnated confined space of the Ti-scarce catalyst particle core in close proximity to the active sites that produced the high molecular weight polymer. These results demonstrate that the catalyst particle architecture directly affects polymer composition, offering the perspective of making high-performance polyethylene from a single reactor system using this modified Phillips catalyst.

BASED ON:
"Polyethylene with Reverse Co-monomer Incorporation: From an Industrial Serendipitous Discovery to Fundamental Understanding", D. Cicmil, J. Meeuwissen, A. Vantomme, J. Wang, I. K. van Ravenhorst, H. E. van der Bij, A. Muñoz-Murillo and B. M. Weckhuysen, *Angew. Chem. Int. Ed.* **2015**, *54*, 13073–13079.

2.1 INTRODUCTION

Even after more than 50 years of industrial and academic research efforts, Cr/SiO_2 Phillips-type catalysts[1–8] for ethylene polymerisation are not yet fully understood and therefore a rational catalyst design in order to improve polymer properties still remains a formidable challenge. Support modifications, *e.g.* sol-gel techniques or surface impregnations, are common strategies to modify the Phillips catalyst. As such, Ti has been used in the polymer industry since several decades to lower the molecular weight (MW) and to broaden the molecular weight distribution (MWD) of the polymer.[9–14] However, Deslauriers and McDaniel revealed that the addition of Ti to the SiO_2 support also leads to an improved distribution of co-monomer in the polymer because the $Cr/Ti/SiO_2$ sites give low molecular weight polymer and have low co-monomer reactivity.[15] More co-monomer is thus incorporated in the high molecular weight fraction of the polymer leading to better mechanical properties.[16]

Several years ago at an industrial ethylene polymerisation plant, the *in-situ* generation of co-monomer on a chromium polymerisation line using the well-known $Cr/Ti/SiO_2$ Phillips-type catalyst was reported.[1–8] Hence, the co-feeding of 1-hexene was significantly reduced in order to keep a polymer with similar content of co-monomer. The interesting finding was that 1-hexene was the major component, while butene and other oligomers were present in lower concentration. Moreover, the properties of the polyethylene (PE) produced were not affected despite the presence of butene. On the contrary, the polymer made even exhibited some improvements. The probable explanation for this finding and the motivation for the research presented in this ***Dissertation*** was the accidental contamination of the polymerisation lines with TEAl co-catalyst, as some of the polymerisation lines were running a Ziegler-Natta-type catalyst. Thus the fundamental question was:

What are the underlying principles for the production of this polymer with advanced properties using a TEAl-modified $Cr/Ti/SiO_2$ catalyst?

This ***Chapter*** presents a new type of Phillips $Cr/Ti/SiO_2$ catalyst, which was selectively surface-titanated on the catalyst particle's outer shell,[14] and by pre-contacting the catalyst with TEAl, *in-situ* ethylene oligomerisation sites could be generated.[1,17] Typically, an olefinic co-monomer (*i.e.*, 1-hexene) is added externally to the reaction mixture and has to diffuse through the growing polymer and catalyst material to arrive at the catalytic sites. It was envisioned that it would be advantageous if the co-monomer was generated on the TEAl-modified active sites within the Ti-scarce catalyst particle close to the active sites that make a high molecular weight polymer. Therefore, *in-situ* produced olefins (*e.g.*, 1-hexene) would be incorporated into longer PE chains. It is shown for the first time that these macroscale polymer properties

can be related to nanoscale chemical imaging data of (early-stage polymerisation) Cr/Ti/SiO_2 catalyst particles by making use of scanning transmission X-ray microscopy (STXM).[18–21]

2.2 EXPERIMENTAL METHODS

2.2.1 Sample preparation

All catalyst samples under investigation were made and provided by Total Research and Technology Feluy, Belgium. A commercially available Phillips-type Cr/SiO_2 catalyst was used with the following properties: ~1 *wt.%* Cr loading, surface area of 500 $m^2 g^{-1}$, pore volume of 1.5 $cm^3 g^{-1}$ and D50 of 85 μm. The pale white pre-catalyst material was titanated and activated according to a procedure described by Debras *et al.*[14] The preparation procedure consists of the following steps. First, the Phillips-type Cr/SiO_2 pre-catalyst was dehydrated at 573 *K* in a fluidised bed in dry nitrogen in order to remove physically adsorbed water, which prevents the formation of crystalline TiO_2. After drying, titanium isopropoxide (TIP, 99.999% trace metals basis, Sigma-Aldrich) was introduced into the nitrogen stream at the same temperature by evaporation of the material, which was added as a suspension into the reactor. The total amount of TIP, flow rate and titanation time was adjusted in order to obtain an overall catalyst titanation amount of ~4 *wt.%*. After titanation, the catalyst was flushed under nitrogen for ~45 *min* at 573 *K*. In a next step, the temperature was gradually increased to 1048 *K* and the atmosphere changed from nitrogen to dry air in which the catalyst material was activated for a period of 6 *h*. After this oxidation step, the prepared surface-titanated Phillips-type polymerisation catalyst had acquired an intense orange colour. X-ray fluorescence (XRF) analysis showed that the surface-titanated Phillips-type polymerisation catalyst had a titanium loading of ~4.7 *wt.%*, slightly above the intended titanium loading. The activated surface-titanated Phillips-type polymerisation catalyst was kept under an inert atmosphere, and then transferred into a glove box under inert atmosphere for storage and further use.

2.2.2 Nitrogen physisorption measurements

The nitrogen physisorption measurements were performed on a Micromeritics TriStar 3000 device at 77 *K*. This instrument determines the nitrogen adsorption and desorption isotherms by static volumetric measurements. The Phillips-type Cr/Ti/SiO_2 sample, stored in a solvent-free argon glove box, was weighed and introduced into a

nitrogen physisorption flask. The sample is evacuated and cooled to the temperature of liquid nitrogen. The adsorption branch is determined by adding stepwise known amounts of nitrogen, until the saturation pressure of nitrogen is reached. The adsorption equilibrium pressure is determined at each addition of nitrogen. The desorption isotherm is determined in a similar way: nitrogen is removed stepwise, and the desorption equilibrium pressure is measured at each desorption step. The specific surface area is calculated from the adsorption isotherm using the Brunauer-Emmet-Teller (BET) model.[22] This value can be considered representative of the true specific surface if the sorption isotherm is of type IV. The pore size distribution is calculated from the desorption isotherm using the Barrett-Joyner-Halenda (BJH) model.[23] The total pore volume was defined as the single-point pore volume at $p/p_o = 0.95$.

2.2.3 Ethylene polymerisation studies in a semi-batch reactor

Slurry polymerisation reactions with a $Cr/Ti/SiO_2$ Phillips-type catalyst in a 4 *L* semi-batch reactor were performed at Total Research and Technology (Feluy, Belgium) and the PE product obtained was used for molecular weight distribution (MWD) and short-chain branching distribution (SCBD) analysis. The catalyst containing 0.5 *wt.%* Cr and 3.9 *wt.%* Ti, prepared following the same procedure as described in the sample preparation section, was used for ethylene polymerisation. The reaction conditions, given in ***Table 2.1***, were chosen in order to target the same molecular weight distribution and co-monomer content in the polymer.

[TABLE 2.1]
Catalyst properties and polymerisation conditions, used for the ethylene polymerisation reaction inside a semi-batch reactor. **Run 1** represents a polymerisation, which was performed without external addition of 1-hexene co-monomer, when *in-situ* polymerisation was induced by the modification of the $Cr/Ti/SiO_2$ catalyst with TEAl. **Run 2** represents a polymerisation, which was performed with externally added 1-hexene with a regular $Cr/Ti/SiO_2$ catalyst.

Run	Cr (wt.%)	Ti (wt.%)	Externally added 1-hexane (wt.%)	Al/Cr ratio	T (K)	H_2 (NL)
1	0.5	3.9	0	2	373	5
2	0.5	3.9	0.6	0	370	0

2.2.4 GPC-IR analysis of the synthesised polyethylene materials

Molecular weight distribution (MWD) of the PEs produced inside the semi-batch reactor was measured on a Polymer Char's GPC-IR instrument with an infrared IR5 detector with thermoelectrically cooled MCT sensor in order to obtain the MWD

curve and short-chain branching distribution (SCBD) within the MWD.[24] The sample preparation included only weighing of the samples (8 cm^3) into the vials, which were filled automatically with trichlorobenzene (TCB) as solvent stabilised with 300 *ppm* of 2,6-di-*tert*-butyl-4-methylphenol (BHT). In order to prevent the polymer samples from being degraded, the vials were kept in a high temperature oven just until the PE was dissolved. After dissolution, the polymer samples were automatically filtered using an in-line filter and 0.2 cm^3 of the polymer solution was injected into the 13 μm GPC columns. The injection time was 55 *min* with a flow rate of 1 $cm^3 min^{-1}$.

All calculations were performed using the GPC One software. MWD and molecular averages are based on a conventional calibration curve made with narrow polystyrene standards. To transform PS values into PE values, a factor Q using a PE as standard was applied. Ethylene-octene co-polymer metallocene-based standards have been used to calibrate the branching content in the IR detector. Short-chain branches per 1000 total carbon (SCB/1000TC) were calculated by subtracting the number of methyl end groups per 1000 TC assuming the absence of vinyl chain ends.

2.2.5 ^{13}C NMR analysis of the synthesised polyethylene materials

Preparation of the PE samples produced inside the 4 *L* semi-batch polymerisation reactor included dissolving 220 *mg* of polymer in 2 cm^3 1,2,4-trichlorobenzene (TCB, 99% spectroscopic grade, Sigma-Aldrich) at 408 *K* with occasional agitation to homogenise the sample, followed by the addition of 0.5 cm^3 hexadeuterobenzene (HDB, spectroscopic grade, Sigma-Aldrich) and 1 or 2 drops of hexamethyldisiloxane (HMDS, 99.5+%).

Proton decoupled ^{13}C NMR spectra were recorded on a Bruker Avance III 500 *MHz* (125.76 *MHz*, 90 ° pulse, 30 *s* delay between pulses, 240 scans, 1.29 *s* acquisition time) with a 10 *mm* cryoprobe at 403 *K* and an inverse-gated pulse sequence to avoid NOE effect. Gaussian multiplication (lb = -0.2 and gb = 0.02) was performed before Fourier-transform. The chemical shifts are referenced to the signal of the internal standard HMDS, with the assigned value of 2.03 *ppm*.

2.2.6 DRIFT spectroscopy during ethylene polymerisation

Diffuse reflectance infrared Fourier-transform (DRIFT) spectroscopy experiments of the Phillips-type $Cr/Ti/SiO_2$ catalyst were performed *in-situ* under controlled atmosphere. The catalyst samples were loaded under inert argon atmosphere into a Praying Mantis High Temperature Reaction Chamber preventing any poisoning by atmospheric oxygen and water. The FT-IR spectra were measured on a Bruker Tensor 37 spectrometer, with a liquid nitrogen-cooled MCT detector, in the spectral range

of 600–4000 cm^{-1} with a 4 cm^{-1} resolution and 32 *s* scan time. All ethylene polymerisation reactions were performed at 373 *K* and 1 *bar*. Lowering the partial pressure of ethylene, compared to the industrial conditions (20-50 *bar*, ***Table 1.1***), helped to avoid saturation of the overall FT-IR signal as well as of the overlapping FT-IR bands of the gaseous reactant, *i.e.* ethylene, with the CH_x stretching bands of the PE formed. As co-catalyst, 0.01 cm^3 of 1.3 *M* solution of TEAl in heptane (~94 *wt.%* TEAl, with ~6 *wt.%* predominately tri-*n*-butylaluminium and less than 0.1 *wt.%* triisobutylaluminium (TIBAl) residue, Acros Organics) was used, which was injected through a silicon septum for an Al:Cr ratio of 2:1. The obtained co-catalyst/heptane mixture was evaporated into the nitrogen stream and let to pre-react with the catalyst by flowing through the catalyst bed, before the feed of the actual ethylene reaction mixture. The excess heptane solvent was flushed off with nitrogen. Only after this step, the reactant mixture consisting of 45 *vol.%* N_2, 45 *vol.%* C_2H_4 and 10 *vol.%* H_2 was fed into the DRIFTS cell for the total flow of 10 $cm^3\ min^{-1}$. All gases were provided by Linde with the following purities N_2 (99.999%), H_2 (99.999%) and C_2H_4 (99.95%). The FT-IR data were analysed with the OPUS Spectroscopy Software. All spectra were normalised to the silica Si-O framework bands in the 1750–2100 cm^{-1} spectral region. The spectral region below 1400 cm^{-1} was not presented due to the high absorption of the Si-O bands of the silica support.

2.2.7 Gas chromatography analysis of the gas phase

The gas phase during the polymerisation of ethylene inside a quartz reactor under the same experimental conditions, as described in ***Section 2.2.6,*** with approximately 300 *mg* of Phillips-type Cr/SiO_2 and $Cr/Ti/SiO_2$ catalysts was continuously collected into 1 dm^3 Sigma-Aldrich Tedlar gas-sampling bags. After reaction, GC analysis of the gas phase was performed on a Varian 430-GC Gas Chromatograph with a FID detector with a VF-5ms column by manual injection of 1 cm^3 of the gas phase using a 1 cm^3 gas-tight GC syringe. Column flow was set at 1 $cm^3\ min^{-1}$ and column temperature kept at 305 *K* during the whole analysis. A calibration curve was made by the dilution of a reference light hydrocarbon gas mixture (Linde Gas), with nitrogen.

2.2.8 SEM-EDX studies on fresh and polymerising catalyst particles

Scanning electron microscopy (SEM) analysis was performed on a FEI company XL30SFEG SEM microscope equipped with an EDAX energy dispersive X-ray (EDX) analyser for elemental analysis. The catalyst samples and the obtained products after ethylene polymerisation within the DRIFTS cell were sprinkled on an aluminium plate covered with a carbon tape, sputter coated with a 10 *nm* layer of platinum in the

Cressington sputter coater 208HR with Cressington thickness controller MTM20, loaded into the sample holder and placed into the apparatus. The acceleration voltage of the electron beam was set to 10–15 *keV*. Several different particles of catalyst material and PE product were analysed by EDX over 4–5 different points and concentrations of the elements were averaged.

2.2.9 UV-Vis-NIR diffuse reflectance spectroscopy

UV-Vis-NIR diffuse reflectance spectroscopy (UV-Vis-NIR DRS) measurements of the fresh Cr/Ti/SiO_2 catalyst, TEAl-modified Cr/Ti/SiO_2 catalyst prior to the ethylene feed and Cr/Ti/SiO_2 catalyst after polymerisation reaction (containing PE) were performed in a home-made sealable quartz cell with a Varian Cary 500 Scan spectrophotometer equipped with a DRS accessory. For each measurement the cell was filled inside an argon glove box, therefore keeping the samples from the contact with air. The spectra were measured against a halon white standard in the 4000–45 000 cm^{-1} range, 33 *ms* data point scan time and spectral resolution of 17 cm^{-1} and 7 cm^{-1} in 12 500–45 000 cm^{-1} and 4000–12 500 cm^{-1}, respectively. Two artefacts in the measured spectra were corrected for the detector/grating and light source changeovers at 12 500 cm^{-1} and 28 570 cm^{-1}, respectively, while the spectral feature appearing at 11 250 cm^{-1} is due to an instrumental artefact.

2.2.10 Electron paramagnetic resonance

The fresh Cr/Ti/SiO_2 catalyst, TEAl-modified Cr/Ti/SiO_2 catalyst prior to the feed of ethylene and the Cr/Ti/SiO_2 catalyst after polymerisation reaction (containing PE) were analysed in sealable J-Young quartz EPR tubes with a diameter of 5 *mm*, which were filled inside a glove box. The electron paramagnetic resonance (EPR) spectra were recorded at 100 *K* with an X-band Bruker EMXPlus spectrometer equipped with an EMX Standard Cavity. The microwave frequency was set to ~9.43 *GHz* at a microwave power of 2 *mW*. The spectrometer settings involved 70 *mT* sweep width with 350 *mT* centre field and a field modulation amplitude of 0.2 *mT* or 600 *mT* sweep width with 300 *mT* centre field and a field modulation amplitude of 0.5 *mT*. Furthermore, to rule out a possible reduction of Ti^{4+} species inside the Cr/Ti/SiO_2 catalyst by TEAl, EPR experiments of the bare TiO_2/SiO_2 material before and after modification with TEAl were performed under the same conditions.

Simulations of the measured EPR spectra were performed with the EasySpin software,[25] using the function "pepper" for solid-state EPR and taking into account an anisotropic broadening (*i.e.*, A and g strain). The Blueprint XAS toolbox (initially developed for other purposes) was used as graphical interface of EasySpin,[26] to opti-

mise parameters for each species that compose the simulation, since it enables visualisation of each spectral component, the sum of the simulation and the experimental EPR spectra simultaneously.

2.2.11 X-ray diffraction

In order to rule out the formation of TiO_2 crystallites after the titanation and activation of the $Cr/Ti/SiO_2$ catalyst in dry air, an XRD analysis of the activated $Cr/Ti/SiO_2$ catalyst was performed with a Bruker-AXS D2 Phaser powder X-Ray diffractometer using a Co k$\alpha_{1,2}$ source with $\lambda = 1.79026$ *Å*. Measurements of the small-angle pattern were carried out between 1.5 and 5 ° 2θ using a step size of 0.022 ° 2θ and a step time of 33 *s*. A wide-angle XRD pattern was acquired between 20 and 80 ° 2θ using a step size of 0.022 ° 2θ and a step time of 13.2 *s*. Furthermore, in order to resolve better the diffractions coming from 100% titania, the analysis was performed in the 25 to 35 ° 2θ range with a high step time of 1320 *s*.

2.2.12 Scanning transmission X-ray microscopy

Sample preparation for the scanning transmission X-ray microscopy (STXM) experiments included the embedding of ***(a)*** the Phillips-type $Cr/Ti/SiO_2$ catalyst and ***(b)*** the PE product formed after the polymerisation in the DRIFTS cell with the Phillips-type $Cr/Ti/SiO_2$ catalyst treated with TEAl into an epoxy-based Struers Epofix Resin.

The third sample ***(c)*** used for STXM analysis to obtain an Al XAS-spectrum and the related spatial distribution was first prepared by wet impregnation of the activated Phillips-type $Cr/Ti/SiO_2$ catalyst for a nominal Al:Cr ratio of 2 with a 1.3 *M* heptane solution of TEAl diluted with 2-methyl pentane (analytical standard, > 99.5%, Sigma-Aldrich) dried over molecular sieves. The suspended catalyst was magnetically stirred for 3 *h*. All steps were performed under inert atmosphere inside the glove box, while the solvents were removed by heating at 323 *K* for 24 *h* in vacuum within a Schlenk line.

The catalyst samples ***(a)*** and ***(c)*** were ultra-microtomed into 300 *nm* slices, while the PE sample ***(b)*** was sectioned into 100 *nm* slices in order to avoid the saturation of the signal during the measurements at the C K-edge. The microtomed samples were placed onto Transmission Electron Microscopy (TEM) copper grids and as such used for the analysis. Due to the delicate sample preparation procedure, the three sets of samples had to be exposed to air prior to the STXM measurements.

The STXM experiments were performed at the Soft X-ray Spectromicroscopy (SM) 10ID-1 beamline of the Canadian Light Source (CLS) in Saskatoon, Canada, with a 40 *nm* zone plate. Several spectral ranges were examined depending on the ele-

ment *i.e.* C K-edge (280–320 *eV*), Ti $L_{2,3}$-edges (452–477 *eV*), O K-edge (525–580 *eV*), Cr $L_{2,3}$-edges (572–592 *eV*), Al K-edge (1550–1595 *eV*) and Si K-edge (1835–1860 *eV*). X-ray absorption spectroscopy (XAS) spectral image sequences were obtained by collecting a series of images over small energy increments in the range of several tenths of *eV* bellow and above an X-ray absorption edge of the examined element. The probed area of single particles was ~100 μm^2 with a spatial resolution of 50–100 *nm*, while the energy resolution varied from 0.1 *eV* around the absorption edge up to 1 *eV* at the pre-edge region where good energy resolution was not necessary in order to minimise the measuring time. The data was processed using the aXis2000 software package[27], which included the alignment of the spectral images and subtraction of the background spectrum after which the XAS spectra were obtained. The XAS spectra were integrated over the whole Phillips-type Cr/Ti/SiO_2 catalyst particle in the examined area in order to acquire better quality spectra of the element with the lowest loading *i.e.* Cr (0.98 *wt.%*) or the element with a higher absorption energy *i.e.* Si and Al due to the small thickness of the sample. By subtracting the pre-edge from the edge spectral image, it was possible to obtain the elemental map of each probed element.

2.3 RESULTS AND DISCUSSION

2.3.1 Industrial scale findings

The hypothetical explanation for the serendipitous finding at the ethylene polymerisation plant of the *in-situ* co-monomer generation was a contamination of the recycling feeds by TEAl, as there were several lines with a common recycling section. One of the polymerisation lines was running a Ziegler-Natta catalyst with TEAl as co-catalyst,[28,29] while the other polymerisation lines ran with a Cr/Ti/SiO_2 Phillips-type catalyst without any co-catalyst.

Further preliminary tests at both pilot and bench scales validated the *in-situ* generation of co-monomer when a Cr/Ti/SiO_2 catalyst and TEAl are used. The observed phenomena could be confirmed by performing slurry-phase ethylene polymerisation experiments in a 4 *L* semi-batch reactor. The polymerisation conditions were chosen to target the same MWD and co-monomer content in the polymer. Hence, 1-hexene was added in one experiment during the polymerisation when the Phillips Cr/Ti/SiO_2 catalyst under investigation was tested without TEAl, as no co-monomer was *in-situ* generated in that particular case. In the second experiment, *in-situ* oligomerisation was induced by modification of the catalyst with TEAl.

[TABLE 2.2]
Physical properties of the polyethylene product and ^{13}C NMR analysis of the short-chain branching of the polyethylene samples produced inside a semi-batch reactor. **Run 1** represents a polymerisation, which was performed without external addition of 1-hexene co-monomer, when *in-situ* polymerisation was induced by the modification of the $Cr/Ti/SiO_2$ catalyst with TEAl. **Run 2** represents a polymerisation, which was performed with externally added 1-hexene with a regular $Cr/Ti/SiO_2$ catalyst. Reaction conditions ***(Table 2.1)*** were chosen in order to achieve the same MWD and co-monomer content in the PE.

Run	Externally added 1-hexane (wt.%)	Olefin incorporation 1-butene (wt.%)	Olefin incorporation 1-hexene (wt.%)	1-octene (wt.%)	Productivity (g g_{cat}^{-1})	HLMI (g $10min^{-1}$)	Density (g cm^{-3})	Wax (wt.%)	Mw/Mn	Mz/Mw
1	0	0.1	0.7	-	1100	35.0	0.953	6.2	10.7	10.6
2	0.6	-	0.9	-	1000	41.1	0.955	5.0	12.6	12.8

The NMR analysis ***(Table 2.2*** and ***Figure 2.1)*** shows a similar amount of olefin incorporation, *i.e. wt.%* of olefin incorporated as short branching of the PE chain, for a catalyst when 1-hexene co-monomer was externally fed and for the catalyst that was modified by pre-contacting with TEAl and with the ethylene oligomers produced *in-situ*.

GPC-IR analysis of the polymers produced, as illustrated in ***Figure 2.2***, clearly shows that less co-monomer was incorporated in the short PE chains than in the long chains when it is generated *in-situ*. Consequently, this so-called "reverse" co-monomer incorporation‡ is enhanced when the co-monomer is generated *in-situ* in the presence of TEAl. This result came as a positive surprise as more co-monomer incorporated in the high molecular weight fraction of the polymer leads to better mechanical properties.[16]

Combined GPC-IR and ^{13}C NMR results have shown that it was possible to produce two different types of polymer with similar overall amount of branching, but with different SCBD. The increased amount of branching in the longer chains, achieved for the TEAl-modified catalyst, is a desired product feature from an industrial point of view as it leads to better mechanical properties.

‡ A co-polymer with reverse co-monomer incorporation shows an increasing *α*-olefin content with increasing co-polymer molecular weight, meaning a higher incorporation of *α*-olefin co-monomer into longer than into shorter polymer chains.[31]

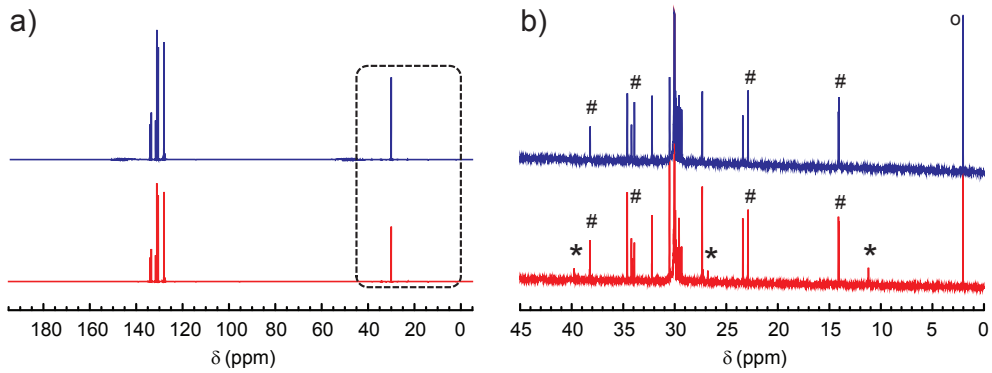

[FIGURE 2.1]
(a) ^{13}C NMR spectra of the polyethylene samples produced inside a semi-batch reactor. (red) Spectrum of the polyethylene produced when *in-situ* polymerisation was induced by modification of the $Cr/Ti/SiO_2$ catalyst with TEAl. (blue) Spectrum of the polyethylene produced with externally added 1-hexene co-monomer with a regular $Cr/Ti/SiO_2$ catalyst. **(b)** Enlarged region of the ^{13}C NMR spectra showing the chemical shifts of ethyl (*) and (#) butyl branches,[30] due to incorporation of 1-butene and 1-hexene, respectively. The chemical shifts are referenced to the signal of HMDS (°), which is assigned to 2.03 *ppm*.

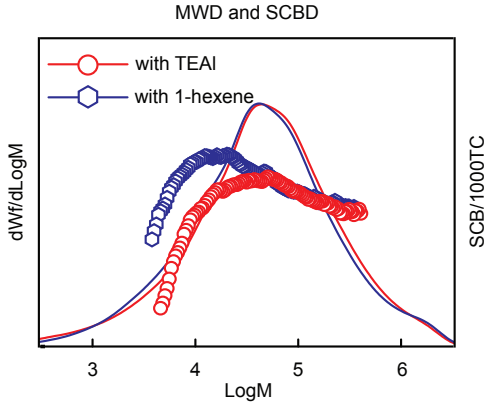

[FIGURE 2.2]
Molecular weight distribution (MWD) and short chain branching distribution (SCBD) of the polyethylene produced with the developed Phillips $Cr/Ti/SiO_2$ catalyst in a 4 *L* semi-batch reactor, with (blue) and without (red) externally added 1-hexene co-monomer. Reverse incorporation of co-monomer into longer polyethylene chains is boosted when co-monomer is *in-situ* generated, while the overall amount of incorporated olefins was kept similar as confirmed by ^{13}C NMR analysis.

2.3.2 Bulk spectroscopy characterisation

In a second series of experiments, the catalyst and its polymerisation behaviour were studied using *in-situ* DRIFT spectroscopy. The obtained DRIFT spectra measured as a function of time-on-stream for the $Cr/Ti/SiO_2$ catalyst are shown in ***Figure 2.3***.

The initial spectrum corresponds to a highly dehydroxylated catalyst as testified by the sharp silanol and titanol stretching bands located at ~3747 cm^{-1} and 3722 cm^{-1}, respectively. During the first 5 *min*, the injection of the TEAl co-catalyst in heptane, for a Al:Cr molar ratio of 2, can be observed by the initial increase of the methyl and methylene stretching bands of these compounds in the 2800–3000 cm^{-1} CH stretching region.[32–36] It must be noted that the addition of TEAl did not lead to a significant decrease of the silanol and titanol groups, suggesting that the added TEAl was also consumed for the reduction of Cr^{6+} to Cr^{2+}, Cr^{3+} and Cr^{5+} species,[37–46] for the transformation of a portion of the polymerisation into the oligomerisation active sites as well as for the scavenging of poisons.[1] Flushing of the excess heptane solvent revealed complex vibrational features of TEAl in the CH stretching region, suggesting alkylation of some of the Cr sites.

UV-Vis-NIR DRS measurements ***(Figure 2.4)*** of the catalyst at this point show that TEAl is inducing a small decrease in the intensity of mono- and polychromate $O\rightarrow Cr^{6+}$ CT bands at ~36 000 cm^{-1}, 28 000 cm^{-1} and 21 500 cm^{-1}, accompanied by the appearance of the d-d bands at ~16 000 cm^{-1} and 10 000 cm^{-1} due to the $^4A_{2g}\rightarrow{}^4T_{2g}$ transition of $Cr^{3+}{}_{Oh}$ and the $^5E_g\rightarrow{}^5T_{2g}$ transition of $Cr^{2+}{}_{Oh}$.[47,48] EPR spectra of Cr species on oxide supports are reported to show three distinct signals, that is, β, γ and δ.[49,50] EPR data ***(Figure 2.5)*** of the fresh catalyst shows only a γ-signal attributed to axially symmetric $[CrO_4]^{3-}$ species (with $g_{xx} = g_{yy} = 1.970$ and $g_{zz} = 1.890$). Besides the reduction of $Cr^{6+/5+}$, as testified by the appearance of a δ-signal from dispersed Cr^{3+} ions (g_{eff} ~3.7–6), reaction with TEAl is causing the appearance of new, axially symmetric ($g_{xx} = g_{yy} = 1.980$ and $g_{zz} = 1.915$) and rhombic Cr^{5+} species ($g_{xx} = 1.980$; $g_{yy} = 1.969$ and $g_{zz} = 1.922$).[49,50] Furthermore, TEAl is not reducing Ti^{4+} species as confirmed by the absence of the EPR signal belonging to the isolated Ti^{3+} ions ***(Figure 2.6)***.[51–53]

After removal of heptane, ethylene and hydrogen were fed into the DRIFTS cell followed by the immediate start of the polymerisation of ethylene. Characteristic PE C-H stretching and deformation vibrations show a rapid rise in the 2800–3000 cm^{-1} region and at 1460 cm^{-1}, respectively.[32–34] The intermolecular interaction of the growing PE chain with the silanol groups caused a decrease of the bands at ~3745 cm^{-1} and 3720 cm^{-1} and their broadening and red shift to respectively 3695 cm^{-1} and 3650 cm^{-1}. After reaction, the UV-Vis-NIR DRS spectrum shows a further increase of the d-d bands of chromium in lower oxidation states at the expense of $O\rightarrow Cr^{6+}$ CT bands.

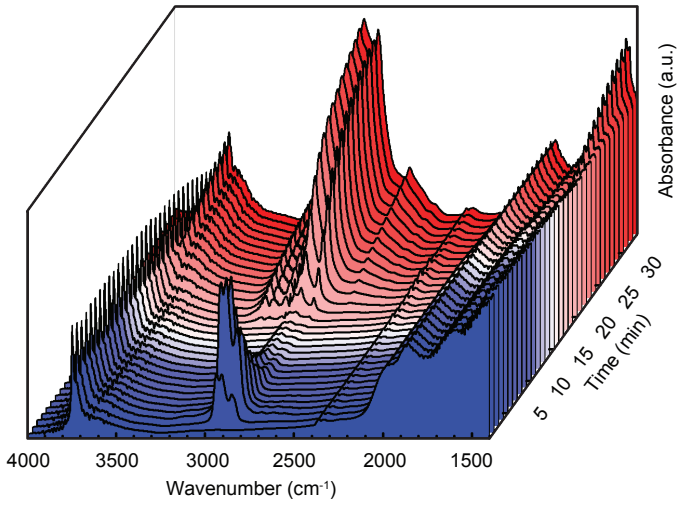

[FIGURE 2.3]
Time evolution of the DRIFT spectra of the $Cr/Ti/SiO_2$ Phillips catalyst under study in the ethylene polymerisation reaction measured at 373 *K* and 1 *bar*. The catalyst was pre-contacted with TEAl during the first 5 *min*, while the actual feed of the ethylene gas reactant mixture was started after 15 *min*. The first spectrum shows (blue) the activated catalyst, middle (grey) the modification with TEAl, while the last spectrum corresponds with the catalyst containing polyethylene (red). The samples at these stages were further examined by SEM-EDX, STXM, EPR and UV-Vis-NIR DRS.

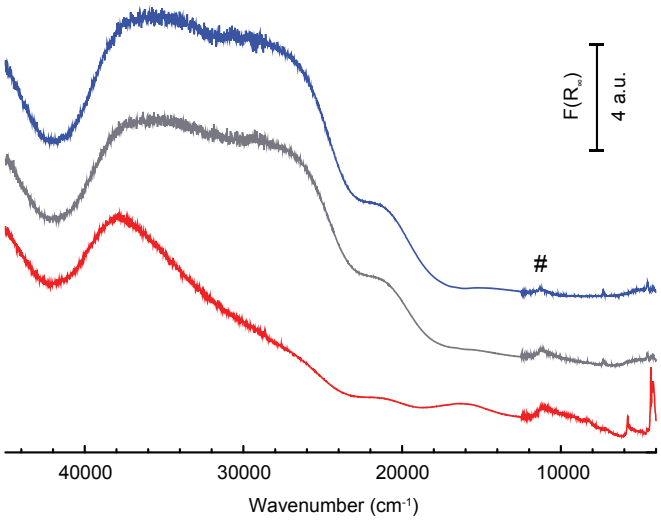

[FIGURE 2.4]
UV-Vis-NIR DRS spectra show reduction of mono- and polychromate species in the fresh catalyst (blue) by TEAl (grey) and ethylene (red). Instrumental artefact is marked with #.

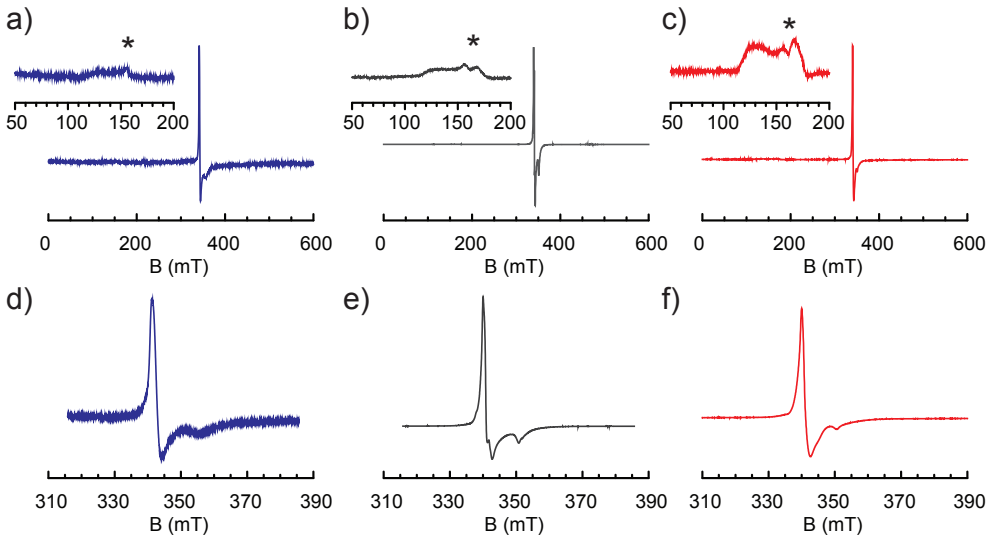

[FIGURE 2.5]
X-band EPR spectra of the fresh (blue), TEAl-modified (grey) and spent (red) Cr/Ti/SiO_2 catalyst. **(a)**, **(b)** and **(c)** show respectively *γ*-signals attributed to $[CrO_4]^{3-}$ species and *δ*-signal from monodispersed Cr^{3+} species dispersed on the Cr/Ti/SiO_2. Insets show magnified EPR spectra in the Cr^{3+} *δ*-signal range, while **(d)**, **(e)** and **(f)** show EPR spectra in the Cr^{5+} *γ*-signal range. It is important to note that the Fe^{3+} impurity is marked with *.

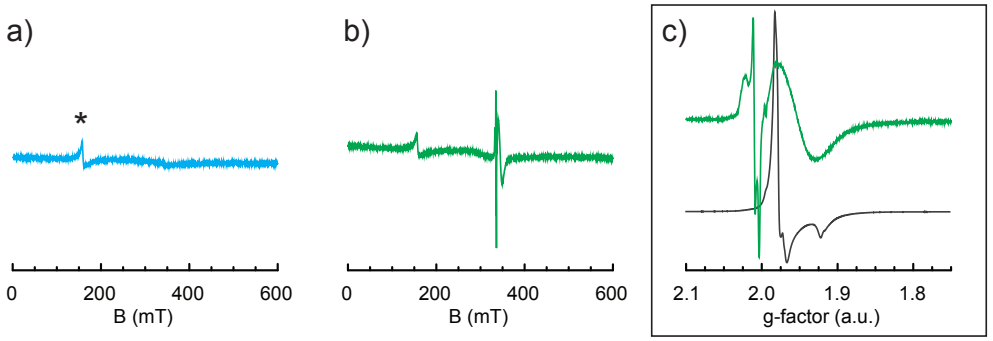

[FIGURE 2.6]
EPR spectra of the fresh **(a)** and TEAl-modified TiO_2/SiO_2 material **(b)** indicate a small reduction of Ti^{4+} species, testified by the appearance of signal of isolated Ti^{3+} ions (g_{xx} = 1.964, g_{yy} = 1.964 and g_{zz} = 1.917) and the formation of superoxide radical anions of type $Ti^{IV}(O_2^-)$ (g>2). It is important to note that the intensities are not substantially higher than the signal of Fe^{3+} impurity marked with *. The overlay **(c)** of the magnified signal of TEAl-modified TiO_2/SiO_2 material (green) and TEAl-modified Cr/Ti/SiO_2 Phillips-type catalyst (grey) shows the absence of the reduction of Ti^{4+} by TEAl inside the Cr/Ti/SiO_2 catalyst, confirming that the observed EPR signal belongs solely to the axially symmetric and rhombic Cr^{5+} species.

The EPR *δ*-signal assigned to dispersed Cr^{3+} species is even more pronounced, while the *γ*-signal shows a further distortion of the axially symmetric Cr^{5+} species, present after modification with TEAl, into new rhombic Cr^{5+} species (g_{xx} = 1.984; g_{yy} = 1.976 and g_{zz} = 1.950). Simulated EPR active species and related simulation parameters are tabulated in ***Tables 2.3*** and ***2.4***.

[TABLE 2.3]
Simulated EPR parameters for the different Cr^{5+} *γ*-signals observed in fresh **(A)**, TEAl-modified **(B** and **C)** and spent Cr/Ti/SiO_2 catalysts **(B'** and **C)**.

Signal	Species	Relative contribution (%)	g-factor			Sg		
			g_{xx}	g_{yy}	g_{zz}	Sg_{xx}	Sg_{yy}	Sg_{zz}
A	Axially symmetric	100	1.970	1.970	1.890	0.010	0.005	0.015
B	Axially symmetric	57	1.980	1.980	1.915	0.008	0.008	0.012
C	Rhombic	43	1.980	1.969	1.922	0.008	0.008	0.012
B'	Rhombic	46	1.984	1.976	1.950	0.010	0.012	0.019
C	rhombic	54	1.980	1.969	1.922	0.010	0.012	0.019

[TABLE 2.4]
Simulated EPR parameters for the signal of isolated Ti^{3+} ions and (O_2^-) superoxide radical anions detected in the TEAl-modified TiO_2/SiO_2 material.

Signal	Species	Relative contribution (%)	g-factor			Sg		
			g_{xx}	g_{yy}	g_{zz}	Sg_{xx}	Sg_{yy}	Sg_{zz}
Ti^{3+}	Axially symmetric	91	1.964	1.964	1.917	0.043	0.043	0.050
$(O_2^-)'$	Rhombic	3	2.004	2.010	2.021	0.003	0.003	0.003
$(O_2^-)''$	Rhombic	3	2.004	2.010	2.025	0.003	0.003	0.003
$(O_2^-)'''$	rhombic	3	2.004	2.010	2.028	0.003	0.003	0.003

2.3.3 SEM-EDX analysis

In order to investigate the morphology and chemical composition of the catalyst material and the PE product formed on the single particle level, SEM-EDX analysis was performed.

It is well-known that at the start of the ethylene polymerisation the reactants diffuse into the pores and the crevices of the polymerisation catalyst. During the propagation step, the growing polymer causes fragmentation of the catalyst particle. This fragmentation was evidenced by the SEM images of the fresh catalyst particles and the particles after polymerisation in the DRIFTS spectroscopy cell using the Phillips-type Cr/Ti/SiO_2 catalyst ***(Figure 2.7)***.[54–56] Due to the relatively mild ethylene partial pressure of 0.45 *bar*, the fragmentation of the catalyst particles was still at an early stage. However, the selection of these experimental conditions offered the unique opportunity to study the ethylene polymerisation process at the initial steps of the fragmentation of the catalyst material induced during the formation of PE before the catalyst particles were completely immersed in the produced PE and the diffusion of ethylene monomer into the catalyst particle core was suppressed.

Figure 2.7a and ***b*** present a couple of Phillips-type Cr/Ti/SiO_2 catalyst particles of ~70 *μm* in diameter. The catalyst particles are mostly of an irregular shape with many cracks and crevices ***(Figure 2.7a, b1*** and ***b2)***, which might be crucial in delivering the ethylene monomer to the active sites inside the catalyst body and on the other hand fragmentation of the catalyst particle by the increasing amount of PE formed. The manner of the fragmentation of the catalyst particle is very important from an industrial point of view since it affects the diffusion of ethylene, PE production rate, yield as well as the optical properties.[54] In the SEM images collected, after the polymerisation of ethylene in the DRIFTS cell at 373 *K* and *1* bar, PE can be clearly observed ***(Figure 2.7c-2.7f1)***. Moreover, due to the milder total pressure of 1 *bar* in comparison to several dozens of bar commonly used in industrial ethylene polymerisation, it is possible to visualise the initial stages of catalyst fragmentation. It is evident that not all catalyst particles were (already) active in the same way as can be concluded from the amount of the produced PE on some of the catalyst particles.

The chemical composition of the Phillips-type catalyst particles and PE formed, as measured by EDX, is presented in ***Table 2.5***. For this purpose, two different catalyst particles and two different PE particles have been examined. The oxygen-to-silicon ratio in the catalyst samples correspond to the ratio of these elements in the silica support. The titanium content is slightly higher than expected from the catalyst preparation. It has to be mentioned that the probed volume of the sample with the EDX analysis is ~1–2 *μm* in diameter from the surface of the material and therefore the Ti content increase could be explained by a higher amount of Ti in the Ti-rich

I) $Cr/Ti/SiO_2$ Phillips catalyst before ethylene polymerisation

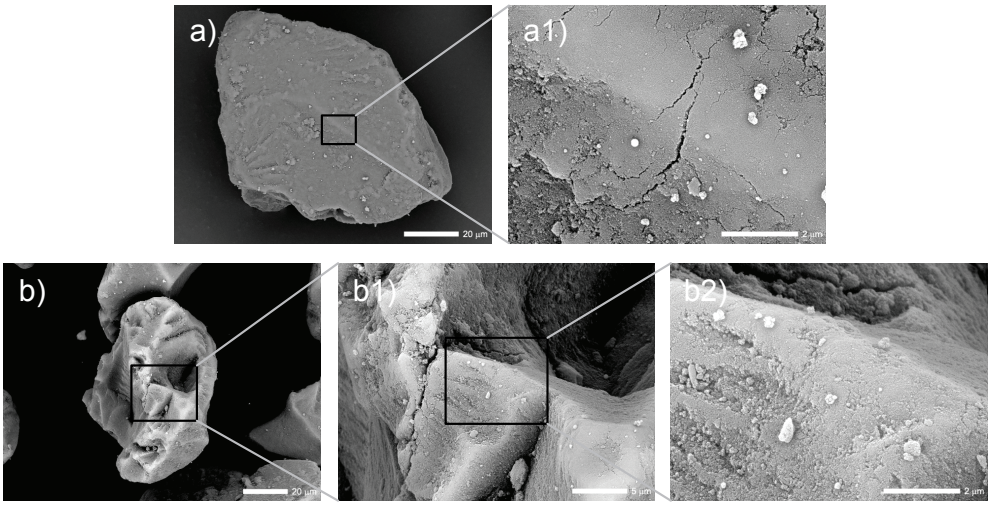

II) $Cr/Ti/SiO_2$ Phillips catalyst - polyethylene product after ethylene polymerisation

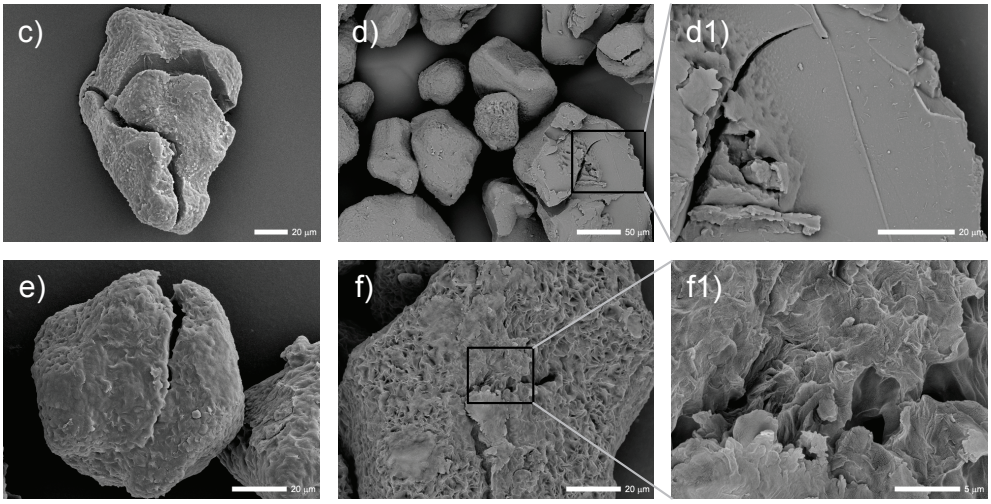

[FIGURE 2.7]
(I) SEM images of the Phillips $Cr/Ti/SiO_2$ catalyst before polymerisation of ethylene **(a)** and **(b)** with magnified images of the highlighted areas **(a1)**, **(b1)** and **(b2)**; **(II)** SEM images of the polyethylene/catalyst mixtures after the *in-situ* polymerisation of ethylene inside the *in-situ* DRIFTS cell at 373 *K* and 1 *bar*, with TEAl co-catalyst and gas mixture of 45 *vol.%* N_2, 45 *vol.%* C_2H_4 and 10 *vol.%* H_2 **(c)**, **(d)**, **(e)** and **(f)** with magnified images of the highlighted areas **(d1)** and **(f1)**; EDX elemental analysis was performed over several points in the regions of **(a)**, **(b1)**, **(d1)** and **(f)**.

[TABLE 2.5]
Elemental composition of two different Phillips-type Cr/Ti/SiO_2 catalyst particles (Cat' and Cat") and two different Cr/Ti/SiO_2 catalyst/polyethylene product particles (PE' and PE") obtained with the EDX analyser by averaging the composition at 4–5 different points.

Sample‡	Pt loading (wt.%)	C loading (wt.%)	Cr loading (wt.%)	Ti loading (wt.%)	O loading (wt.%)	Si loading (wt.%)
Cat' (a)	21	6	1	5	36	31
Cat" (b1)	34	3	1	7	30	26
PE' (d1)	6	68	1	0	15	10
PE" (f)	43	52	0	1	2	3

‡ The labels in the parenthesis correspond to the SEM images ***(Figure 2.7***) of the samples where the EDX analysis was performed.

shell of the catalyst particle. The amount of Ti in the areas probed by EDX can be estimated by excluding Pt from the mass balance, which gives the concentrations of 7 and 11 *wt.%* of Ti in the catalyst samples Cat' and Cat", respectively. The content of Cr has to be taken with caution due to the low concentration, detection limitation of the instrument and the overlapping of the Cr band with Ti and O bands in the X-ray spectra. After ethylene polymerisation, no Cr or Ti could be basically detected, and the main contribution in the X-ray spectra comes from the carbon of the PE, including the signal from the Pt coating ***(Figure 2.8)***. The Al K-edge originating from the addition of TEAl co-catalyst cannot been seen in the EDX spectra of the catalyst/PE

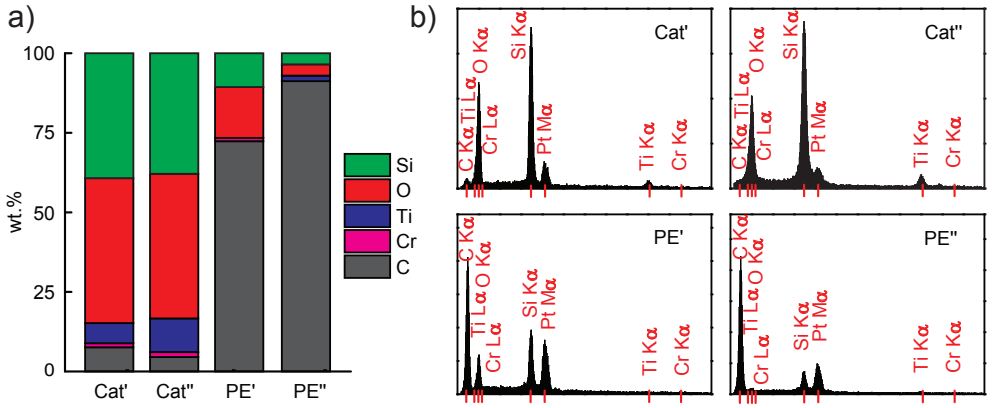

[FIGURE 2.8]
EDX analysis in a SEM instrument of the Phillips-type Cr/Ti/SiO_2 catalyst under study and the polyethylene product formed after the polymerisation in the DRIFTS cell at 373 *K* and 1 *bar*. **(a)** The elemental composition of the two different catalyst particles (Cat' and Cat") and the two polyethylene particles (PE' and PE") was averaged over 4–5 measurement points per sample. **(b)** The EDX spectra belong to one of the measurement points of each particle.

particle after ethylene polymerisation due to the fact of a too low amount of added TEAl through the gas lines by evaporation (aimed for an Al:Cr ratio of 2:1). It is important to mention that the small amounts of carbon present in the fresh catalyst, which has not yet been contacted with TEAl, originate from the carbon tape on which the particles were placed for the SEM analysis to improve the conductivity of a non-conductive silica-supported catalyst.

The acquired data offered the possibility to study the catalyst and the catalyst/PE particles at the micro- and nanoscale. In this respect, SEM-EDX was very useful for studying the morphology of the PE, the fragmentation of the catalyst particle and the related elemental analysis. Unfortunately, the nature of the EDX analysis and the overlapping of the bands of probed elements could not give any further information on the coordination, phase and oxidation state of the constituting elements of the catalyst particle.

2.3.4 Nanoscale chemical imaging

As DRIFTS, EPR and UV-Vis-NIR DRS are bulk techniques, which give only an averaged set of information over a large amount of material, it is important to call in another more local characterisation method. As a result, STXM was performed as this method is a less invasive technique than energy dispersive X-ray (EDX) analysis commonly attached to a SEM instrument with respect to the sensitive PE material. STXM offers nanoscale spatial information on the electronic and chemical structure of the catalyst and catalyst/polymer materials. ***Figure 2.9*** shows the X-ray absorption spectroscopy (XAS) spectra of all of the elements of the fresh Phillips Cr/Ti/SiO_2 catalyst, collected using soft X-rays in the range of 450–1860 *eV*. The Si K-edge XAS spectrum in the spectral range from 1835–1860 *eV* is indicative for T_d coordinated Si^{4+} present within the SiO_2 support. Regarding the O K-edge in the spectral region of 525–580 *eV*, it was possible to distinguish between the O K-edge XAS spectrum of SiO_2 and that of the epoxy resin, which was used for embedding the catalyst particle. Indeed, the O K-edge of SiO_2 shows a 1 *eV* blue shift to 538 *eV* and a higher post-edge feature at ~560 *eV*. Interestingly, the Ti $L_{2,3}$-edge XAS spectrum in the range of 452–477 *eV* shows separated L_3 and L_2 regions due to the spin-orbit coupling of Ti 2p core electrons. Compared to reference spectra,[35,57] it can be concluded that Ti^{4+} is in an O_h coordination.

Ti^{4+} does not belong to TiO_2 crystallites, but is a part of a mixed amorphous oxide support of titania-silica showing no ordering or crystalline phases, which is confirmed by XRD ***(Figure 2.10)***. The titanation procedure employed for the preparation of the catalyst materials included a reaction of TIP with a highly dehydrated pre-catalyst (*i.e.*, a Phillips-type Cr/SiO_2) in a way which prevented the formation

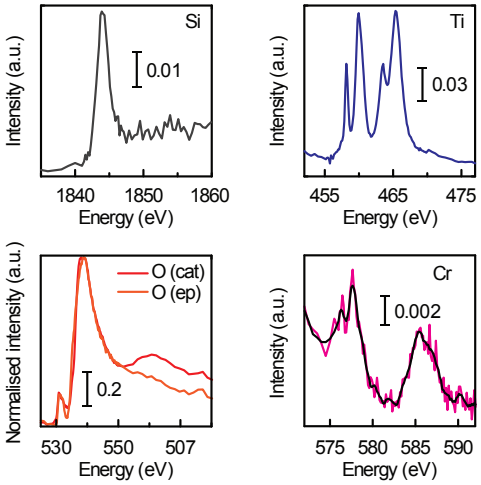

[FIGURE 2.9]
X-ray absorption spectroscopy (XAS) data of the chemical elements present in the fresh Phillips Cr/Ti/SiO_2 catalyst under study: Si K-edge (grey), Ti $L_{2,3}$-edge (blue), O K-edge from the SiO_2 support (red), O K-edge from the epoxy resin (orange) and Cr $L_{2,3}$-edge (magenta) with a smoothed spectrum (black). The spectra were integrated over the examined region of the entire catalyst particle for achieving the best signal-to-noise ratio.

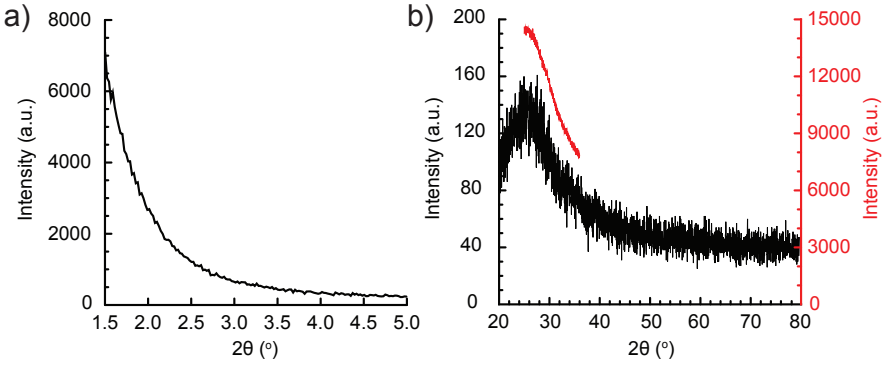

[FIGURE 2.10]
(a) The small-angle X-ray diffractogram of the fresh Cr/Ti/SiO_2 catalyst showing no ordering of the catalyst material. **(b)** Wide-angle X-ray diffractogram of the fresh Cr/Ti/SiO_2 catalyst showing only amorphous silica support (black) even for high accumulation times (red) for the angles were the 100%-peaks of TiO_2 are expected to appear.

of bulk TiO_2. Ti becomes chemically bonded to the pre-catalyst instead of the forming of TiO_2 crystallites on the catalyst surface. Therefore, the X-ray diffractograms show only an amorphous oxide support, although the size and amount of the TiO_2 crystallites could be too small to be detected with XRD. No ordering can be noted in the small-angle XRD diffractogram, while no TiO_2 crystallites were found in the wide-angle part of the diffractogram, even for the high step time in the 2θ range where 100% TiO_2 diffractions are expected. Due to the presented results, STXM, as an XAS technique, is critical for the characterisation of these types of materials since it is probing the local "short-range" structure and coordination of the examined elements, independent of the overall lack of crystallinity.

The most challenging aspect of the performed STXM study is the low Cr content of the Cr/Ti/SiO_2 Phillips catalyst. To the best of our knowledge, the first Cr $L_{2,3}$-edge XAS spectrum of Phillips-type catalyst using STXM is presented in ***Figure 2.9***. The spin orbit splitting of Cr causes distinct L_2 and L_3 regions in the spectral range of 572–592 *eV*. In comparison with the literature reference spectra,[58] it can be concluded that Cr is most probably in a distorted O_h state in the form of a dispersed Cr_2O_3-like phase. The oxidation number of the activated catalyst, calcined in dry O_2, is expected to be +6. Therefore, the lower oxidation state of 3+ can be explained by the exposure of the activated catalyst to air, water and epoxy resin during the required preparation procedure for the STXM measurements, where Cr^{6+} has been partially converted into Cr^{3+}.‡

Besides a detailed analysis of the measured XAS data, the STXM technique gives the opportunity of elemental mapping of a sample at the nanoscale. By subtracting a pre-edge image from the absorption edge spectral image it is possible to acquire an elemental map of each element under investigation. Using this procedure it was possible to obtain ***Figure 2.11a***, which shows the elemental distribution of a Phillips Cr/Ti/SiO_2 catalyst particle, including a chemical element overlay map ***(Figure 2.11b)***.

The STXM Si and O maps show the mesoporous structure, which can also be inferred from nitrogen physisorption data ***(Figure 2.12)*** of the catalyst material. Less than 1.5% of the total pore volume accounts for the volume of micropores therefore confirming that the catalyst material after the titanation and activation in dry air possesses mesopores. Furthermore, the absence of the sharp closure of the hysteresis

‡ The sample preparation for the STXM analysis is quite delicate and demanding, and certain steps could not be avoided. Although the obtained Cr does not completely reflect the Cr species of the activated catalyst, the nano-scale level distributions of elements, most importantly Cr, Ti and Al, were shown in this ***Thesis.*** The presence of Cr and Al (originating from TEAl) in the particle core, without Ti in their vicinity, is crucial to explain the *in-situ* ethylene oligomerisation and subsequent incorporation of oligomers over the sites making longer PE chains. It has to be acknowledged that Cr is indeed modified and therefore the additional UV-Vis-NIR DRS and EPR spectroscopic data and XRD analysis, discussed earlier in this ***Chapter***, were performed to complement the STXM analysis, in which it was able to manipulate the sample without exposing it to air.

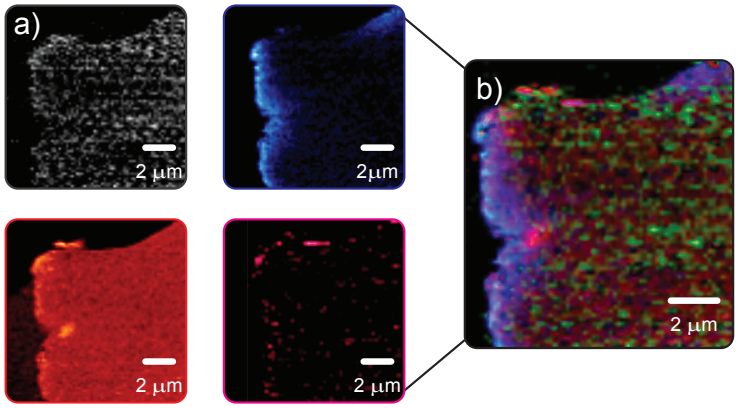

[FIGURE 2.11]
(a) Scanning transmission X-ray microscopy (STXM) elemental maps of Si (grey), Ti (blue), O (red) and Cr (magenta) inside the fresh Phillips Cr/Ti/SiO_2 catalyst particle with **(b)** an overlay of the STXM elemental maps.

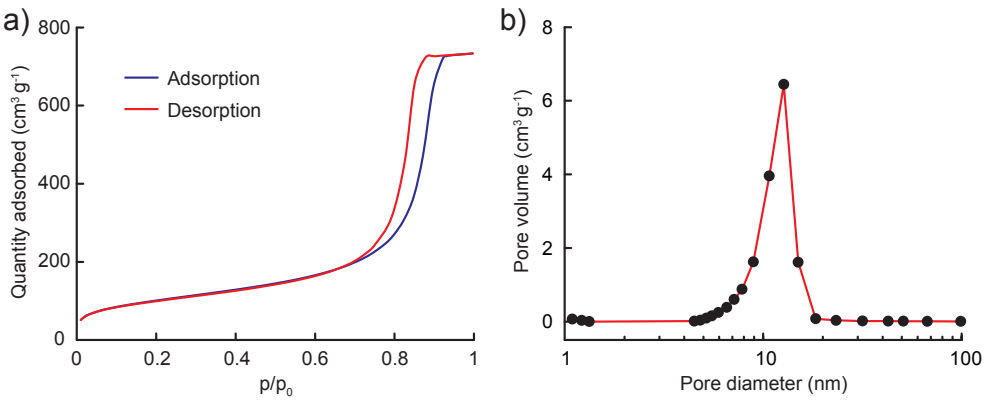

[FIGURE 2.12]
Adsorption/desorption curves **(a)** and pore size distribution **(b)** of the activated Cr/Ti/SiO_2 Phillips-type catalyst obtained using nitrogen physisorption. The titanation and activation at 1048 *K* in dry air of the commercial pre-catalyst lead to a material with the following properties: mean pore diameter of 12.4 *nm*, BET surface area of 367 $m^2\,g^{-1}$ and pore volume of 1.13 $cm^3\,g^{-1}$ of which only 0.0018 $cm^3\,g^{-1}$ belongs to the micropore volume.

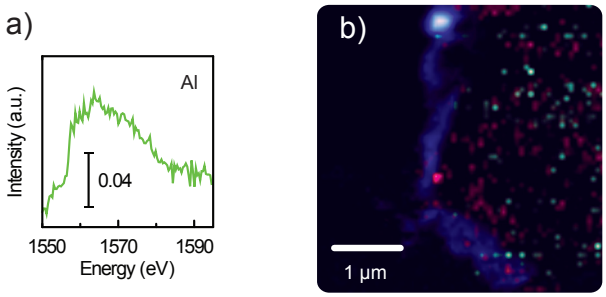

[FIGURE 2.13]
Al K-edge **(a)** and elemental maps **(b)** of Ti (blue), Cr (magenta) and Al (green) of the Cr/Ti/SiO_2 catalyst after the wet impregnation with TEAl for a nominal Al:Cr ratio of 1.

loop confirms that there are no cavity-like pores and that all mesopores in the tested catalyst material are open, which is crucial for the diffusion of TEAl as well as ethylene to the oligomerisation and polymerisation sites inside the catalyst particle.

The STXM Ti map shows that Ti species are mostly located at the surface of the Cr/Ti/SiO_2 catalyst particle forming a core-shell structure, which is in line with the applied preparation route and impregnation of the titanate ester. On the other hand, Cr species were found to be present more evenly throughout the whole catalyst particle. This non-uniform distribution of Ti and Cr is considered to be essential in the formation of at least two different types of active sites on a single particle, one mainly positioned in the Ti-abundant and the other one dominantly present in Ti-scarce catalyst particle regions, which are able to produce different types of PE. Moreover, the elemental map of the Cr/Ti/SiO_2 sample pre-treated with TEAl for the Al:Cr ratio of 1 ***(Figure 2.13)***, shows that Al is well-dispersed into the catalyst core, which indicates that ethylene oligomerisation sites are neighbouring the (Ti-scarce) ethylene polymerisation sites.

In order to evaluate this working hypothesis, a detailed STXM study was conducted on the Phillips Cr/Ti/SiO_2 catalyst after treating with the TEAl co-catalyst and ethylene feeding at 373 *K* and 1 *bar* in the *in-situ* DRIFTS cell. The overall XAS image of the catalyst/PE particle embedded in the epoxy resin, given in ***Figure 2.14a***, shows a clear start of the catalyst fragmentation process. In the STXM Ti map, presented in ***Figure 2.14b***, the Ti-abundant shell of the Phillips catalyst particles can still be seen with discontinuities in the cracks, which are filled with the produced PE.

As with the fresh Phillips Cr/Ti/SiO_2 catalyst, the XAS spectra of the Ti $L_{2,3}$- and Cr $L_{2,3}$-edges were measured and are shown in ***Figure 2.15***. After ethylene poly-

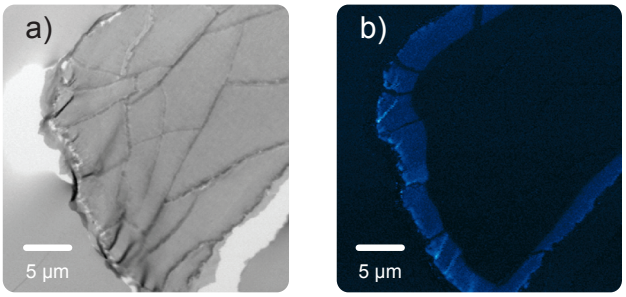

[FIGURE 2.14]
(a) The overall X-ray absorption spectroscopy (XAS) image and **(b)** STXM Ti map of the polyethylene/Cr/Ti/SiO_2 catalyst particle after the polymerisation of ethylene at 373 *K* and 1 *bar* in the DRIFTS cell shows the shell distribution of Ti and a clear start of the catalyst fragmentation process.

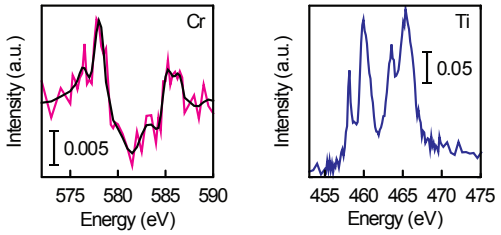

[FIGURE 2.15]
X-ray absorption spectroscopy (XAS) data of the Ti $L_{2,3}$-edge (blue) and Cr $L_{2,3}$-edge (magenta) with a smoothed spectrum (black) in the Cr/Ti/SiO_2 catalyst/polyethylene sample after the polymerisation of ethylene at 373 *K* and 1 *bar* inside the DRIFTS cell.

merisation, the Ti^{4+} remains O_h coordinated, while Cr species were still detectable after reaction since the Cr/Ti/SiO_2 catalyst fragments were not yet dispersed in the PE matrix due to the initial phase of the polymerisation and the related early stages of the fragmentation process. The XAS spectrum of the Cr $L_{2,3}$-edge shows that Cr is distorted O_h coordinated in the form of dispersed Cr_2O_3 phase.

One of the most interesting aspects of this study has been the investigation of the absorption edge of the carbon species of the catalyst/PE sample, probed in the energy range of 281–297 *eV*. Due to the distinctively different C K-edge XAS spectra it is possible to distinguish the carbon species of the produced PE and the epoxy resin used for sample preparation. ***Figure 2.16a*** shows the elemental maps of the Ti, Cr and C together with a map overlay in ***Figure 2.16b***. It was found that Ti remains located close to the surface of the catalyst particle except in the cracks of the fragmenting catalyst particle. In contrast, the Cr species are dispersed throughout the entire catalyst particle in the form of clusters, while the produced PE is detected both on the outer

surface of the catalyst particle and in the pores within the catalyst particle core with the highest optical density in the cracks of the fragmenting catalyst particle.

In order to investigate in detail the influence of the active polymerisation sites in the different regions within the catalyst particle, a more detailed analysis of the C K-edge in several parts of the particle has been performed. Two main different types of PE were detected, as shown in ***Figure 2.16c***. Besides the characteristic C1s→$\sigma^*_{C\text{-}H/Ryd}$ transitions at 287.5 *eV* and 288 *eV* of the CH_2 groups of PE species, inside the pores and the fragmentation cracks of the catalyst, the produced PE shows an absorption spectrum very similar to the spectrum of the reference polypropylene sample with a more distinct C1s→$\sigma^*_{C\text{-}C}$ transition band.[59–63] Furthermore, detailed analysis of the C1s→$\sigma^*_{C\text{-}H/Ryd}$ bands shows a small widening towards lower energies caused by the C1s→$\sigma^*_{C\text{-}H}$ transition at 285.1 *eV* of the CH_3 groups. These are the indications of the higher amount of branching of the PE induced by the co-polymerisation of the ethylene with the *in-situ* generated ethylene oligomers, such as 1-hexene, inside the confined space of the catalyst pores. Furthermore, low intensity band at 285.2 *eV* assigned to C1s→$\pi^*_{C=C}$ indicates the presence of olefin oligomers still adsorbed or trapped inside the catalyst.

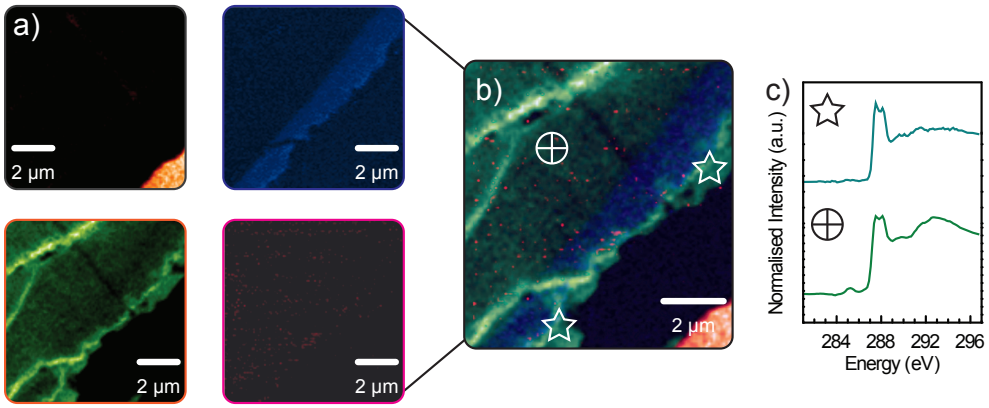

[FIGURE 2.16]
(a) Scanning transmission X-ray microscopy (STXM) elemental maps of the Phillips Cr/Ti/SiO_2 catalyst particle after ethylene polymerisation at 373 *K* and 1 *bar*. Carbon from the epoxy resin (orange), carbon from the polyethylene (green), Ti (blue) and Cr (purple). **(b)** An overlay of the STXM elemental maps. **(c)** XAS data of the C K-edge from the PE layer on the outer rim of the catalyst particle (top) and of the PE within the cracks of the inner core of the catalyst particle (bottom).

2.3.5 Gas chromatography

The *in-situ* production of olefins was also confirmed with the GC analysis of the gas phase after the polymerisation of ethylene using the Cr/SiO_2 and the examined $Cr/Ti/SiO_2$ Phillips type catalyst ***(Figure 2.17)***. The Ti-free Cr/SiO_2 catalyst, chemically similar to the Ti-scarce core of the $Cr/Ti/SiO_2$ catalyst particle analysed with STXM, is clearly able to produce a higher amount of olefins, with better selectivity towards 1-hexene, which on the other hand confirms the observed higher *in-situ* branching in the catalyst particle core. A detailed study of the influence of Ti on the selective oligomerisation of ethylene will be presented in ***Chapter 3***.

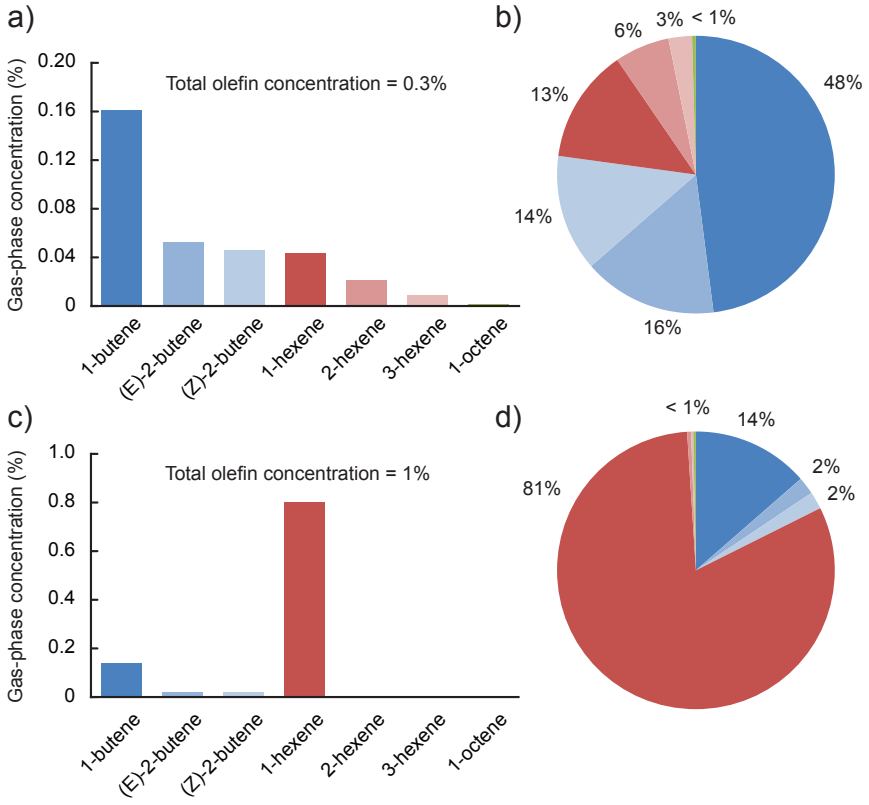

[FIGURE 2.17]
Gas phase concentrations of the olefinic products produced *in-situ* in the ethylene polymerisation reactions with **(a)** a $Cr/Ti/SiO_2$ and **(c)** a Cr/SiO_2 catalyst pre-contacted with TEAl. The relative ratio of olefinic species for both catalyst materials is given in the pie charts **(b)** and **(d)**. The Cr/SiO_2 catalyst pre-contacted with TEAl is producing more ethylene co-monomers than the $Cr/Ti/SiO_2$ catalyst; *i.e.*, 0.3 vs. 1%. Moreover, the olefin selectivity is clearly shifted towards the formation of 1-hexene when a non-titanated Phillips-type Cr/SiO_2 catalyst pre-contacted with TEAl is used.

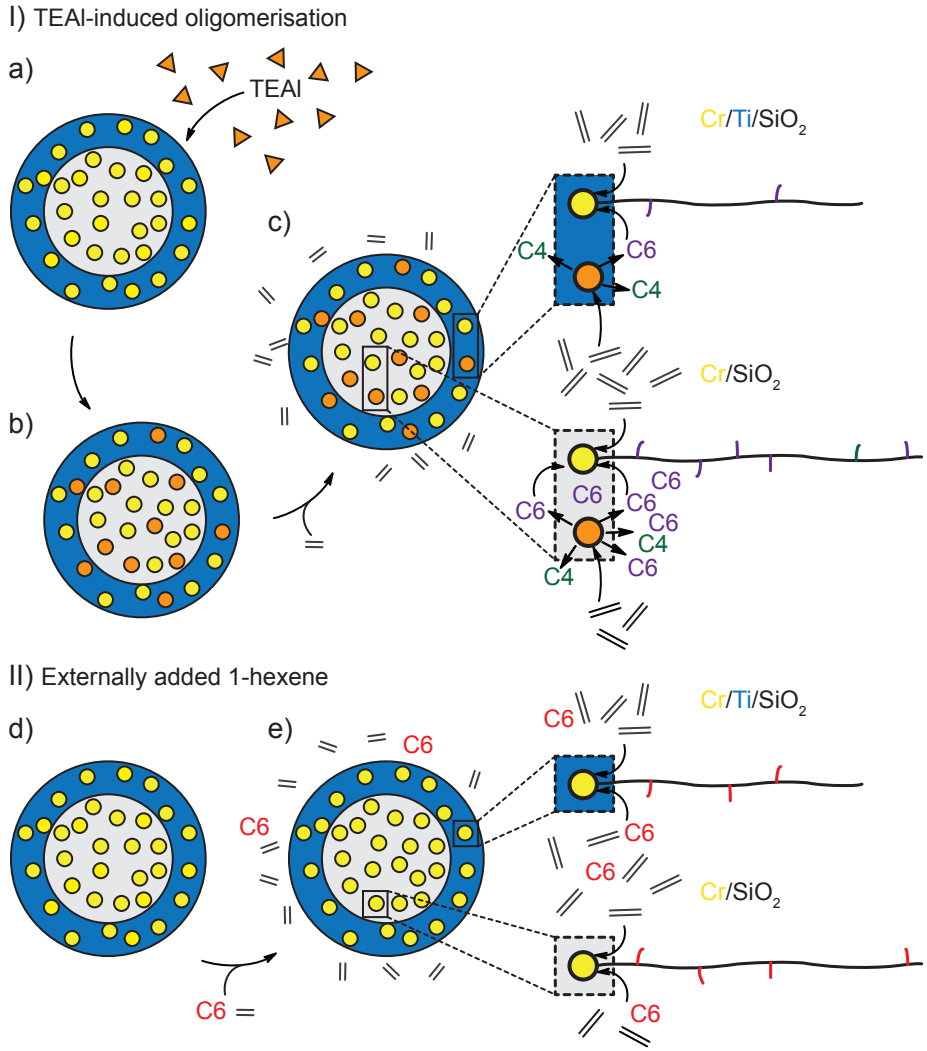

[FIGURE 2.18]
(I) Schematic representation of the polymerisation and oligomerisation active sites of a TEAl-modified shell-titanated Cr/Ti/SiO_2 Phillips-type catalyst. **(a)** TEAl (Δ) is transforming some of the Cr polymerisation sites (O) into **(b)** ethylene oligomerisation sites (O). **(c)** Oligomerisation sites within the Ti-rich particle shell are producing less oligomers, *i.e.* 1-hexene (C6) and 1-butene (C4). Therefore, near-by PE polymerisation sites that are making shorter chains in comparison to polymerisation active sites within the Ti-scarce particle core,[1] incorporate low amount of co-monomer. Oligomerisation sites within the Ti-scarce particle core are very efficient for the oligomerisation of ethylene, producing 1-hexene predominantly. Hence, PE polymerisation sites close-by, which are producing longer chains in comparison to polymerisation active sites close to Ti,[1] incorporate a higher amount co-monomer. This catalyst generates polyethylene with more co-monomer in the long chains, *i.e.* reverse co-monomer incorporation. **(II)** If 1-hexene is externally added into the reactor using a pristine Cr/Ti/SiO_2 catalyst **(d)**, co-monomer concentration is similar for all active sites, which leads to a typical Cr-based polyethylene with more co-monomer in short chains **(e)**.

2.4 CONCLUSIONS

A novel TEAl-modified Phillips Cr/Ti/SiO_2 ethylene polymerisation catalyst with two distinct active regions has been developed. STXM proved to be an indispensable method able to discriminate between the active sites producing low molecular weight linear chain and high molecular weight short-chain branched PE within a single Phillips catalyst particle.

It can be concluded that the active sites in the outer rim of the catalyst particle, containing predominantly both Ti and Cr, produce more linear type of PE with a lesser amount of branching than the core of the catalyst particle, which contains almost exclusively Cr. In this respect, it is important to mention that in the studies of the co-polymerisation of ethylene with linear alpha olefins, such as 1-hexene,[1] it is known that the presence of Ti on the Phillips catalyst tends to inhibit the incorporation of the co-monomer. Moreover, Ti could also inhibit co-monomer *in-situ* generation and lead to a more pronounced reverse co-monomer incorporation, as co-monomer will mainly be generated in Ti-scarce areas where longer chains are produced.

This observation is in line with our data as the two distinct regions of the Cr/Ti/SiO_2 catalyst particle clearly had different catalytic behaviour as the Ti-scarce active sites inside the core tend to induce the branching of the PE chain, while the Ti-rich active sites inside the shell of the catalyst particle give a more linear type of PE. This offers a clear experimental proof of the position of the active sites responsible for the *in-situ* oligomerisation of ethylene and the subsequent incorporation of the *in-situ* produced light olefins, such as 1-hexene, into the growing PE chain ***(Figure 2.18)***. It is anticipated that the two different types of PE produced by this bifunctional ethylene oligomerisation-polymerisation catalyst offer a clear perspective into advancing the production of an industrially important polyethylene with a simple Phillips-type catalyst from a single reactor system.

2.5 ACKNOWLEDGMENTS

Marjan Versluijs-Helder and Hans Meeldijk, both from Utrecht University (UU), are acknowledged or performing SEM-EDX and ultramicrotomy, respectively. The authors thank CLS for providing beamtime and the 10ID-1 beamline scientists and the UU team, including Mustafa al Samarai, Korneel Cats, Sam Kalirai and Ramon Oord, for help in acquiring the STXM data. Mario Delgado Jaime (UU) is acknowledged for the use of the Blueprint XAS program, Z. Öztürk (UU) for the XRD measurements, while Gerrit van Hauwermeiren and Julien Decrom (Total Research and Technology, Feluy) are acknowledged for the preparation of the catalyst materials.

2.6 REFERENCES

[1] M. P. McDaniel, *Adv. Catal.* **2010**, *53*, 123–606.

[2] E. Groppo, C. Lamberti, S. Bordiga, G. Spoto, A. Zecchina, *Chem. Rev*. **2005**, *105*, 115–184.

[3] B. M. Weckhuysen, R. A. Schoonheydt, *Catal. Today* **1999**, *51*, 215–221.

[4] A. Zecchina, E. Groppo, *Proc. R. Soc. A Math. Phys. Eng. Sci.* **2012**, *468*, 2087–2098.

[5] R. Cheng, Z. Liu, L. Zhong, X. He, P. Qiu, M. Terano, M. S. Eisen, S. L. Scott, B. Liu, *Adv. Polym. Sci.* **2013**, *257*, 135–202.

[6] D. S. McGuinness, N. W. Davies, J. Horne, I. Ivanov, *Organometallics* **2010**, *29*, 6111–6116.

[7] J. P. Hogan, R. L. Banks, US2825721, **1958**.

[8] J. P. Hogan, R. L. Banks, US2951816, **1960**.

[9] R. Cheng, C. Xu, Z. Liu, Q. Dong, X. He, Y. Fang, M. Terano, Y. Hu, T. J. Pullukat, B. Liu, *J. Catal.* **2010**, *273*, 103–115.

[10] T. J. Pullukat, R. E. Hoff, M. Shida, *J. Polym. Sci. Polym. Chem. Ed.* **1980**, *18*, 2857–2866.

[11] M. P. McDaniel, M. B. Welch, M. J. Dreiling, *J. Catal.* **1983**, *82*, 118–126.

[12] S. J. Conway, J. W. Falconer, C. H. Rochester, *J. Chem. Soc. Faraday Trans. 1* **1989**, *85*, 71–78.

[13] S. J. Conway, J. W. Falconer, C. H. Rochester, G. W. Downs, *J. Chem. Soc. Faraday Trans. 1* **1989**, *85*, 1841–1851.

[14] G. Debras, J.-P. Dath, EP0882743 B1, **1998**.

[15] P. J. Deslauriers, M. P. McDaniel, *J. Polym. Sci. Part A Polym. Chem.* **2007**, *45*, 3135–3149.

[16] L. L. Böhm, H. F. Enderle, M. Fleißner, *Adv. Mater.* **1992**, *4*, 234–238.

[17] C. Barzan, D. Gianolio, E. Groppo, C. Lamberti, V. Monteil, E. A. Quadrelli, S. Bordiga, *Chem. Eur. J.* **2013**, *19*, 17277–17282.

[18] F. M. F. de Groot, E. de Smit, M. M. van Schooneveld, L. R. Aramburo, B. M. Weckhuysen, *ChemPhysChem* **2010**, *11*, 951–962.

[19] A. M. Beale, S. D. M. Jacques, B. M. Weckhuysen, *Chem. Soc. Rev.* **2010**, *39*, 4656–4672.

[20] B. M. Weckhuysen, *Angew. Chem. Int. Ed.* **2009**, *48*, 4910–4943.

[21] I. L. C. Buurmans, B. M. Weckhuysen, *Nat. Chem.* **2012**, *4*, 873–886.

[22] S. Brunauer, P. H. Emmett, E. Teller, *J. Am. Chem. Soc.* **1938**, *60*, 309–319.

[23] E. P. Barrett, L. G. Joyner, P. P. Halenda, *J. Am. Chem. Soc.* **1951**, *73*, 373–380.

[24] B. Monrabal, J. Sancho-Tello, J. Montesinos, R. Tarín, A. Ortín, P. del Hierro, M. Bas, "High Temperature Gel Permeation Chromatograph (GPS/SEC) with integrated IR5 MCT detector for Polyolefin Analysis: a breakthrough in sensitivity and automation". Published at *The Applications Book (LCGC) Europe and North America*, **2012** (Application Note by Polymer Char, http://www.polymerchar.com/application_notes).

[25] S. Stoll, A. Schweiger, *J. Magn. Reson.* **2006**, *178*, 42–55.

[26] M. U. Delgado-Jaime, C. P. Mewis, P. Kennepohl, *J. Synchrotron Radiat.* **2010**, *17*, 132–137.

[27] A. P. Hitchcock, "aXis 2000," can be found under http://unicorn.mcmaster.ca/aXis2000.html, **1997**.

[28] G. Wilke, *Angew. Chem. Int. Ed.* **2003**, *42*, 5000–5008.

[29] L. L. Böhm, *Angew. Chem. Int. Ed*. **2003**, *42*, 5010–5030.

[30] G. B. Galland, R. F. de Souza, R. S. Mauler, F. F. Nunes, *Macromolecules* **1999**, *32*, 1620–1625.

[31] J. B. P. Soares, T. F. L. McKenna, *Polyolefin Reaction Engineering*, Wiley-VCH, Weinheim, **2012**, pp. 17–27.

[32] G. Socrates, *Infrared and Raman Characteristic Group Frequencies: Tables and Charts*, John Wiley & Sons Ltd, Chichester, **2004**, pp. 259–282.

[33] E. Groppo, C. Lamberti, S. Bordiga, G. Spoto, A. Zecchina, *J. Catal.* **2006**, *240*, 172–181.

[34] C. Lamberti, A. Zecchina, E. Groppo, S. Bordiga, *Chem. Soc. Rev.* **2010**, *39*, 4951–5001.

[35] P. Guttmann, C. Bittencourt, S. Rehbein, P. Umek, X. Ke, G. Van Tendeloo, C. P. Ewels, G. Schneider, *Nat. Photonics* **2011**, *6*, 25–29.

[36] C. N. Nenu, E. Groppo, C. Lamberti, A. M. Beale, T. Visser, A. Zecchina, B. M. Weckhuysen, *Angew. Chem. Int. Ed.* **2007**, *46*, 1465–1468.

[37] B. Liu, P. Šindelář, Y. Fang, K. Hasebe, M. Terano, *J. Mol. Catal. A Chem*. **2005**, *238*, 142–150.

[38] W. Xia, B. Liu, Y. Fang, K. Hasebe, M. Terano, *J. Mol. Catal. A Chem.* **2006**, *256*, 301–308.

[39] W. Xia, B. Liu, Y. Fang, T. Fujitani, T. Taniike, M. Terano, *Appl. Catal. A Gen*. **2010**, *389*, 186–194.

[40] J. H. Lunsford, S.-L. Fu, D. L. Myers, *J. Catal.* **1988**, *111*, 231–234.

[41] B. Rebenstorf, *J. Mol. Catal.* **1989**, *56*, 170–182.

[42] D. L. Myers, J. H. Lunsford, *J. Catal.* **1986**, *99*, 140–148.

[43] D. L. Myers, J. H. Lunsford, *J. Catal.* **1985**, *92*, 260–271.

[44] M. P. Conley, M. F. Delley, G. Siddiqi, G. Lapadula, S. Norsic, V. Monteil, O. V. Safonova, C. Copéret, *Angew. Chem. Int. Ed.* **2014**, *53*, 1872–1876.

[45] M. F. Delley, M. P. Conley, C. Copéret, *Catal. Lett*. **2014**, *144*, 805–808.

[46] M. F. Delley, F. Núñez-Zarur, M. P. Conley, A. Comas-Vives, G. Siddiqi, S. Norsic, V. Monteil, O. V. Safonova, C. Copéret, *Proc. Natl. Acad. Sci. U. S. A.* **2014**, *111*, 11624–11629.

[47] B. M. Weckhuysen, L. M. De Ridder, R. A. Schoonheydt, *J. Phys. Chem.* **1993**, *97*, 4756–4763.

[48] B. M. Weckhuysen, A. A. Verberckmoes, A. L. Buttiens, R. A. Schoonheydt, *J. Phys. Chem.* **1994**, *98*, 579–584.

[49] B. M. Weckhuysen, L. M. De Ridder, P. J. Grobet, R. A. Schoonheydt, *J. Phys. Chem.* **1995**, *99*, 320–326.

[50] B. M. Weckhuysen, R. A. Schoonheydt, F. E. Mabbs, D. Collison, *J. Chem. Soc. Faraday Trans.* **1996**, *92*, 2431–2436.

[51] M. Anpo, M. Che, B. Fubini, E. Garrone, *Top. Catal.* **1999**, *8*, 189–198.

[52] R. Bal, K. Chaudhari, D. Srinivas, S. Sivasanker, P. Ratnasamy, *J. Mol. Catal. A Chem.* **2000**, *162*, 199–207.

[53] K. Chaudhari, D. Srinivas, P. Ratnasamy, *J. Catal.* **2001**, *203*, 25–32.

[54] W. C. Conner, S. W. Webb, P. Spanne, K. W. Jones, *Macromolecules* **1990**, *23*, 4742–4747.

[55] K. W. Jones, P. Spanne, S. W. Webb, W. C. Conner, R. A. Beyerlein, W. J. Reagan, F. M. Dautzenberg, *Nucl. Instruments Methods Phys. Res.* **1991**, *B56/57*, 427–432.

[56] X. Zheng, M. Smit, J. C. Chadwick, J. Loos, *Macromolecules* **2005**, *38*, 4673–4678.

[57] F. M. F. de Groot, J. C. Fuggle, B. T. Thole, G. A. Sawatzky, *Phys. Rev. B* **1990**, *41*, 928–937.

[58] C. N. Nenu, J. N. J. van Lingen, F. M. F. de Groot, D. C. Koningsberger, B. M. Weckhuysen, *Chem. Eur. J.* **2006**, *12*, 4756–4763.

[59] H. W. Ade, A. P. Smith, G. R. Zhuang, J. Kirz, E. G. Rightor, A. P. Hitchcock, *J. Electron Spectros. Relat. Phenomena* **1996**, *84*, 53–72.

[60] O. Dhez, H. W. Ade, S. G. Urquhart, *J. Electron Spectros. Relat. Phenomena* **2003**, *128*, 85–96.

[61] S. G. Urquhart, A. P. Hitchcock, A. P. Smith, H. W. Ade, E. G. Rightor, *J. Phys. Chem. B* **1997**, *101*, 2267–2276.

[62] S. G. Urquhart, A. P. Hitchcock, A. P. Smith, H. W. Ade, W. Lidy, E. G. Rightor, G. E. Mitchell, *J. Electron Spectros. Relat. Phenomena* **1999**, *100*, 119–135.

[63] G. Hähner, *Chem. Soc. Rev.* **2006**, *35*, 1244–1255.

[This page is intentionally left blank]

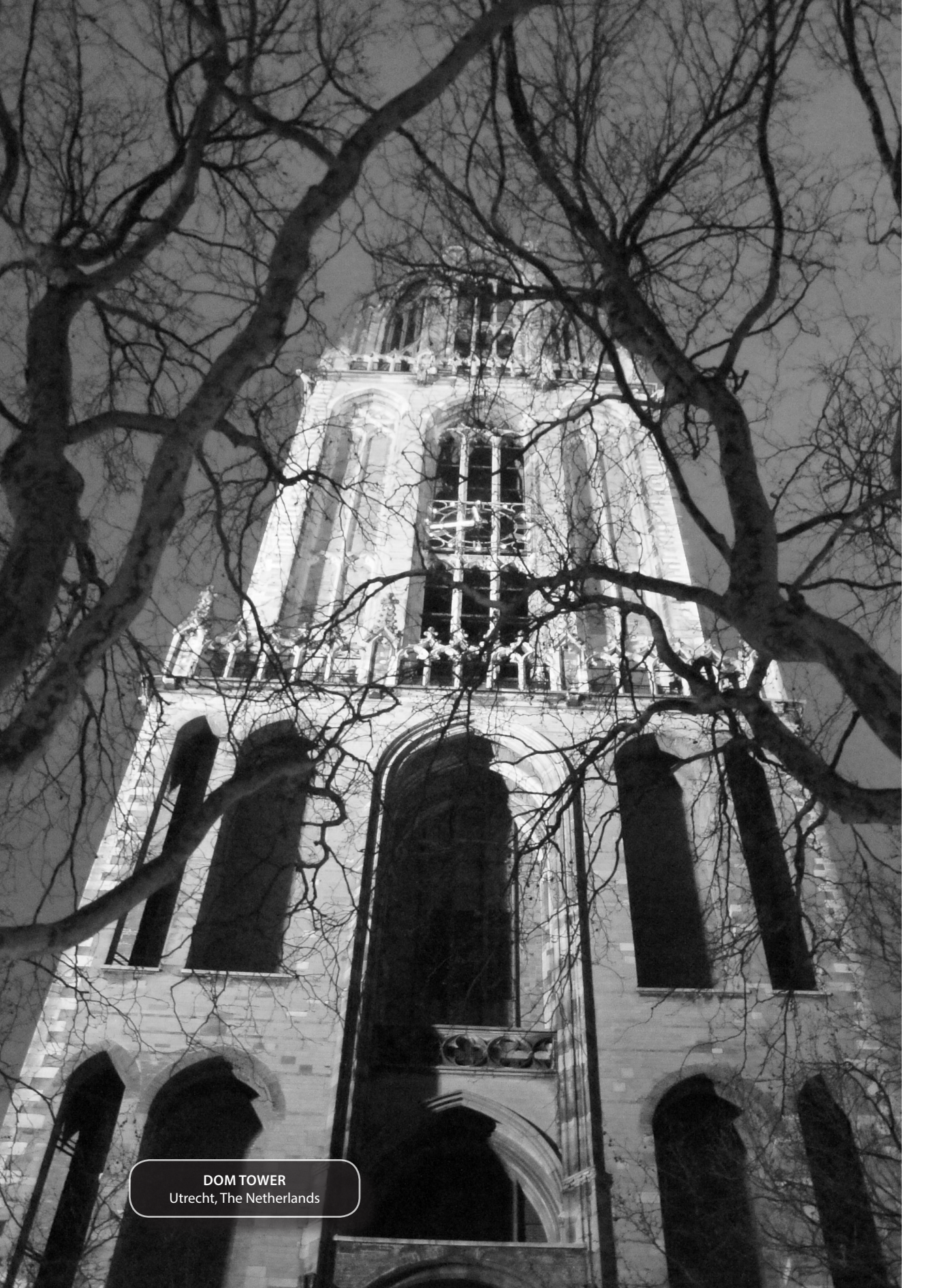

DOM TOWER
Utrecht, The Netherlands

III

Real-time Analysis of a Working $Cr/Ti/SiO_2$ Ethylene Polymerisation Catalyst with In-situ DRIFT Spectroscopy

The spectroscopic characterisation of Phillips-type catalysts, in powder form and under high-pressure conditions (20-50 *bar*) that are used in the industrial polymerisation of ethylene, is rather challenging. Infrared spectroscopy studies performed so far included mostly "model" systems of the pre-reduced catalyst at low reaction temperatures and pressures. In this ***Chapter***, a diffuse reflectance infrared Fourier-transform (DRIFT) study conducted at 373 *K* and 1 *bar* revealed a highly promoting effect of the titanium-based modifier on the industrial $Cr/Ti/SiO_2$ Phillips-type catalyst with triethylaluminium (TEAl) as co-catalyst on the reaction rate of the polymerisation of ethylene, which was monitored by the increase of the methylene stretching band of the growing polyethylene (PE). By varying the titanium content inside the catalyst the acidity of the surface hydroxyl groups could be altered. The increase of Ti loading causes the appearance of more acidic hydroxyl groups, which modify the Cr polymerisation sites, ultimately shortening the induction time and increasing the initial polymerisation rate. After an initial period of mixed kinetics, the propagation of the PE chains proceeds as a pseudo-zero order reaction with the reaction rate constantly increasing with increasing titanium loading. Furthermore, the assignment of the 3610 cm^{-1} band was clarified and attributed to the stretching vibration of bridging titanol groups.

BASED ON:
"Real-time Analysis of a Working $Cr/Ti/SiO_2$ Ethylene Polymerisation Catalyst with *In-situ* DRIFT Spectroscopy", D. Cicmil, J. Meeuwissen, A. Vantomme and B. M. Weckhuysen, *in preparation*.

3.1 INTRODUCTION

The ability of the Phillips catalyst[1–5] to polymerise ethylene without the intervention of any activator that would introduce an initial alkyl ligand, from which the polyethylene (PE) chain could grow, makes it rather different from Ziegler-Natta[6–9] and metallocene catalysts.[10–13] In order for ethylene polymerisation to start, Cr^{6+} species of the activated catalyst need to be reduced to Cr species in lower oxidation states, while the redox products (*i.e.* aldehydes and ketones)[14] should desorb from the coordination sphere of Cr. Subsequently, a hydride or an alkyl ligand has to be formed where a monomer can be inserted. Without the presence of any alkylating agents, these roles have to be performed by the ethylene monomer and are the cause of the reported induction period before the start of the ethylene polymerisation.

These silica-supported chromium catalysts for the polymerisation of ethylene have been extensively studied with infrared (IR) spectroscopy[15-17] in order to elucidate the nature of chromium polymerisation sites.[4,8,19] Most of the research included studies of model catalysts, where the main Cr species of the activated catalyst, *i.e.* Cr^{6+}, are reduced with CO to Cr^{2+} species, which are suspected to be the active ethylene polymerisation sites by the majority of researchers.[20] The catalyst in this form is afterwards examined with different probe molecules including CO, NO and ethylene itself, in time-, temperature- and pressure-resolved experiments.[21] In order to study this highly active system, temperatures and pressures are often set to very low values, *i.e.* 77 K and under vacuum, which are needed in order to freeze possible reaction intermediates or examine the adsorption and desorption of probe molecules.[13,22-24] The experiments showed a high heterogeneity of Cr^{2+} sites, classified into three families *i.e.* Cr_A^{2+}, Cr_B^{2+} and Cr_C^{2+}, with respect to their ability to coordinate probe molecules (A > B > C). The exact initiation mechanism has not yet been agreed on, except that the initiation step follows ethylene coordination on Cr^{2+} *via* formation of d-π complexes.[4,25] It is for these reasons that the kinetic studies of ethylene polymerisation using the Phillips-type catalysts are rather difficult to perform.

This ***Chapter*** focuses on a DRIFTS characterisation study of the Phillips-type catalyst in its activated form, without the pre-reduction of Cr^{6+} species, in order to elucidate the influence of the titanium modification and use of TEAl as co-catalyst on the ethylene polymerisation kinetics over both Cr/SiO_2 and $Cr/Ti/SiO_2$ Phillips-type catalysts.

3.2 EXPERIMENTAL METHODS

3.2.1 Sample preparation

The catalyst samples were provided by Total Research and Technology Feluy, Belgium. A silica pre-catalyst with ~0.5 *wt.%* Cr loading, surface area of 318 $m^2 g^{-1}$, pore volume of 1.55 $cm^3 g^{-1}$ and D50 particle size diameter of 47 μm was heated to 543 *K* for dehydration under a nitrogen flow. Surface titanation of the samples with a target Ti loading of 2 *wt.%* and 4 *wt.%* was performed using titanium isopropoxide (99.999 % trace metals basis, Sigma-Aldrich) added dropwise to the fluidised bed, following the method described in Debras *et al.*[26] The catalyst was subsequently activated at 1048 *K* in dry air to anchor and stabilise Cr^{6+} on the support and burn off organic groups. After the activation step, the catalyst was transferred to an Ar glove box under inert atmosphere. The sample containing Ti was prepared using a wide-pore silica support treated under the same procedure as the Cr pre-catalyst. The pure silica sample used as a reference included only calcination of Aerosil 300 at 1048 *K* in dry air. The prepared catalysts and their properties are summarised in ***Table 3.1***.

[TABLE 3.1]
Overview of the prepared Phillips-type ethylene polymerisation catalysts and support materials with their textual properties.

Sample name	Activation temperature (K)	Cr loading (wt.%)	Ti loading (wt.%)	Surface area ($m^2 g^{-1}$)	Pore volume ($cm^3 g^{-1}$)
S	1048	0	0	246	1.39
TS	1048	0	4.7	254	1.51
CS	1048	0.52	0	296	1.30
CTS1	1048	0.62	2.2	293	1.44
CTS2	1048	0.56	3.9	277	1.39

3.2.2 DRIFT spectroscopy

Ethylene polymerisation reactions were performed with a specially designed *in-situ* setup ***(Figure 3.1)***, under a controlled atmosphere inside a Praying Mantis High Temperature Reaction Chamber with ZnSe windows, while the catalyst and the PE product were studied with *in-situ* diffuse reflectance infrared Fourier-transform (DRIFT) spectroscopy. The catalyst samples were loaded inside an Ar glove box into the DRIFTS cell, preventing any contamination with moisture and oxygen, which

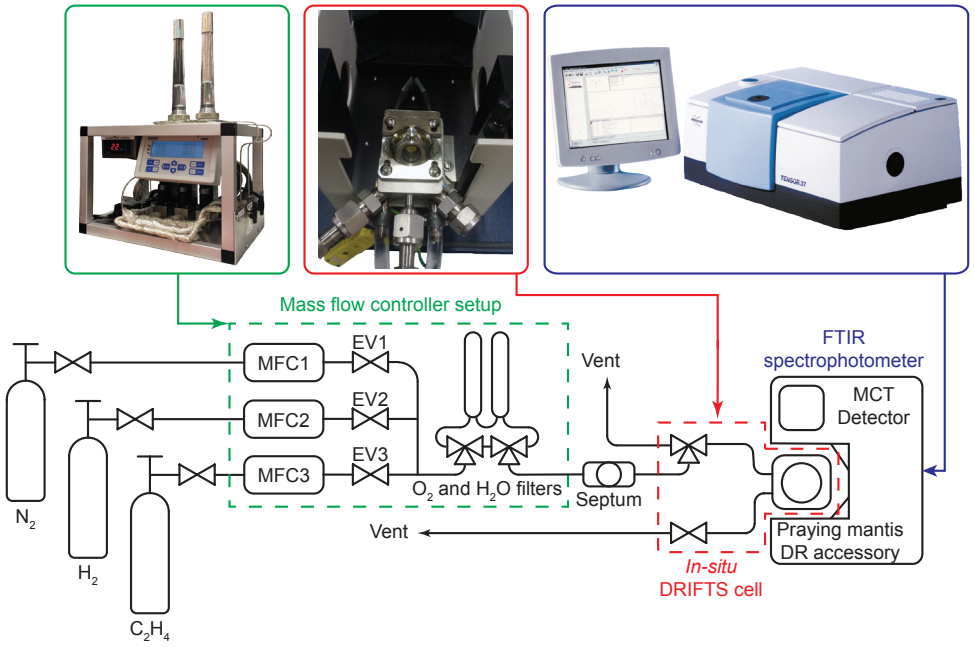

[FIGURE 3.1]
DRIFT spectroscopy setup developed for the testing of solid catalysts at 1 *bar* and temperatures in the range of RT to 1100 *K*. The *operando* setup includes changeable gas reactant sources, a mass flow controller setup (green), a septum for the injection of co-catalyst, a Praying Mantis High Temperature Reaction Chamber (red) and a Bruker Tensor 37 spectrophotometer (blue). All lines and the reactor are traced and heated to the desired reaction temperature as monitored by a number of thermocouples.

was placed in the Praying Mantis accessory on a Bruker Tensor 37 spectrometer with a liquid nitrogen-cooled MCT detector.

Two types of experiments were performed at 1 *bar* and 373 *K* using the gas reactant mixture consisting of 45 *vol.%* N_2, 45 *vol.%* C_2H_4 and 10 *vol.%* H_2, *i.e.* ethylene polymerisation with ***(a)*** the activated catalysts and ***(b)*** the catalysts pre-treated with a triethylaluminium (TEAl) co-catalyst. Modification with TEAl was performed by the injection of 5 μL of 1.3 *M* solution of TEAl in heptane (~94 *wt.%* TEAl, with ~6 *wt.%* predominately tri-*n*-butylaluminium and less than 0.1 *wt.%* triisobutylaluminium residue, Acros Organics) through a septum into the nitrogen stream, aiming for a nominal Al:Cr ratio of 2:1. After evaporation, the mixture was carried to the catalyst bed and allowed to react with the catalyst. The excess solvent was flushed away with nitrogen, leaving the TEAl-modified catalyst. All of the gases were provided by Linde Gas with the following purities N_2 (99.999%), H_2 (99.999%) and C_2H_4 (99.95%), and the total gas flow was kept to 10 $cm^3\ min^{-1}$.

FT-IR measurements were performed every 60 *s*, in the spectral range of 600–4000 cm^{-1} with a 4 cm^{-1} resolution and 32 *s* scan time. The FT-IR data were analysed with the OPUS spectroscopy software.

3.3 RESULTS AND DISCUSSION

3.3.1 DRIFTS experiments with the Phillips-type catalysts without TEAl modification

In a first set of experiments, Cr/Ti/SiO_2 (CTS1 and CTS2) and Cr/SiO_2 (CS) Phillips-type catalysts were tested for the ethylene polymerisation reaction without prior modification with TEAl. The reactions were monitored *in-situ* with DRIFT spectroscopy. As a showcase, the time evolution of the DRIFT spectra in the 600–4000 cm^{-1} region during the polymerisation of ethylene over the CTS2 Cr/Ti/SiO_2 catalyst are presented in ***Figure 3.2a.*** The spectra of several key points, *i.e.* before the reaction, at the addition of ethylene and after the reaction, are presented in ***Figure 3.2b***. The fresh catalyst shows a highly dehydroxylated catalyst support, as testified by the sharp silanol stretching vibration at 3746 cm^{-1}. Another band observed at 3719 cm^{-1}, which appears only in the titanated catalyst samples, is assigned to the stretching vibration of isolated titanol group and is an indication of the increased surface acidity. Thirdly, the low intensity band appearing at 3610 cm^{-1} is more difficult to assign. Recently, a band at similar wavenumber has been assigned by Conley *et al.* to the stretching vibration of bridging Si-(μ-OH)-Cr^{3+} hydroxyl groups formed upon contact of ethylene with Cr^{3+} catalyst material, used to explain the initiation mechanism that involves the heterolytic activation of the Cr^{3+}-O bonds.[27a,28] However, it was shown later that the combination of bands from the C-H vibrations of polyethylene could appear at the same wavenumbers, making it impossible to assign this vibration unequivocally to the Si-(μ-OH)-Cr^{3+}.[27b] In the DRIFTS measurements performed for this ***Chapter***, such a band was observed in the activated Phillips-type catalyst before any contact with ethylene, co-catalyst or other organic compound possessing CH_2 or CH_3 groups. Furthermore, during the activation of the catalyst at 1048 *K*, all of the organic groups originating from Ti and Cr precursors were burnt off, therefore leading to the conclusion that the band at ~3610 cm^{-1} could be assigned to the bridging hydroxyl groups interacting with chromium or even titanium species, which could both exist at the silica surface. Besides the absorption bands in the OH stretching region, the high-intensity bands appearing below 2100 cm^{-1} belong to the vibrational modes of the silica support, limiting the information that can be obtained from this region. Fur-

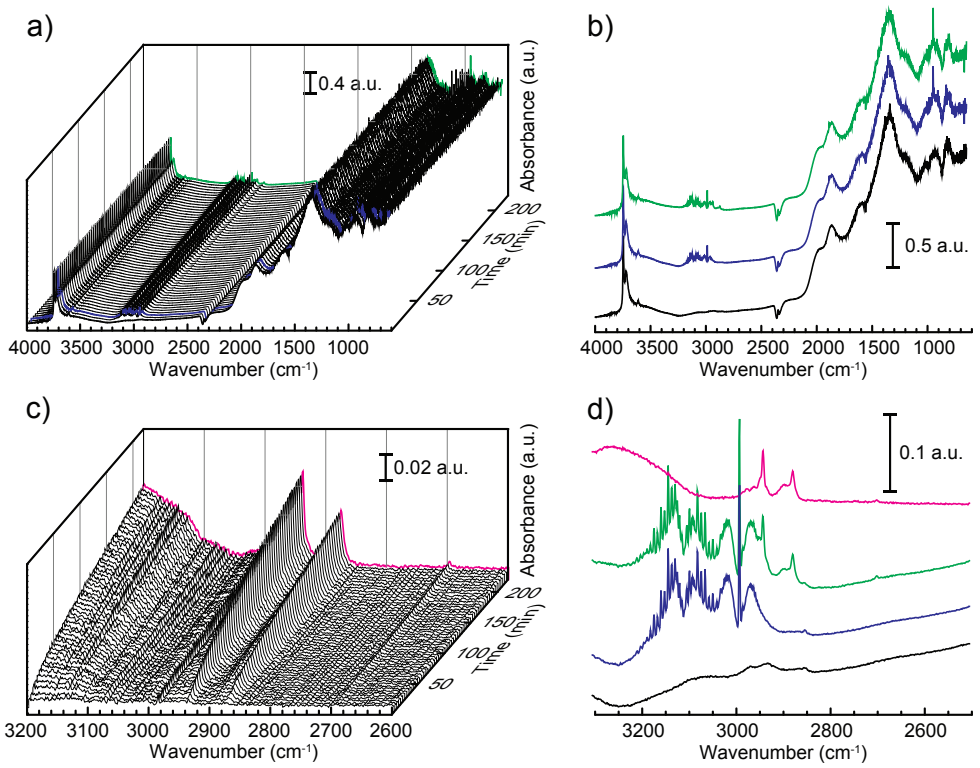

[FIGURE 3.2]

(a) *In-situ* DRIFT spectra of the CTS2 Cr/Ti/SiO_2 catalyst during the reaction with ethylene inside the DRIFTS cell when no co-catalyst is used show a minor polymerisation activity. **(b)** Individual spectra of several key points, *i.e.* before the reaction (black), start of the ethylene feed (blue) and after the reaction (green). The CH_x stretching region after the subtraction of the spectrum of gaseous ethylene **(c)** show an increase of the bands of asymmetric and symmetric stretching vibrations of the methyl and methylene groups of the growing polyethylene. Part **(d)** shows individual spectra in the CH_x stretching region of the fresh catalyst (black), start of the ethylene feed (blue) and after reaction (green) before ethylene subtraction, and the ethylene-subtracted spectrum after the reaction (magenta).

thermore, due to the titanation of the catalyst, the so-called "silica window" in the 850–1000 cm^{-1} region is obscured by the absorption of Ti-O-Si vibrational modes.

The introduction of the reactant mixture into the DRIFTS cell can be seen by the distinct gas phase ethylene spectra in the 2900–3200 cm^{-1} region possessing characteristic rotational structure, which includes R-, P- and Q-branches depending on the rotational selection rules.[29] Ethylene polymerisation starts slowly with the characteristic asymmetric and symmetric stretching vibrations of the CH_2 groups of the polymer, steadily increasing at 2938 cm^{-1} and 2875 cm^{-1}, respectively, and of the CH_3 groups at 2962 cm^{-1} and 2892 cm^{-1}. ***Figure 3.2c*** shows the different spectra in the CH_x stretching region after subtracting the first spectrum after the ethylene is added,

as gas-phase ethylene partially obscures the asymmetric CH_x bands of the polymer. The polymerisation of ethylene proceeds slowly, even after long contact time with ethylene, which can be related to the lower partial pressure of ethylene in the gas reactant mixture. However, the experimental conditions applied can possibly provide the study and the detection of the first polyethylene chains formed on the catalyst.

Furthermore, the CS Cr/SiO_2 catalyst containing no titanium, the CTS1 Cr/Ti/SiO_2 catalyst with the titanium loading of 2.2 *wt.%* and the materials containing no chromium (TS and S), summarised in ***Table 3.1***, were analysed in the same manner. The latter showed no activity in the ethylene polymerisation reaction, while the activity of the supported Cr catalyst was notably influenced by the Ti content. The increase of Ti loading shortens the induction period and increases the overall ethylene polymerisation rate. ***Figure 3.3*** shows the development of the symmetric stretching vibrations of the methylene groups of the growing polymer. The curves can be divided into two parts, *i.e.*, an initial nonlinear and a subsequent linear region. These differences in the operation of the catalyst can be explained by the assumption of the reaction rate given with the following equation:

$$r = k\,[C^*]^m\,[M]^n \qquad \textbf{[EQUATION 3.1]}$$

where *k* is the reaction rate constant, *[C*]* concentration of the polymerisation active sites, *[M]* concentration of ethylene monomer and *m* and *n* are the reaction orders in respect to the active sites and monomer. Due to the constant flow and excess of ethylene monomer, the reaction rate can be assumed independent on the concentration of monomer and reaction order n = 0, meaning that the catalyst surface is saturated

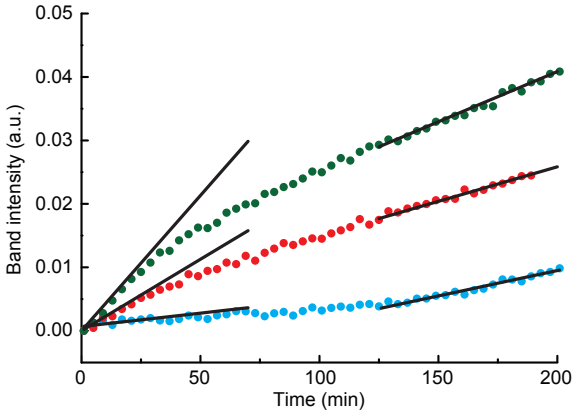

[FIGURE 3.3]
Comparison of the intensity change of the symmetric $\nu_s(CH_2)$ stretching vibration at 2874 cm^{-1} with CS (black), CTS1 (red) and CTS2 (green) catalysts differing in their Ti loading of 0, 2.2 and 3.9 *wt.%,* respectively.

with the monomer, which simplifies the equation to:

$$r = k\,[C^*]^m \qquad \textbf{[EQUATION 3.2]}$$

During the initial period of development of the methylene stretching bands, the reaction rate is determined by the formation and activity of the active sites. At the start of the polymerisation, the initial reaction rate ***(Table 3.2)*** increases with an increasing amount of titanation (CS < CTS1 < CTS2). A higher titanium loading promotes the faster creation of active sites by making Cr^{6+} species more reducible.[1] During this period, the reaction rate order cannot be explained by either first or second order reactions, leading to the mixed reaction order kinetics.

Over the course of time, the reaction rate reaches a steady state exhibiting zero order kinetics. At this stage of the reaction, the reaction rate is independent of the concentration of the Cr active sites and monomer, and equals the reaction rate constant ***(Table 3.2)***. At this point, all ethylene polymerisation active sites have been created. The differences in the rate constants between the polymerisation reactions with the catalysts with varying titanium loading most probably originate from slightly different molecular structures of the active sites. The titanation of the catalyst increases the amount of acid sites, which are able to withdraw electron density from the Cr sites making them more Lewis acidic, which can facilitate easier π-coordination of the ethylene monomer.

[TABLE 3.2]
Overview of the initial rate of ethylene polymerisation (r_i), determined as the slope at the start of the polymerisation, and the rate after the steady-state is reached (r_s), determined as the slope of the linear fit, for the TEAl-unmodified CS, CTS1 and CTS2, and TEAl-modified CTS2 Phillips-type catalysts.

Sample name	Ti loading (wt.%)	Al:Cr	r_i (10^{-4} min^{-1})	$r_s = k_s$ (10^{-4} min^{-1})	R^2 (r_s)
CS	0	0	0.4	0.8	0.9973
CTS1	2.2	0	2.3	1.1	0.9917
CTS2	3.9	0	4.3	1.6	0.9786
CTS2	3.9	2	200	2500	0.9915

3.3.2 DRIFTS experiment with the Cr/Ti/SiO_2 Phillips-type catalyst with TEAl modification

In the second part of the study, *in-situ* DRIFTS measurements were performed during the modification of the Cr/Ti/SiO_2 catalyst with TEAl and subsequent polymerisation of ethylene, which will be showcased for the CTS2 catalyst. ***Figure 3.4*** shows the time evolution of the baseline-corrected DRIFTS spectra in the 600–4000 cm^{-1}

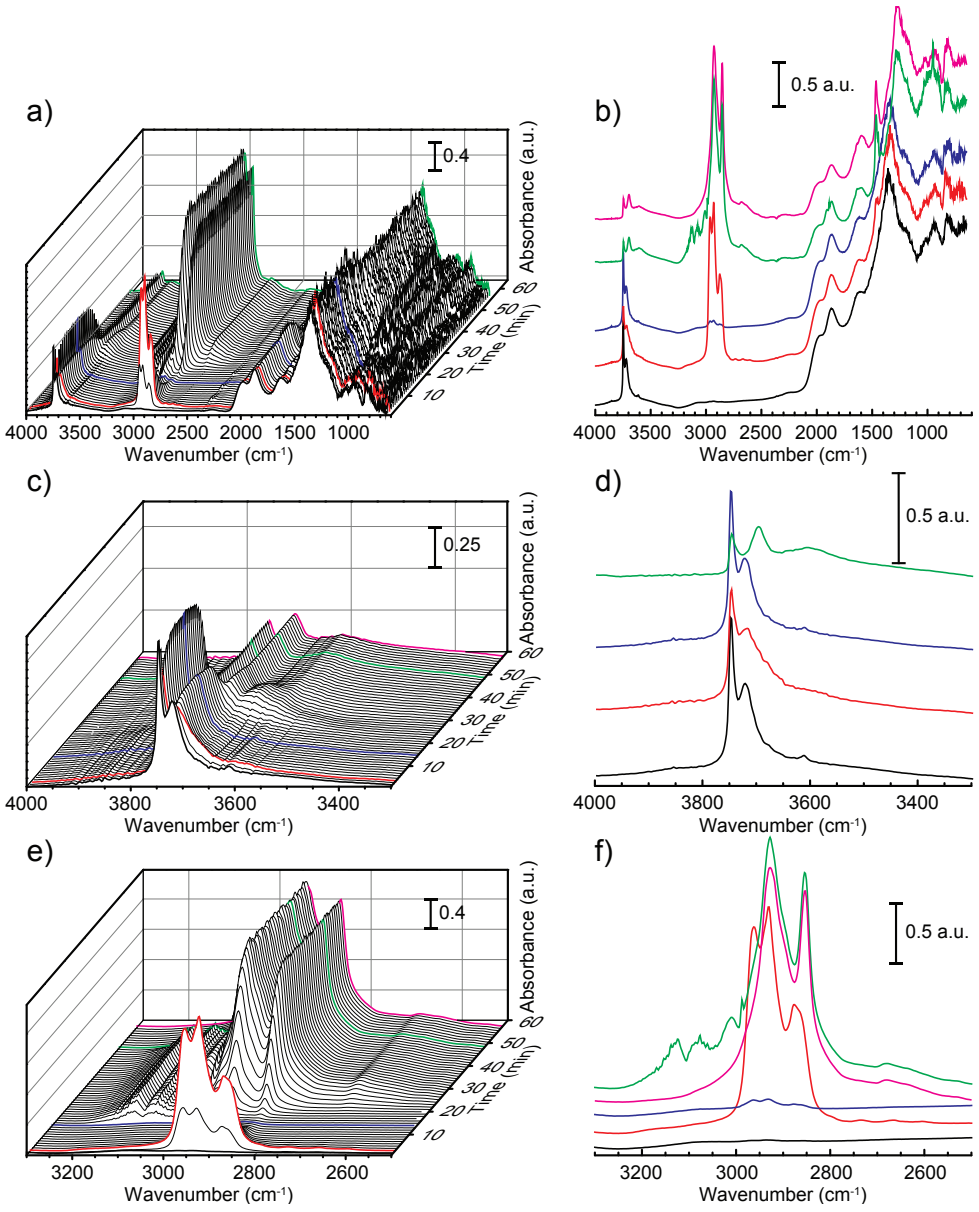

[FIGURE 3.4]
(a) *In-situ* DRIFT spectra of the CTS2 Cr/Ti/SiO_2 catalyst during the pre-reaction with TEAl co-catalyst and subsequent ethylene polymerisation inside the DRIFTS cell show a significant change in the polymerisation activity. **(b)** Individual spectra of several key points, *i.e.* before the reaction (black), injection of TEAl dissolved in heptanes (red), after flushing of excess solvent (blue), at the end of the reaction (green) and after flushing of ethylene reactant (magenta). Spectra **(c)** and **(d)** show the OH and the CH_x stretching regions, respectively, while the individual spectra of the same regions are shown in **(d)** and **(f)**, with the colour code described earlier.

spectral region. In order to facilitate comparisons, spectra of several key moments are presented in ***Figure 3.4b***, including the spectrum of the fresh CTS2 catalyst, spectra during and after modification with TEAl, and spectra after the polymerisation of ethylene and flushing of ethylene reactant. ***Figure 3.4c-d*** and ***Figure 3.4e-f*** show the characteristic OH stretching and CH stretching regions, respectively.

The spectrum of the freshly activated $Cr/Ti/SiO_2$ catalyst and the absorption bands appearing at 3746 cm^{-1}, 3716 cm^{-1} and 3610 cm^{-1}, is already described in the previous set of experiments. However, in this case, the catalyst was treated with the TEAl solution in heptanes, which was introduced into the DRIFTS cell by evaporation. The arrival of the co-catalyst is immediately observed by the rising CH_2 and CH_3 stretching vibration absorption bands in the 2800–3000 cm^{-1} region. After injection, excess solvent is flushed off by the constant nitrogen flow, leaving only the TEAl-modified catalyst. As discussed in ***Chapter 1***, TEAl can perform several plausible roles, few of which can be deducted from the DRIFTS data at this stage. TEAl indeed reacts with the free hydroxyl groups of the support, albeit to a small degree, as testified by the small intensity decrease of the OH stretching vibration bands. The reduction of chromium species cannot be observed as it is obscured by the high absorption of the support. On the other hand, TEAl is alkylating the catalyst surface shown by the remaining CH_2 and CH_3 bands of the ethyl groups after modification with the co-catalyst. This initial alkylation is considered to induce the formation of the first polyethylene chain, significantly decreasing the induction time.

Upon the start of ethylene flow and observing the gas phase ethylene ro-vibrational spectrum, ethylene polymerisation starts rapidly. The absorption signal of methyl and methylene stretching vibrations quickly reaches saturation, while the signal of the methyl groups can be hardly distinguished due to the high activity of the catalyst and production of longer chains with small amount of methyl end groups. Possible formation of shorter unsaturated oligomers cannot be deduced from the experiment performed under these applied conditions. The OH stretching region shows very interesting changes in the absorption profile. During the course of ethylene polymerisation, the intensity of the isolated OH group band at 3746 cm^{-1} and lower acidity OH group at 3719 cm^{-1} decreases with the simultaneous development of the bands at 3696 cm^{-1} and ~3650 cm^{-1}. The isosbestic point appearing at ~3700 cm^{-1} suggests the conversion of "free" hydroxyls groups to hydroxyl species hydrogen-bonded to the CH_x groups of the growing PE chains. Furthermore, the broadening of the new bands is in line with the nature of the intermolecular interactions *via* hydrogen bonding. The low intensity band observed at 3610 cm^{-1} assigned to the silanols interacting with Cr species disappears during ethylene polymerisation implying changes to the ethylene polymerisation sites during the reaction. At slightly lower energies at ~3600 cm^{-1}, a

new band evolves, which can be assigned to the combination of the CH_x vibrations bands of the PE. The treatment of the Cr/Ti/SiO_2 Phillips-type catalyst with TEAl significantly changes the polymerisation activity of the catalyst as can been seen by the comparison of the development of the CH_x stretching bands of the growing PE in ***Figure 3.5***. The activity of the catalyst is increased, showing basically no induction time, due to the alkylation of the polymerisation sites. In the case of the original catalyst, the CH_2 and CH_3 stretching vibrations appear at slightly higher energies, which can be explained by the lower amount of intermolecular interactions between the chains due to considerably lower quantity of the produced PE.

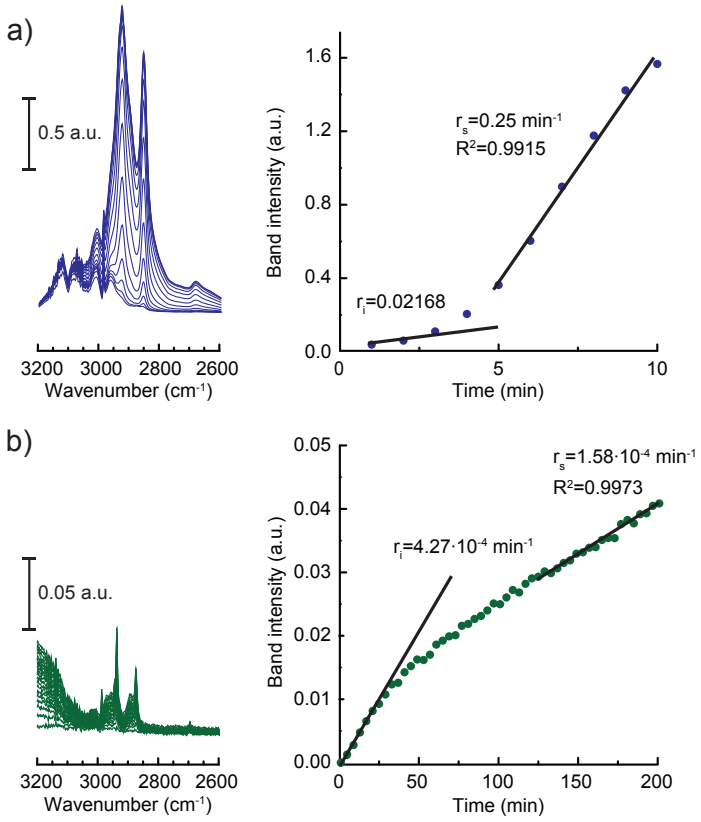

[FIGURE 3.5]
The TEAl-modified CTS2 Cr/Ti/SiO_2 catalyst **(a)** exhibits significantly higher polymerisation activity than the original catalyst, which was not pre-treated with TEAl **(b)**. For the sake of clarity, the gas phase ethylene spectrum was subtracted from the DRIFT spectra of the latter. Right hand side plots show the development of the band intensity of the symmetric $\nu_s(CH_2)$ stretching vibration after the start of the polymerisation.

The analysis of the kinetic data shows a considerably higher initial rate of the reaction and the rate of propagation in the case of a TEAl-modified catalyst ***(Table 3.2)***. The quicker formation of the active sites can be attributed to the scavenging properties of TEAl in order to remove adsorbed ethylene oxidation products. In this manner, TEAl can also facilitate the easier formation and the increase of the number of ethylene polymerisation active sites. Furthermore, due to the alkylation of a part of the chromium sites, their local structure can be changed, allowing a more favourable coordination of the monomers and their insertion into the PE chain during the chain propagation step, which is reflected in an increase of the reaction rate constant.[30]

3.3.3 Comparison of the TEAl-modified Phillips-type catalysts and support materials

In order to investigate the influence of the titanation of the catalyst, besides the CS and CTS1 catalysts containing no and an intermediate amount of Ti, respectively, pure silica support (S) and titanated silica (TS) were also examined in order to rule out possible polymerisation activity of these two materials modified with TEAl. The comparison of the DRIFT spectra in the hydroxyl stretching group region of the fresh catalysts and support materials before the modification with TEAl is presented in ***Figure 3.6a***. The absence of any methyl and methylene groups confirms the successful calcination of these materials and removal of the organic groups, which could have remained after the titanation with titanium isopropoxide. The hydroxyl group stretching region reveals the highly dehydroxylated nature of the materials. Besides the isolated silanol vibration at 3746 cm^{-1}, in the case of the titanated catalyst including the titanated silica sample additional band appears at 3719 cm^{-1} with the intensity proportional to the Ti loading. The low intensity band at 3610 cm^{-1}, previously assigned to the bridging silanol groups interacting with Cr or Ti centres, can be seen in the titanated samples regardless of the presence of Cr, leading to the conclusion that the origin of this band is the bridging silanols interacting with Ti species rather than with Cr species. This finding rules out the previous literature proposal of the 3610 cm^{-1} absorption band assignment to the vibration of Si-(μ-OH)-Cr^{3+},[27a] which was questioned by the scientific community and later by the authors themselves.[27b]

Modification of the catalyst and support materials with TEAl, as already described in the case of the CTS2 catalyst, causes a small decrease in the intensities of the silanol and titanol stretching bands ***(Figure 3.6b)***. Furthermore, the reaction of TEAl with Ti centres diminishes their interaction with the hydroxyl groups leading to the decrease of the band at 3610 cm^{-1}. The CH_x stretching region ***(Figure 3.6c)*** reveals methyl and methylene groups present on the examined materials after their modification with TEAl.

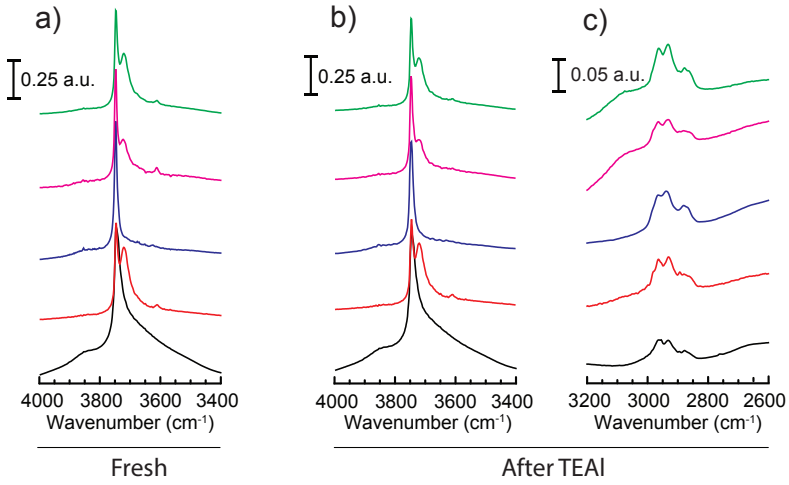

[FIGURE 3.6]
The hydroxyl group stretching region of the DRIFT spectra of **(a)** the fresh catalysts *i.e.* silica gel S (black), TS (red), CS (blue), CTS1 (magenta) and CTS2 (green) and **(b)** after reaction with TEAl in heptane and subsequent flushing with N_2. The methyl and methylene group stretching region **(c)** shows the alkylation of the materials after reaction with TEAl. The DRIFT spectra are characterised by intensive absorption by the silica support in the region below 2100 cm^{-1}, which was excluded from the figure.

Figure 3.7 shows the DRIFTS spectra after the polymerisation of ethylene. The CS Cr/SiO_2 and CTS1 and CTS2 Cr/Ti/SiO_2 samples exhibit high activity upon the modification with TEAl, producing PE with the characteristic absorption profile in the CH_x stretching region. As with the CTS2 catalyst, the decrease of the silanol and titanol stretching vibrations and their broadening and shift to lower energy can be observed as the consequence of the intermolecular interactions with the PE chains. The CS sample however, due to the absence of titanium and titanol groups, shows a simpler absorption profile containing only infrared absorptions due to the silanol groups. Interestingly, silica (S) and especially titanated silica (TS) modified with TEAl still show certain reactivity towards ethylene, which can be seen in the CH_x stretching region after the reaction and flushing of ethylene reactant. The observed absorption bands between 2850 cm^{-1} and 3000 cm^{-1} originate from the CH_2 and CH_3 groups of the hydrocarbon products formed. In literature, Ti(OR_4)/$AlEt_3$ catalyst systems are already known for the selective dimerisation of ethylene.[31] In the case of the titanated silica, such ethylene oligomerisation sites could have been created upon reaction of the material with TEAl. However, the absence of the absorption bands above 3000 cm^{-1} suggests the production of mainly saturated ethylene oligomers.

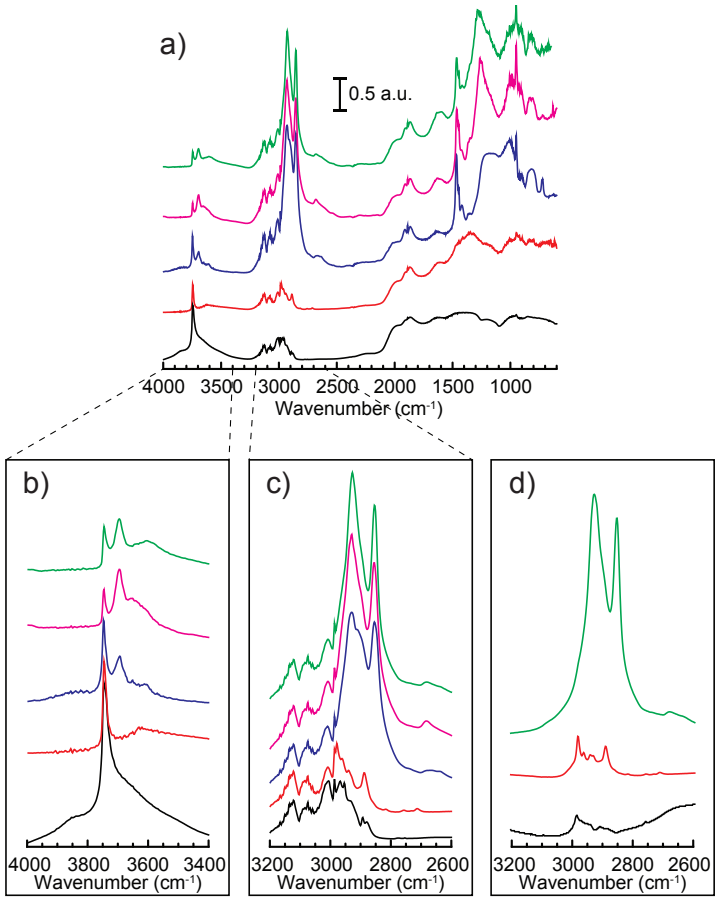

[FIGURE 3.7]
(a) DRIFT spectra of the TEAl-modified catalyst materials: silica gel S (black), TS (red), CS (blue), CTS1 (magenta) and CTS2 (green) after polymerisation of ethylene inside the DRIFTS cell at 373 *K* and 1 *bar*. The hydroxyl and CH_2/CH_3 groups stretching regions are presented in **(b)** and **(c)**, respectively. **(d)** Shows the CH_2/CH_3 stretching region of the silica gel, TS and CTS2 catalyst after purging the DRIFTS cell with N_2.

3.4 CONCLUSIONS

The performed *in-situ* DRIFTS studies discussed in this ***Chapter*** allowed the investigation of the working Cr/SiO_2 and $Cr/Ti/SiO_2$ Phillips-type catalysts at 1 *bar* and 373 *K* with a minimal sample preparation, without the previous reduction step with CO or modification of its form by pressing the catalyst powder into pellets. This offered the possibility of an investigation of the vibrational properties of a genuine catalyst material. In that respect, several catalyst formulations with an increasing degree of

titanation have been characterised. The increase of the titanium loading exhibited a promotional effect on the shortening of the induction time and the increase of both the initial polymerisation rate and the rate after steady-state has been reached. At this point the reaction follows pseudo-zero order kinetics and the reaction rate becomes independent of the concentration of the monomer and active sites. The reaction rate constant is influenced by the degree of titanation. This can be explained by an increased acidity of the support, which is the highest for the CTS2 Cr/Ti/SiO_2 catalyst with the highest Ti loading.

Furthermore, the catalysts and the support materials were also studied in the ethylene polymerisation reaction after modification with TEAl as co-catalyst. The possible polymerisation properties of TEAl-modified Ti/SiO_2 can be excluded, while the observed alkylation of the Cr/SiO_2 (CS) and Cr/Ti/SiO_2 (CTS1 and CTS2) catalysts showed a promotional effect on the polymerisation activity, which is deduced from the fast development of the methylene absorption bands of the produced PE in the *operando* DRIFT spectra and quantified by the comparison of the reaction rates of the TEAl-modifed CTS2 and unmodified CTS2 catalyst.

Recently, Copéret *et al.* proposed the 3610 cm^{-1} band to be due to the bridging silanol Si-(μ-OH)-Cr^{3+} vibration.[27a] The work performed in this ***Chapter*** clearly demonstrates that this is not the case as this band is also observed in the titanated silica support containing no chromium, while absent in the case of a Cr/SiO_2 catalyst. Therefore, from the analysis of the absorption bands in the hydroxyl group stretching region, we propose that the assignment of the 3610 cm^{-1} absorption band can be attributed to the stretching vibration of bridging titanol groups.

3.5 ACKNOWLEDGMENTS

Gerrit van Hauwermeiren and Julien Decrom (Total Research and Technology, Feluy) are acknowledged for the preparation of the catalysts. Fouad Soulimani and Ad Mens (Utrecht University) are acknowledged for their help with the construction of the DRIFTS setup.

3.6 REFERENCES

[1] M. P. McDaniel, *Adv. Catal.* **2010**, *53*, 123–606.

[2] R. Cheng, Z. Liu, L. Zhong, X. He, P. Qiu, M. Terano, M. S. Eisen, S. L. Scott, B. Liu, *Adv. Polym. Sci.* **2013**, *257*, 135–202.

[3] B. M. Weckhuysen, I. E. Wachs, R. A. Schoonheydt, *Chem. Rev.* **1996**, *96*, 3327–3350.

[4] E. Groppo, C. Lamberti, S. Bordiga, G. Spoto, A. Zecchina, *Chem. Rev.* **2005**, *105*, 115–184.

[5] C. Barzan, E. Groppo, E. A. Quadrelli, V. Monteil, S. Bordiga, *Phys. Chem. Chem. Phys.* **2012**, *14*, 2239–2245.

[6] G. Wilke, *Angew. Chem. Int. Ed.* **2003**, *42*, 5000–5008.

[7] L. L. Böhm, V. Busico, R. Cheng, M. S. Eisen, G. Fink, X. He, B. Liu, B. Monrabal, L. A. Novokshonova, P. Qiu, S. L. Scott, T. Taniike, M. Terano, V. A. Zakharov, L. Zhong, *Polyolefins: 50 Years after Ziegler and Natta I*, Springer, Berlin, **2013**.

[8] L. A. Novokshonova, V. A. Zakharov, *Adv. Polym. Sci.* **2013**, *257*, 99–134.

[9] L. L. Böhm, *Angew. Chem. Int. Ed.* **2003**, *42*, 5010–5030.

[10] H. Sinn, W. Kaminsky, H.-J. Vollmer, R. Woldt, *Angew. Chem. Int. Ed.* **1980**, *19*, 390–392.

[11] H. H. Brintzinger, D. Fischer, R. Mülhaupt, B. Rieger, R. M. Waymouth, *Angew. Chem. Int. Ed.* **1995**, *34*, 1143–1170.

[12] W. Kaminsky, *Macromolecules* **2012**, *45*, 3289–3297.

[13] B. M. Weckhuysen, R. A. Schoonheydt, *Catal. Today* **1999**, *51*, 215–221.

[14] L. M. Baker, W. L. Carrick, *J. Org. Chem.* **1968**, *33*, 616–618.

[15] T. Armaroli, T. Bécue, S. Gautier, *Oil Gas Sci. Technol.* **2004**, *59*, 215–237.

[16] J. Ryczkowski, *Catal. Today* **2001**, *68*, 263–381.

[17] F. C. Meunier, *Chem. Soc. Rev.* **2010**, *39*, 4602–4614.

[18] A. Zecchina, E. Groppo, A. Damin, C. Prestipino, in *Top. Organomet. Chem.* (Eds.: C. Copéret, B. Chaudret), Springer, Berlin, **2005**, pp. 1–35.

[19] E. Groppo, K. Seenivasan, C. Barzan, *Catal. Sci. Technol.* **2013**, *3*, 858–878.

[20] O. M. Bade, R. Blom, M. Ystenes, *J. Mol. Catal. A Chem.* **1998**, *135*, 163–179.

[21] O. M. Bade, R. Blom, I. M. Dahl, A. Karlsson, *J. Catal.* **1998**, *173*, 460–469.

[22] A. Zecchina, E. Groppo, Proc. *R. Soc. A Math. Phys. Eng. Sci.* **2012**, *468*, 2087–2098.

[23] C. Lamberti, A. Zecchina, E. Groppo, S. Bordiga, *Chem. Soc. Rev.* **2010**, *39*, 4951–5001.

[24] A. Zecchina, E. Garrone, G. Ghiotti, S. Coluccia, *J. Phys. Chem.* **1975**, *79*, 972–978.

[25] I. R. Subbotina, V. B. Kazanskii, *Kinet. Catal.* **2002**, *43*, 115–121.

[26] G. Debras, J.-P. Dath, EP0882743 B1, **1998**.

[27] a) M. P. Conley, M. F. Delley, G. Siddiqi, G. Lapadula, S. Norsic, V. Monteil, O. V. Safonova, C. Copéret, *Angew. Chem. Int. Ed.* **2014**, *53*, 1872–1876. b) M. P. Conley, M. F. Delley, G. Siddiqi, G. Lapadula, S. Norsic, V. Monteil, O. V. Safonova, C. Copéret, *Angew. Chem. Int. Ed.* **2015**, *53*, 6657–6671.

[28] M. F. Delley, M. P. Conley, C. Copéret, *Catal. Lett.* **2014**, *144*, 805–808.

[29] D. N. Sathyanarayana, *Vibrational Spectroscopy Theory and Applications*, New Age International (P) Ltd. Publishers, New Delhi, 1st ed., **2004**, pp. 271–293.

[30] W. Xia, B. Liu, Y. Fang, K. Hasebe, M. Terano, *J. Mol. Catal. A Chem.* **2006**, *256*, 301–308.

[31] R. Robinson, D. S. Mcguinness, B. F. Yates, *ACS Catal.* **2013**, *3*, 3006–3015.

[This page is intentionally left blank]

DAVID DE WIEDGEBOUW
Utrecht, The Netherlands

IV

Structure-Performance Relationships of $Cr/Ti/SiO_2$ Catalysts Modified with TEAl for Oligomerisation of Ethylene:

Tuning the Selectivity Towards 1-Hexene

A study on the influence of hydrogen, the degree of titanation and activation temperature of a Cr/SiO_2 Phillips polymerisation catalyst on the selective oligomerisation of ethylene induced by pre-contacting the catalyst with triethylaluminium (TEAl) is presented. Ethylene oligomerisation reactions were performed at 373 *K* and 1 *bar*, inside a quartz reactor of a specially designed *operando* setup, which allowed examination of the catalysts by UV-Vis-NIR diffuse reflectance spectroscopy, while the gas phase was continuously monitored by on-line mass spectrometry and subsequently analysed by gas chromatography. This combination of techniques revealed detailed insight into the different distributions of produced oligomers, which turned out to be highly dependent on the catalyst structure. The addition of small amounts of Ti significantly changes the electronic environment of Cr oligomerisation sites by the formation of Cr-O-Ti-O-Si linkages, favouring β-H-transfer and increasing the selectivity towards butene at the expense of 1-hexene. Moreover, ethylene oligo-/polymerisation reactions follow at least two different pathways, *i.e.* metallacyclic for olefinic species with a broken Schulz-Flory distribution, and Cossee-Arlman for other hydrocarbon species.

BASED ON:
"Structure-Performance Relationships of $Cr/Ti/SiO_2$ Catalysts Modified with TEAl for Oligomerisation of Ethylene: Tuning the Selectivity Towards 1-Hexene", D. Cicmil, I. K. van Ravenhorst, J. Meeuwissen, A. Vantomme and B. M. Weckhuysen, *Catal. Sci. Technol.* **2015**, *DOI: 10.1039/c5cy01512j*

4.1 INTRODUCTION

Phillips-type Cr/SiO_2 polymerisation catalysts are responsible for the commercial production of more than one third of all polyethylene (PE) sold worldwide.[1–4] This has attracted a great deal of research attention both in academia and chemical industries since their discovery in the early 1950s by J.P. Hogan and R.L. Banks at Phillips Petroleum Company.[5,6] Despite the numerous research efforts on the oxidation states of the catalyst,[7–11] the molecular structure of the active sites,[2,12–16] and the mechanism of ethylene polymerisation with Phillips-type catalysts,[17–23] however, these key scientific questions still require further attention.

No univocal consensus has been yet achieved, especially in studies with polymerisation conditions similar to industrial ones, as many of the research studies involved model systems, temperatures and pressures, which were quite different from the conditions utilised in industrial systems. One of the reasons is the very high sensitivity of the Cr/SiO_2 ethylene polymerisation catalyst to trace amounts of catalytic poisons, *i.e.* water, oxygen and small oxygenated organic compounds. Furthermore, the fast rate of polymerisation and high productivity of the catalysts make the study of the initial stages of ethylene polymerisation very challenging.

Certain adjustments of the catalyst furthermore complicate the picture. Cr/SiO_2 ethylene polymerisation catalysts can often be modified by incorporation of titania, yielding a $Cr/Ti/SiO_2$ catalyst with increased activity and capability of producing PE with a lower molecular weight and broader molecular weight distribution than the pristine catalyst. Titanation can be performed in two manners, either by a co-precipitation with silica gel, when titania becomes highly dispersed in the bulk catalyst material,[24] or by reaction of a titanium compound with the hydroxyl groups of the support, therefore coating the silica surface with a layer of titania.[25–28] Consequently, both methods include the formation of Cr-O-Ti-O-Si linkages,[29] which change the electronic environment of the active sites and influence the mechanism of ethylene polymerisation.

One of the unique aspects of Phillips-type Cr/SiO_2 catalysts is that they do not require activation by a metal alkyl co-catalyst as compared to Ziegler-Natta and metallocene polymerisation catalysts and therefore these compounds are often excluded, even at industrial production sites.[30–32] However, when metal alkyls are used in combination with Phillips-type Cr/SiO_2 catalysts, the development of the polymerisation rate is commonly accelerated and the induction time is decreased. It is believed that these effects are caused by a more facile reduction of the Cr^{6+} species of the activated catalyst to Cr species in a lower oxidation state, which are thought to be responsible for the polymerisation of ethylene.[1] Most of the authors attribute the poly-

merisation-active sites to Cr^{2+} species of different coordinative unsaturations[19,33–35] although other species of higher valences, *i.e.* Cr^{3+}, Cr^{4+} and Cr^{5+}, should still be taken into consideration,[8,10,36–38] especially in view of the recent work of the group of Copéret.[20,21,39] Secondly, metal alkyl co-catalysts can improve the polymerisation rate by alkylation of Cr sites and provide chain initiation similarly to Ziegler-Natta catalysts. However, with Phillips-type catalysts, this chain initiation by a co-catalyst is not necessary. Thirdly, as highly reactive compounds, metal alkyls can remove the poisons still present in the gas feed or in the system, such as ethylene oxidation products formed during the initiation stage, which might remain adsorbed on the Cr sites. Depending on the type of co-catalyst, there is an optimal amount expressed as the metal-to-Cr ratio, which gives the highest catalytic activity. Besides the improvement of the activity and decrease of the induction time, further increase of the co-catalyst amount can deteriorate the polymerisation rate or even destroy the catalyst due to attack on Cr-support bonds. Some of the metal alkyls can act as chain transfer agents, exchanging the alkyl groups with Cr polymerisation sites, and therefore affect the properties of the produced PE, although less than in Ziegler-Natta and metallocene catalysis. Co-catalysts can also influence the polymerisation sites by reacting with Cr or neighbouring groups and directly modifying the polymerisation activity and the type of PE that is produced.

One of the most interesting facts regarding co-catalysts and their interaction with the Cr sites is that the addition of metal alkyl compounds to the reactor containing a Phillips-type catalyst changes the amount of short-chain branching of the produced PE, even if no α-olefin co-monomers were added to the system. This short-chain branching of the PE chain originates from the co-polymerisation of ethylene with the *in-situ* produced ethylene α-oligomers on modified polymerisation active sites, as shown in ***Chapter 2***.[40,41] *In-situ* branching attracts high interest in the industrial world due to the possibility of reducing or even eliminating the separate feed of α-olefin co-monomers, their transportation, storage and purification, therefore simplifying manufacturing procedures and production costs of MDPE and LLDPE. The recent drop in ethylene price of more than $500 per metric ton from January 2014 to January 2015,[42] decreases the production cost of PE and increases the economic importance of *in-situ* ethylene oligomerisation. Therefore, an accurate description and finding the means to directly influence *in-situ* ethylene oligomerisation, *i.e.* selectivity, olefin distribution and their yield, proves to be one of the hottest topics in ethylene polymerisation industry.

Although a lot of progress has been made in the last few decades in resolving these issues by applying advanced characterisation techniques,[18,40,43–46] no unifying picture has yet been achieved. In this ***Chapter***, an *operando* UV-Vis-NIR diffuse re-

flectance study (DRS) of a Cr/Ti/SiO_2 catalyst is presented in order to elucidate the TEAl-induced *in-situ* ethylene oligomerisation properties of this system, which were described in ***Chapter 2***.

4.2 EXPERIMENTAL METHODS

4.2.1 Sample preparation

The catalyst samples were provided by Total Research and Technology Feluy, Belgium. Catalyst preparation includes the treatment of two commercially available Cr/SiO_2 pre-catalysts containing either a higher or a lower Cr loading, with the following properties: a pre-catalyst with ~1.0 *wt.%* Cr loading, surface area of 500 $m^2 g^{-1}$, pore volume of 1.5 $cm^3 g^{-1}$ and a D50 particle size diameter of 72 μm, and a pre-catalyst with ~0.5 *wt.%* Cr loading, a surface area of 318 $m^2 g^{-1}$, a pore volume of 1.55 $cm^3 g^{-1}$ and a D50 particle size diameter of 47 μm. The pale white silica pre-catalyst was placed in a fluidised bed reactor under nitrogen flow and slowly heated to 543 *K* for dehydration. While still under nitrogen flow, in the case of the titanated samples, the pre-catalyst material was surface-titanated, according to the procedure described by Debras *et al.*, to either 2 *wt.%* or 4 *wt.%* of the total Ti loading using titanium isopropoxide (99.999% trace metals basis, Sigma-Aldrich), which was added dropwise to the fluidised bed.[25] After flushing under nitrogen for 45 *min*, the gas flow was changed to dry air and the temperature was slowly increased to the desired activation temperature. During the 6 *h* oxidation step, the colour of the prepared Cr/SiO_2 and Cr/Ti/SiO_2 catalysts changed to intense yellow/orange due to the formation of Cr^{6+} species. After cooling down to RT and switching back to nitrogen flow, the activated Cr/SiO_2 and Cr/Ti/SiO_2 catalysts could be obtained under inert nitrogen atmosphere and transferred to an argon glove box for storage and further use. An overview of the catalysts' properties and activation temperatures is given in ***Table 4.1***.

4.2.2 *Operando* setup

The prepared catalyst materials were tested in a specially designed setup ***(Figure 4.1)***, which allows an *operando* UV-Vis-NIR DRS study of the catalyst under working conditions and a real-time analysis of the reaction products with on-line mass spectrometry (MS) and gas chromatography (GC). The setup is suitable for polymerisation reactions with gaseous reactants and solid catalysts at 1 *bar* and temperatures in the range from RT to 473 *K*. Each part of the setup will be explained separately in the following sections.

[TABLE 4.1]
Overview of the prepared Phillips-type ethylene polymerisation catalysts and support materials, their properties and the positions of the $O \rightarrow Cr^{6+}$ charge transfer bands.

Sample name	Activation temperature (K)	Cr loading (wt.%)	Ti loading (wt.%)	Surface area ($m^2 g^{-1}$)	Pore volume ($cm^3 g^{-1}$)	$O \rightarrow Cr^{6+}$ charge transfer (cm^{-1})		
S	1048	0	0	246	1.39			
TS	1048	0	4.7	254	1.51			
CS	1048	0.52	0	296	1.30	38 500	29 500	21 900
CTS1	1048	0.62	2.2	293	1.44	38 100	28 700	21 700
CTS2	1048	0.56	3.9	277	1.39	37 500	27 800	21 600
CTS3	923	0.56	4.0	289	1.34	37 200	27 800	21 600
CTS4	823	0.55	3.8	294	1.35	36 500	27 500	21 600
CTS5	1048	0.98	4.7	367	1.13	36 500	27 500	21 700

4.2.3 Ethylene oligo-/polymerisation

Approximately 300 *mg* of a catalyst sample was loaded into a quartz cell under inert atmosphere and heated to a reaction temperature of 373 *K*. Before the feed of ethylene, the catalyst was pre-contacted with 0.1 cm^3 of 1.3 *M* (for an Al:Cr ratio of 2:1) triethylaluminium co-catalyst (TEAl) in heptanes (~94 *wt.%* TEAl, with ~6 *wt.%* predominately tri-*n*-butylaluminium and less than 0.1 *wt.%* triisobutylaluminium residue, Acros Organics), which was injected through a silicon septum into a N_2 stream of 10 $cm^3 min^{-1}$. After the stabilisation of the spectra, a gas reaction mixture consisting of either 45 *vol.%* N_2, 45 *vol.%* C_2H_4 and 10 *vol.%* H_2 or 50 *vol.%* N_2 and 50 *vol.%* C_2H_4 was fed into the cell for a total flow of 10 $cm^3 min^{-1}$. The gases were provided by Linde Gas with the following purities N_2 (99.999%), H_2 (99.999%) and C_2H_4 (99.95%). Modification of the catalyst with TEAl and polymerisation reaction were simultaneously monitored with *operando* UV-Vis-NIR DRS, while the gaseous products were analysed on-line with MS and collected for GC analysis.

4.2.4 UV-Vis-NIR diffuse reflectance spectroscopy

UV-Vis-NIR DRS measurements were performed with a Varian Cary 500 Scan UV-Vis-NIR spectrophotometer equipped with a diffuse reflectance accessory. To obtain the diffuse reflectance spectra of the catalyst materials, a reference spectrum of a halon white standard was first measured and automatically subtracted from the actual DRS data using the Cary Win UV Scan Application. All data were acquired in

the spectral range of 4000–45 000 cm^{-1}, with 17 cm^{-1} spectral resolution and 33 *ms* data point scan time in the UV-Vis region (12 500–45 000 cm^{-1}) and 7.1 cm^{-1} spectral resolution and 33 *ms* data point scan time in the NIR region (4000–12 500 cm^{-1}). The UV-Vis-NIR DRS spectra were corrected for the detector/grating and light source changeover steps at 12 500 cm^{-1} and 28 570 cm^{-1}, respectively, and smoothed in the UV-Vis region using a FFT filter with a 0.00147 cut-off frequency. The spectra were repeatedly taken every 120 *s*.

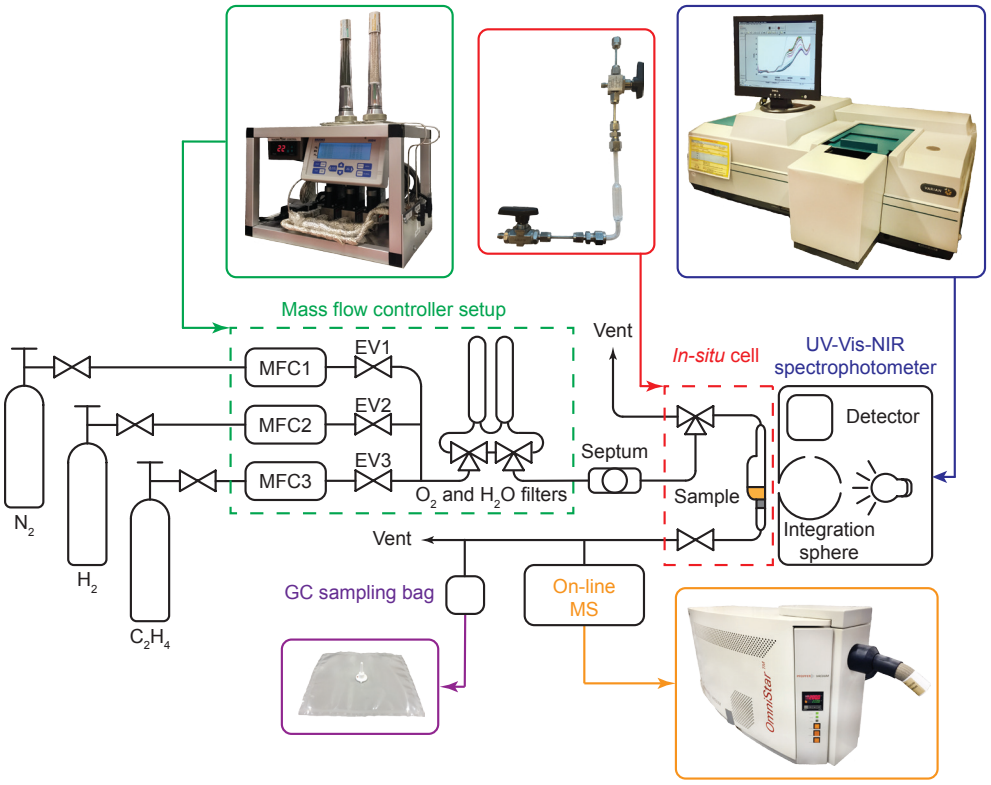

[FIGURE 4.1]
UV-Vis-NIR diffuse reflectance spectroscopy, mass spectrometry and gas chromatography setup developed for the testing of solid catalysts and products obtained in gas phase in reactions at 1 *bar* and temperatures in the range from RT to 473 *K*. The *operando* setup includes changeable gas reactant sources, mass flow controller setup (green), septum for the injection of co-catalyst, 4 cm^3 airtight quartz reactor (red), Varian Cary 500 spectrophotometer (blue), OmniStar mass spectrometer (orange) and gas sampling bag for the GC(-MS) analysis of gas phase (magenta). All lines and the reactor are traced and heated to the desired reaction temperature monitored by a couple of thermocouples.

4.2.5 On-line mass spectrometry

The released gasses during the pre-treatment with TEAl and polymerisation of ethylene were analysed by a quadruple on-line Pfeiffer OmniStar mass spectrometer, which was connected at the exit of the quartz reactor. Ion currents were recorded for 33 different *m/z* values in the range between 2 and 114, selected to detect and distinguish different produced hydrocarbon species. Data were recorded using the program Quadstar 32-Bit.

4.2.6 Gas chromatography-mass spectrometry

The identification of hydrocarbon species from the gas phase, collected into 1 litre Sigma-Aldrich Tedlar gas-sampling bags during the polymerisation of ethylene, was performed on a QP2010 Shimadzu GC-MS apparatus with a VF-5ms column by manual injection of 1 cm^3 of the gas phase using a 1 cm^3 gas-tight GC syringe. The column flow was set at 1 $cm^3\,min^{-1}$ and column temperature was kept constant at 305 *K* during the whole analysis. Quantification of the amount of hydrocarbon species in the gas phase was performed on a Varian 430-GC gas chromatograph with a FID detector. The same type of column and experimental settings as for the GC-MS experiments were used. The calibration curve was made by the dilution of a reference light hydrocarbon gas mixture, provided by Linde Gas, with nitrogen.

4.3 RESULTS AND DISCUSSION

4.3.1 Integration of UV-Vis-NIR diffuse reflectance spectroscopy, mass spectrometry and gas chromatography: an experiment example

For the sake of clarity, the results obtained by the integration of multiple analytical techniques within the specially designed setup ***(Figure 4.1)***, will be first explained for the ethylene polymerisation reaction using the CS catalyst ***(Table 4.1)***, after which the differences between the catalyst structures and reaction conditions will be discussed in the following sections.

Figure 4.2a shows the on-line MS analysis and time evolution of several fragments of the compounds of interest during the pre-run, catalyst modification with TEAl, ethylene oligo-/polymerisation reaction and post-run. The UV-Vis-NIR DRS spectra were repeatedly collected during the TEAl-modification stage and polymerisation reaction, while the gas phase was sampled for the GC analysis during the reac-

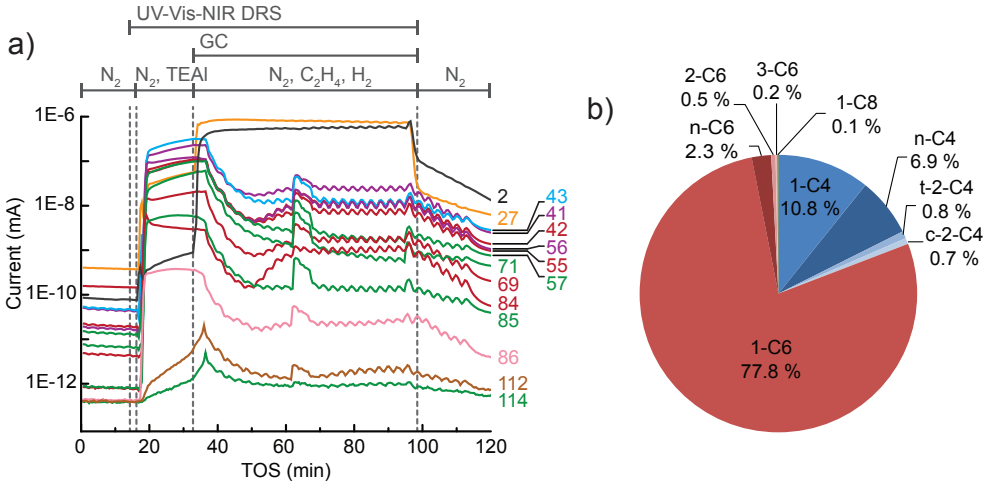

[FIGURE 4.2]
(a) On-line MS analysis of the gas phase during the modification of the CS Phillips-type Cr/SiO_2 catalyst with the TEAl co-catalyst and subsequent oligo-/polymerisation of ethylene using the in-house designed *operando* setup. UV-Vis-NIR DRS repeated measurements were started at t = 14 *min*. At t = 16 *min*, TEAl was injected into the system *via* evaporation into the N_2 stream. After 17 *min*, gas feed was changed to the reaction mixture consisting of 45% N_2, 45% C_2H_4 and 10% H_2, at a total flow rate of 10 $cm^3 min^{-1}$ and the gas phase was sampled for the GC analysis. After 60 *min* of reaction, the gas feed was changed back to N_2 and UV-Vis-NIR DRS and GC sampling stopped. Assignment of the *m/z* is given in ***Table 3.2***. **(b)** GC analysis of the gas phase collected during oligo-/polymerisation of ethylene after the modification of the catalyst with TEAl.

tion stage. Numerous mass fragments were monitored although only the evolution of the most relevant fragments was presented, based on the GC analysis shown in ***Figure 4.2b***,‡ with an overview given in ***Table 4.2***. The injection of TEAl solution in heptanes into the nitrogen stream results in a sudden increase of the detector current and saturation of the signal due to the high concentration of the solvents. After 17 *min* of flushing off the solvent, the gas feed was changed to the reaction mixture consisting of 45 *vol.%* N_2, 45 *vol.%* C_2H_4 and 10 *vol.%* H_2. The change in the gas composition is testified by a high rise of the signal with *m/z* values of 2 and 27 due to H_2 and C_2H_4 reactants, respectively. After the start of the reaction, the signals belonging to the fragments of the *in-situ* produced 1-hexene slowly rise and remain constant until the feed of the reaction mixture was switched off. Furthermore, the TEAl-modified CS catalyst is able to oligomerise ethylene to 1-butene, although in smaller amounts than 1-hexene. At ~30 *min* of the reaction, a sudden increase of the signals suggests

‡ The concentration of the oligomers in the gas phase may be altered by the consumption of the oligomers in the polymer. However, it is assumed that the oligomer consumption by polymer formation is negligible due to the small amount of PE formed and low reactivity of *α*-olefins with the Phillips-type catalyst. For example, Cr/SiO_2 incorporates only 1.85 *mol.%* of 1-hexene at a constant concentration in the reactor.[1]

[TABLE 4.2]
Overview of the fragments detected using an on-line mass spectrometer during the polymerisation of ethylene with CS catalyst modified with TEAl. Main contributors are highlighted in bold.

Fragment *m/z*	Compound of origin
2	hydrogen
27	**ethylene, 1-butene, 1-hexene, hexane,** TEAl, butane, heptanes
43	**1-butene,** butane, heptanes, octane
41	**1-butene, 1-hexene, hexane,** butane, heptanes
56	**1-hexene, hexane,** 1-butene
42, 55, 69, 84	1-hexene, 1-octene
57	**hexane, TEAl,** heptanes
71, 85	TEAl, octane
71, 85, 114	TEAl
86	hexane
112	1-octene

a temporary production of the oligomers with carbon numbers higher than 6. After 60 *min* of reaction, the gas feed was switched back to nitrogen. The signals due to C_2H_4 and H_2 immediately drop due to the abrupt change and continue to decline slowly together with the signals belonging to the oligomerisation products.

The origin of the fragments detected during the on-line MS analysis could be identified and confirmed by the GC-MS and GC analysis of the sampled gas phase ***(Figure 4.2b)***. In this particular case when the CS catalyst was used, the main oligomer product detected was 1-hexene. Moreover, a small amount of the *in-situ* produced saturated and unsaturated ethylene dimers and tetramers was identified. GC and MS results unambiguously confirm the ethylene oligomerisation properties of the tested catalyst material.

Furthermore, the UV-Vis-NIR DRS spectrometer integrated within the setup offered monitoring of the catalyst material during the course of the reaction. Analysis of the UV-Vis part is suitable for inspecting the electronic spectra of supported transition metal ions, which allows determination of the oxidation number, coordination state and symmetry of a transition metal ion by studying d-d and charge transfer (CT) transitions.[47,48] Moreover, the NIR part offers the possibility of examining vibrational properties *i.e.* combination bands and overtones of the vibrational modes

[TABLE 4.3]
Assignment of the bands in the UV-Vis-NIR DRS spectra of the Cr/Ti/SiO_2 Phillips-type polymerisation catalyst and polyethylene.[14, 16, 48-50]

Assignment	Wavelength (cm^{-1})
$\sigma \rightarrow \sigma^*$ C-C	~67 000
$\pi \rightarrow \pi^*$ C=C	52 000–59 000
$O \rightarrow Ti^{4+}$ CT	37 500–40 000
$O \rightarrow Cr^{6+}$ CT	37 600–39 600
$O \rightarrow Cr^{6+}$ CT	27 000–31 000
$O \rightarrow Cr^{6+}$ CT	21 000–22 000
Cr^{3+}_{Oh} d-d	~16 000
Cr^{2+}_{Oh} d-d	~10 000
$3\nu_{as}(CH_2/CH_3)$	8423; 8233
2ν(SiOH)	7325
2ν(TiOH)	7270
$2\nu_{as/s}(CH_2/CH_3)+\delta(CH_2/CH_3)$	7189; 7059; 6966; 6482
$2\nu_{as/s}(CH_2/CH_3)$	5777; 5668
$\nu(H_2O)+\delta(H_2O)$	5260
ν(SiOH)+δ(SiOH)	4525
$\nu_{as/s}(CH_2/CH_3)+\delta(CH_2/CH_3)$	4325; 4250
$\nu_{as}(CH_2/CH_3)+w(CH_2/CH_3)$	4185

of the materials and reaction products. The expected electronic and vibrational bands due to the silica-supported Cr and Ti species (if present inside the catalyst),[14,16,49,50] and polymer[51] produced therewith are summarised in ***Table 4.3***.

During the pre-treatment of the CS catalyst with TEAl (***Figure 4.3a*** and ***b***), the UV-Vis-NIR DRS spectra of the catalyst show a small intensity increase of the bands at 16 000 cm^{-1} and 10 000 cm^{-1} due to the $^4A_{2g} \rightarrow {}^4T_{2g}$ and $^5E_g \rightarrow {}^5T_{2g}$ d-d transitions of the formed Cr^{3+}_{Oh} and Cr^{2+}_{Oh} species. Due to the small amount of modified surface sites, the reduction is more evident after the subtraction of the fresh catalyst spectrum from the final spectrum of the sample after TEAl modification, as shown in ***Figure 4.4***. The negative bands at 21 000–22 000 cm^{-1}, 27 000–31 000 cm^{-1} and 37 000 –40 000 cm^{-1} originating from the decrease of the CT bands of Cr^{6+} species are accompanied with the positive bands of the reduced Cr^{3+}_{Oh} and Cr^{2+}_{Oh} species. The ad-

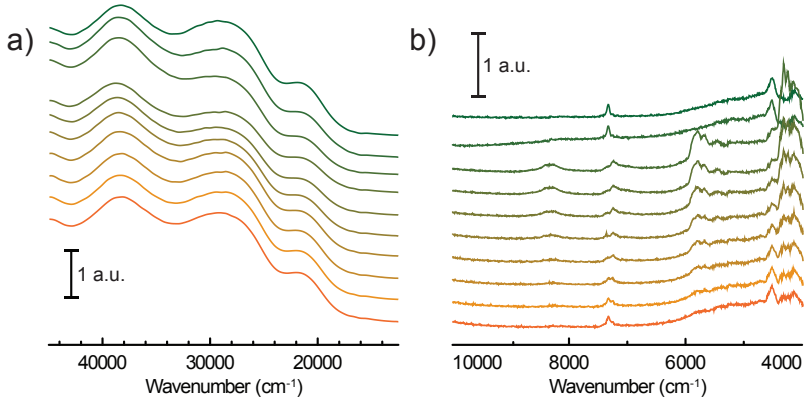

[FIGURE 4.3]
Time evolution (from green to orange) of the *operando* UV-Vis-NIR DRS spectra of the Cr/SiO_2 Phillips-type catalyst (CS sample) during the addition of TEAl, in the UV-Vis **(a)** and NIR **(b)** region.

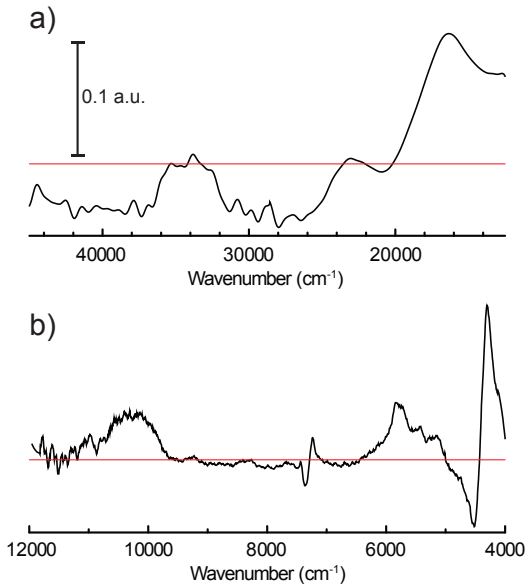

[FIGURE 4.4]
Difference spectrum of the catalyst modified with TEAl and the fresh Cr/SiO_2 Phillips-type catalyst in the UV-Vis **(b)** and Vis-NIR **(b)** region showing the reduction of some of the Cr^{6+} species as testified by the negative O→Cr^{6+} charge transfer bands and positive bands of the formed Cr^{3+} and Cr^{2+} species at approximately 16 000 and 10 000 cm^{-1}, respectively. Zero is presented with the red line.

dition of the co-catalyst can be clearly noted in the NIR region of the time-resolved spectra ***(Figure 4.3b)***. The intensity increase of the bands at 4000–4400 cm^{-1} is due to the combination modes of stretching and deformation vibrations of CH_2/CH_3 groups originating from the adsorbed alkyl groups of the TEAl and heptane solvents. At higher wavenumbers, the first overtone of the fundamental symmetric and asymmetric CH_2/CH_3 stretching vibration appears in the 5600–5900 cm^{-1} region. Furthermore, the first stretching vibration overtone and deformation band can be observed in the 6900–7200 cm^{-1} region. In the first overtone OH stretching region, consumption of the silanol groups at 7325 cm^{-1} occurs due to the interaction with adsorbed TEAl and heptanes. After flushing with nitrogen, the OH functionality of the catalysts is mostly restored, giving almost identical spectra to those obtained before the treatment with TEAl, although a broadening and red shift of the associated absorption band can be noted.

At this stage, ethylene polymerisation reaction with the CS catalyst was started by changing the nitrogen flow in the quartz reactor to the gas reactant mixture consisting of 45 *vol.%* C_2H_4, 45 vol.% N_2 and 10 *vol.%* H_2. ***Figure 4.5a*** shows the time evolution of the UV-Vis-NIR DRS spectra in the UV-Vis region during the *in-situ* polymerisation of ethylene using the Cr/SiO_2 (CS) catalyst. During the reaction, the intensities of the $O \rightarrow Cr^{6+}$ CT bands belonging to mono- and dichromates are decreasing due to the reduction of Cr^{6+} species by ethylene with a simultaneous increase of the d-d transition bands of Cr^{3+}_{Oh} and Cr^{2+}_{Oh} species at ~16 000 cm^{-1} and ~10 000 cm^{-1}, respectively. Consumption of surface silanol groups is evidenced in the NIR region ***(Figure 4.5b)*** by the disappearance of the OH stretching overtone and combination bands at ~7325

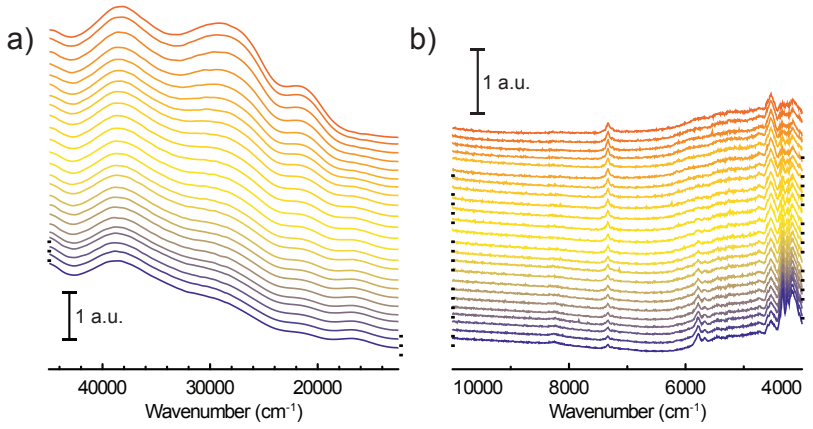

[FIGURE 4.5]
Time evolution (from orange to blue) of the *operando* UV-Vis-NIR DRS spectra of the fresh Cr/SiO_2 Phillips-type catalyst (CS sample) during the oligo-/polymerisation of ethylene, in the UV-Vis **(a)** and the NIR **(b)** region.

cm^{-1} and 4535 *cm*$^{-1}$. On the other hand, the formation of the polymerisation product can be monitored *in-situ* by the growing bands originating from the CH_2 and CH_3 of the growing polymer chain and possible shorter oligomers. These bands evolve in the regions of 4000–4400 *cm*$^{-1}$, 5600–5900 *cm*$^{-1}$ and 6900–7200 *cm*$^{-1}$ with the assignation given in ***Table 4.3.***

From the on-line MS and *operando* UV-Vis-NIR DRS data two stages of the catalyst reaction can be identified. During the first stage, right from the start of the ethylene feed, the catalyst is being reduced. No bands due to the polymer product can yet be seen in the NIR region of the spectra. On the other hand, it is possible to observe a rise of the MS signal belonging to the fragments of the produced ethylene oligomers. In this stage, ethylene oligomerisation sites were being created and ethylene oligomerised mainly to 1-hexene. The second stage starts later and includes the production of heavier oligomers and PE, as confirmed by the growing NIR bands of the CH_2 and CH_3 groups. It must be noted that the oligomerisation activity of the catalyst is still preserved during the later stage.

4.3.2 UV-Vis-NIR diffuse reflectance spectroscopy

In this ***Chapter***, the influence of titanium and hydrogen on the oligomerisation properties of a TEAl-modified Phillips-type ethylene polymerisation catalyst was investigated and therefore the catalysts tested with different amounts of titanation ***(Table 4.1)*** and a different content of the gas reactant mixture. As was shown in the previous section, the UV-Vis-NIR DRS spectra of the fresh CS catalyst show a highly dehydroxylated catalyst surface, evidenced by a sharp 2ν(SiOH) stretching overtone at ~7325 *cm*$^{-1}$ and a combination ν(SiOH)+δ(SiOH) band at ~4525 *cm*$^{-1}$. The addition of Ti during the preparation of the catalyst materials introduces a 2ν(TiOH) overtone band at 7270 *cm*$^{-1}$ as a shoulder of the silanol stretching band, with the intensity increasing with increasing Ti loading. This group increases the acidity of the catalyst surface and appears at lower wavenumbers as expected due to the increased reduced mass of the functional group. Another characteristic of the fresh catalysts is the presence of three $O \rightarrow Cr^{6+}$ CT bands of mono- and polychromate species appearing in the UV-Vis region. The exact positions of these absorption bands ***(Table 4.1)*** are dependent on the catalyst architecture since any changes in the electronic environment influence the energy levels of Cr. Titanation and an increased amount of Ti from CS to CTS2 cause a shift of the maxima of the UV-Vis bands towards lower energy. This is triggered by the formation of Si-O-Ti-O-Cr bonds where Si is replaced with the less electronegative Ti atom, causing a slight shift of the electron cloud towards the O closest to Cr, populating its energy levels and narrowing the $O \rightarrow Cr^{6+}$ CT energy gap, therefore decreasing the energy required for the charge transfer to occur.[52]

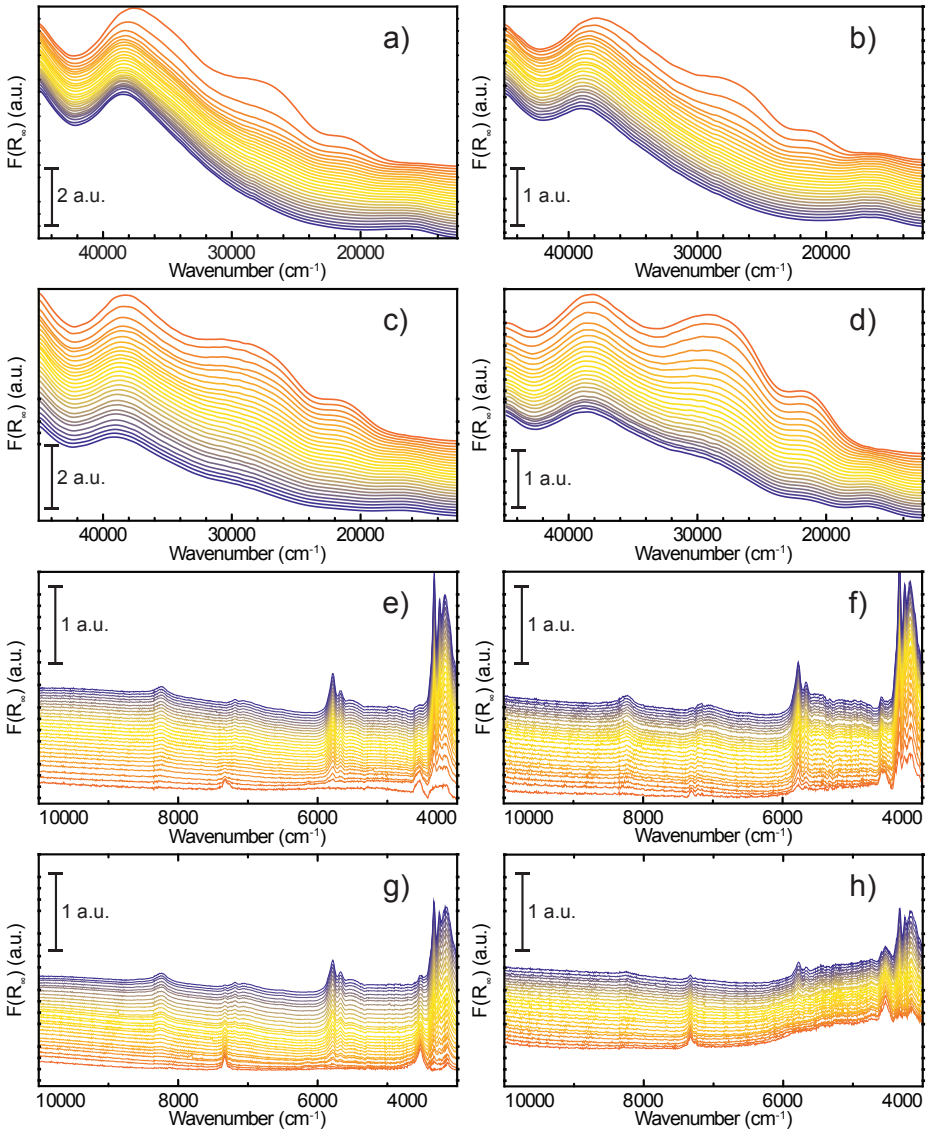

[FIGURE 4.6]
UV-Vis part of the *operando* UV-Vis-NIR DRS spectra of CTS2 and CS Phillips catalysts during polymerisation of ethylene without H_2 **(a)** and **(c)**, and with H_2 **(b)** and **(d)**, respectively, after pre-reacting the catalyst with the TEAl co-catalyst. NIR part of the *operando* UV-Vis-NIR DRS spectra of CTS2 and CS Phillips catalysts during polymerisation of ethylene without H_2 **(e)** and **(g)**, and with H_2 **(f)** and **(h)** after pre-reacting the catalyst with the TEAl co-catalyst. Time evolution of the spectra is indicated by colour transition from orange to blue with 2 *min* between each successive spectrum.

Prior to ethylene polymerisation, all of the tested catalysts were pre-contacted with TEAl. Some of the Cr^{6+} sites were reduced to Cr^{3+} and Cr^{2+} species, as testified by a small intensity decrease of the O→Cr^{6+} CT bands and the appearance of the $^4A_{2g}$→$^4T_{2g}$ d-d transition band of $Cr^{3+}{}_{Oh}$ and the ^5E_g→$^5T_{2g}$ d-d transition band of $Cr^{2+}{}_{Oh}$. Furthermore, TEAl also reacts with the hydroxyl groups of the support, as shown by the broadening and lowering of the intensity of the silanol and titanol group stretching first overtone. However, these changes in the UV-Vis-NIR DRS spectra are not substantial, suggesting that TEAl modifies only some of the Cr sites, which were still enough to produce ethylene oligomers.

Figure 4.6 shows the evolution of the UV-Vis-NIR DRS spectra during ethylene polymerisation using the CS and CTS2 catalysts, with and without hydrogen, after the modification with TEAl. During ethylene polymerisation, Cr^{6+} mono- and dichromate species become significantly reduced by the ethylene reactant to Oh coordinated Cr^{3+} and Cr^{2+} species.[9] Some of these new-formed sites may not only be the active ethylene polymerisation species, but also the products of deactivation of polymerisation sites as a slight shift of the 16 000 cm^{-1} band to higher energies indicates a possible formation of crystalline Cr_2O_3 on the catalyst surface. The influence of titanation on the polymerisation of ethylene can be clearly seen in the time evolution of the *operando* UV-Vis-NIR DRS spectra. By changing the electronic and spatial environments around Cr sites, Ti gives rise to a new type of Cr^{6+} species, which prove to be more reducible than the Cr^{6+} species of the non-titanated catalyst. This effect is evidenced by a more rapid intensity decrease of the O→Cr^{6+} CT bands in the case of CTS2 compared to CS. Consequently, easier reducibility causes a faster development of the polymerisation rate, which can be seen by the growth rate of the overtone and combination vibrational bands of the CH_x groups of the growing PE. In the presence of hydrogen ***(Figure 4.6b*** and ***d)***, the reduction of Cr is even more pronounced due to the reducing properties of hydrogen.

The UV-Vis absorption bands of the polymerisation products could not be measured, since they appear outside of the detectable range of the UV-Vis-NIR DRS spectrophotometer. Absorption, due to the $\sigma \rightarrow \sigma^*$ transition of saturated hydrocarbons, is expected at ~67 000 cm^{-1}. Unsaturation of the C bond, in the case of alkene species, introduces an additional $\pi \rightarrow \pi^*$ transition band in the 52 000–59 000 cm^{-1} range.[53]

4.3.3 Gas chromatography analysis of the reaction products

Although *operando* UV-Vis-NIR DRS is a spectroscopic technique useful to study both the catalyst and the product during the polymerisation reaction, it cannot discriminate between different types of products due to the overlap of NIR bands appearing at the same wavenumbers. ***Figure 4.7-4.9*** show the GC analysis results of the

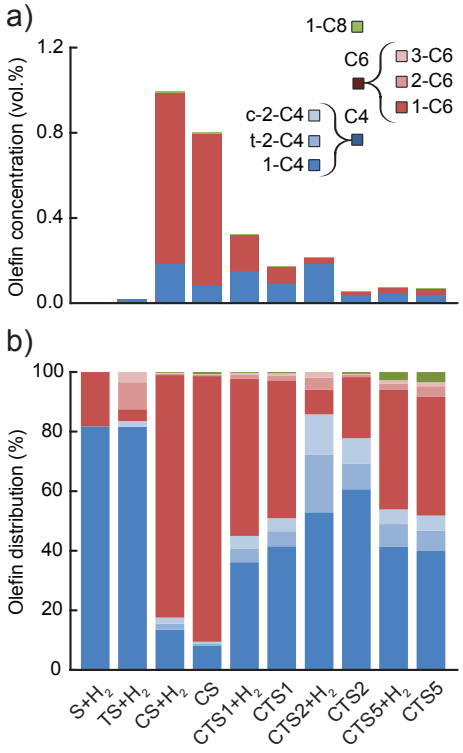

[FIGURE 4.7]
GC analysis of the gas phase during ethylene polymerisation with various Phillips-type catalysts showing different gas phase concentrations **(a)** of the *in-situ* produced C4 (blue), C6 (red) and C8 (green) olefins depending on the catalyst composition. Olefin distribution normalised to 100% **(b)** reveals that the titanation of the catalysts has a detrimental effect on ethylene oligomerisation and selectivity towards industrially important 1-hexene fraction.

gas phase sampled during the polymerisation of ethylene using several different catalysts, with varying Ti loading (0, ~2 and ~4 *wt.%* Ti), Cr loading (0, ~0.5 and ~1 *wt.%* Cr) and activation temperature (823, 923 and 1048 *K*), as summarised in ***Table 4.1***.‡ Each catalyst was tested both with and without 10 *vol.%* hydrogen, while the ratio of ethylene and nitrogen was kept at 1:1.

For the sake of excluding any ethylene oligomerisation activity of the silica carrier or the titania on the silica carrier,§ two additional materials without any Cr were tested, *i.e.* wide-pore silica support (S) and 4 *wt.%* titanated silica (TS), both activated using the same procedure as the actual catalyst. During ethylene polymerisations using these materials with hydrogen and the TEAl co-catalyst, no substantial ethylene

‡ See the footnote on page 92.

§ Supported Ti alkoxides on silica reduced by metal alkyl co-catalyst are reported as active catalysts for ethylene dimerisation.[65] In the case the studied catalysts, it is assumed that virtually all alkoxide groups have been burnt off during the calcination step.

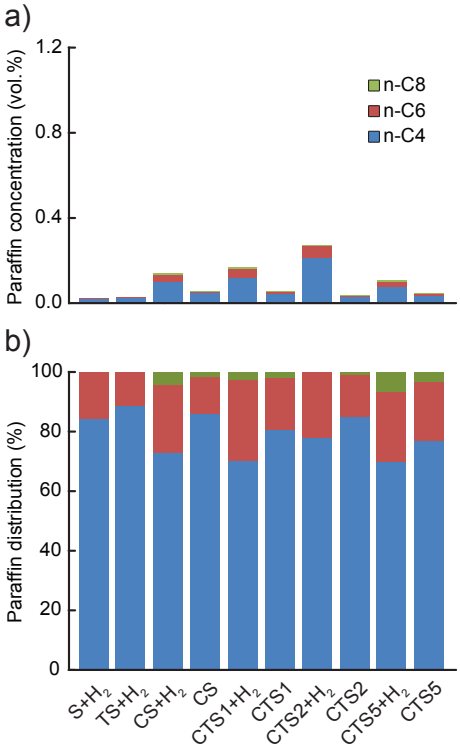

[FIGURE 4.8]
GC analysis of the gas phase during ethylene polymerisation with various Phillips-type catalysts showing different gas phase concentrations **(a)** of the *in-situ* produced C4 (blue), C6 (red) and C8 (green) paraffins depending on the catalyst composition. Paraffin distribution normalised to 100% **(b)** reveals that the titanation of the Phillips-type catalysts does not change significantly the ratio of produced oligomers.

oligomerisation was reported ***(Figure 4.7a*** and ***4.8a)***.

For the actual Phillips-type catalysts, it was observed that the concentration of the produced ethylene oligomers greatly depends on the composition of the catalyst. The highest yield of all oligomers was obtained with the CS catalyst containing no Ti, and it decreases with increasing Ti loading. Detailed analysis of the amounts of olefinic and paraffinic fractions shows that the yield of olefins significantly drops with increasing Ti loading, while the yield of paraffins is slightly increased. The addition of hydrogen to the reaction mixture caused an increase in the overall oligomer yield, with a higher influence on the production of saturated oligomers. Therefore, hydrogen might be involved in the termination of polymer chain growth at the early stages, increasing the concentration of saturated oligomers in the gas phase.

Figure 4.7b and ***4.8b*** show a detailed distribution of the *in-situ* produced olefinic and paraffinic hydrocarbons, respectively, normalised to 100%. Firstly, a clear de-

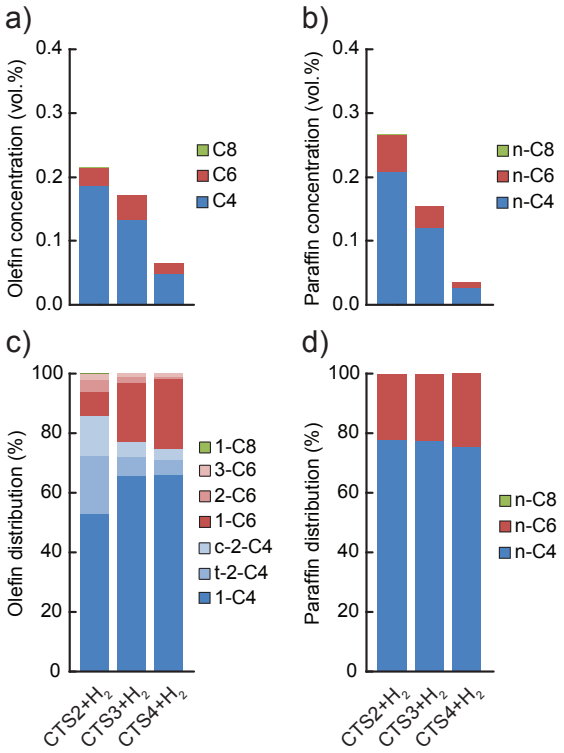

[FIGURE 4.9]
GC analysis of the gas phase during ethylene polymerisation with CTS2, CTS3 and CTS4 Cr/Ti/SiO_2 catalysts activated at 1048 *K*, 923 *K* and 823 *K*, respectively. Decrease of the activation temperature lowers the yields of the *in-situ* produced C4 (blue) and C6 (red) olefins **(a)** and paraffins **(c)**. A lower activation temperature slightly shifts the distribution of *in-situ* produced olefins towards *α*-olefins, particularly 1-hexene **(b)**, having practically no influence on the distribution of paraffins **(d)**.

pendence of the ratio of butenes, hexenes and octenes can be observed, depending on the amount of Ti present in the catalyst. The CS system, without any Ti, exhibited the highest selectivity towards ethylene trimerisation, predominantly producing 1-hexene. The addition of Ti caused a further decrease in the overall ethylene trimerisation selectivity as can be noted for the CTS1 catalyst with ~2 *wt.%* Ti. The most pronounced Ti effect is observed for the catalyst with the highest Ti loading of ~*4 wt.%* where a strong inhibition of ethylene trimerisation sites diminished the amount of hexenes compared to the higher yield of butenes and octenes. In the reaction with the CTS5 catalyst, which contains double the amount of Cr loading compared to the other examined catalysts, the distribution of olefins matches the distribution produced with the CTS1 catalyst of a similar Cr-to-Ti ratio. The distribution of paraffins shows that the relative ratio of the *in-situ* produced *n*-butane, *n*-hexane and *n*-octane is independent of the Ti loading inside the catalyst and that the differences can mainly be

attributed to the presence of hydrogen in the reactant gas mixture. Overall, a higher Ti loading decreases the olefin-to-paraffin ratio within the ethylene oligomers of all chain lengths.

A higher activation temperature of the catalyst showed the promoting effect on the *in-situ* ethylene oligomerisation as can be seen by the increasing amount of produced oligomers starting from the CTS4, over CTS3 to CTS2 catalyst, activated in dry air at 823 *K*, 923 *K* and 1048 *K*, respectively ***(Figure 4.9)***. A higher activation temperature improves the dehydroxylation of the catalyst surface, liberating the coordination sphere of Cr producing more reactive Cr sites, which increases the gas phase oligomer yield. A rise in the activation temperature also shifts the olefin distribution towards butenes and promotes the isomerisation and production of linear β- and γ-olefins.

Figure 4.10 shows the total distribution of hydrocarbon oligomers, split into olefin and paraffin contributions, which can be further presented as Schulz-Flory (SF) diagrams. A clear 1-hexene spike can be observed with the CS catalyst with no Ti. An

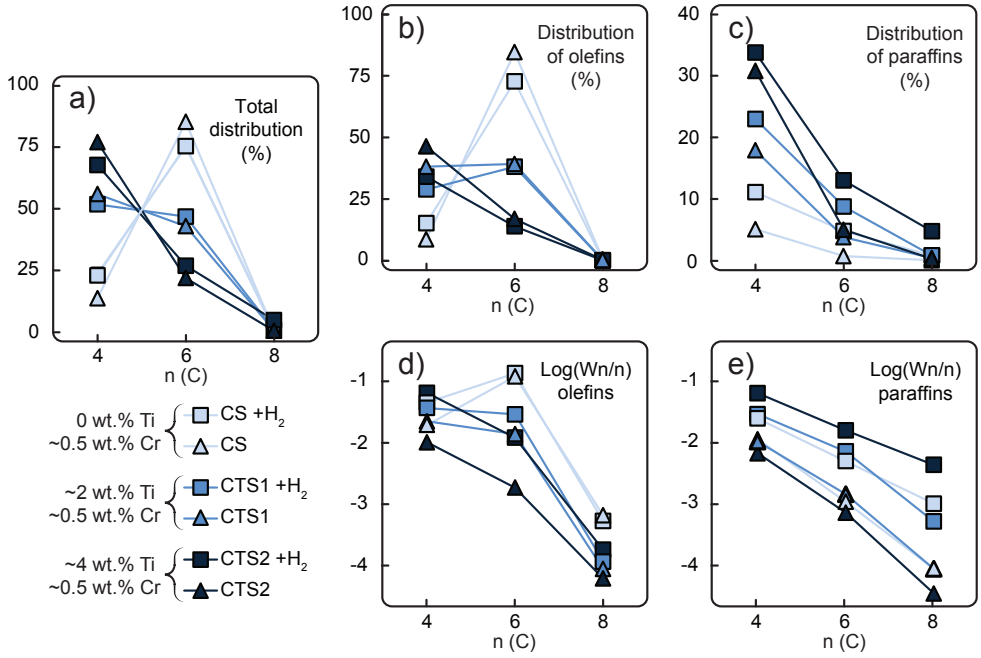

[FIGURE 4.10]
The increase of Ti loading inside the Phillips-type catalyst (from light to dark blue) shifts the selectivity towards C4 at the expense of C6 products in the experiments with (▪) and without (▸) hydrogen. A different trend in the distribution of olefin species **(a)** compared to paraffinic species **(b)** is also clearly visible in Schulz-Flory plots. While paraffinic species show linear curves independent of the Ti loading **(d)**, olefinic species exhibit a discrepancy from linearity with increasing Ti loading **(c)**, indicating an oligomerisation mechanism, which does not follow SF distribution.

[TABLE 4.4]
Chain-growth probability factor *α* for the paraffinic oligomers produced in ethylene oligomerisation reactions.

Catalyst name	α no H_2	α with H_2
CS	0.30	0.45
CTS1	0.33	0.37
CTS2	0.27	0.51
CTS5	0.38	0.46

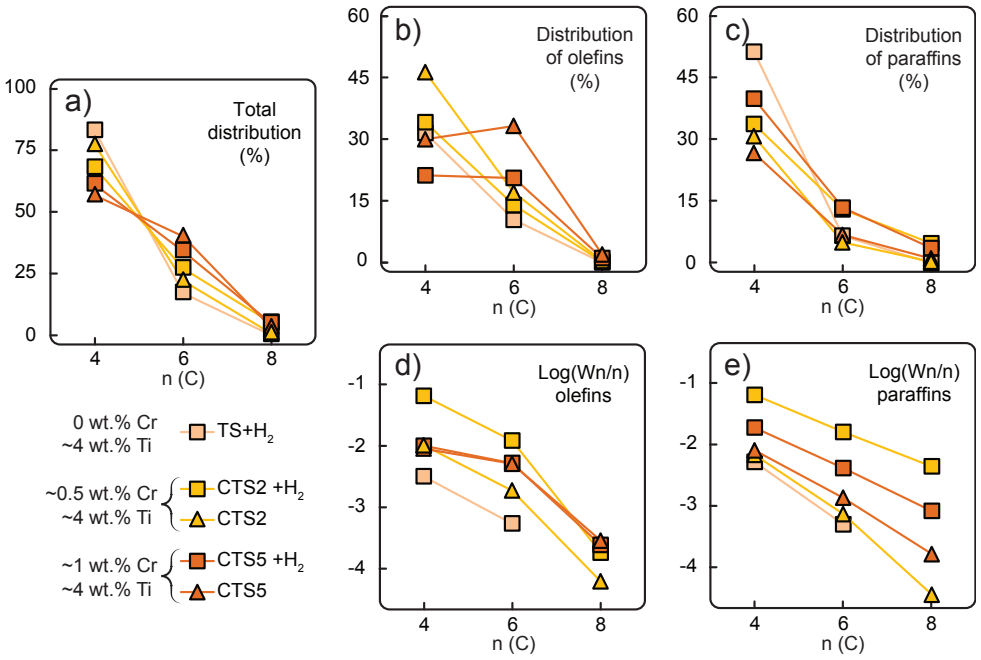

[FIGURE 4.11]
The increase of Cr loading inside the Phillips-type catalyst (from light yellow to orange) increases the selectivity towards C6 products in the experiments with (▪) and without (▸) hydrogen. A different trend in the distribution of olefinic species **(a)** compared to paraffinic species **(b)**, also visible in the Schulz-Flory plots **(c)** and **(d)**, causes a discrepancy from linearity with increasing Cr loading. A higher amount of Cr, while keeping the Ti loading constant, increases the amount of ethylene trimerisation sites, which produce higher amounts of 1-hexene.

increase of the Ti loading significantly decreases the 1-hexene selectivity. If the products follow the SF distribution, caused by the linear-insertion mechanism, a straight curve can be expected with the slope, which represents the chain-growth probability α, determined by the rates of chain growth and termination. The distribution of the *in-situ* produced paraffins exhibits an exponential decay with the increase of carbon number, which is reflected in linear SF curves with α values given in ***Table 4.4.*** Addition of 10 *vol.%* H_2 to the reactant mixture increases α and therefore decreases the selectivity to shorter paraffin oligomers, *i.e. n*-butane. On the other hand, the olefinic oligomers do not show a linear trend in the SF plot in the case of the CS catalyst containing no Ti. With increasing Ti loading, due to the decrease in 1-hexene selectivity, the curves become more linear.

Similar trends can be observed with the CTS5 catalyst with the increased Cr loading of ~1 *wt.%* ***(Figure 4.11)***. A higher Cr loading, while keeping the amount of Ti constant, increases the number of Ti-free Cr sites, which are able to produce selectively ethylene trimers, as illustrated by the non-exponential decay of olefins and the presence of 1-hexene spike. This catalyst samples still contained Ti, which explains the higher amount of ethylene dimers. Nevertheless, the increase in Cr loading appeared to be beneficial for the promotion of ethylene trimerisation.

4.3.4 Ethylene oligomerisation pathway

The analyses of the gas phase collected during the ethylene polymerisation show that the titanation of the Cr/SiO_2 Phillips-type catalyst significantly reduces the yield of ethylene oligomers and shifts the selectivity towards butene fractions. A lower Ti-to-Cr loading ratio appeared to be beneficial for the promotion of the trimerisation of ethylene, as the number of Cr sites, which are not inhibited by Ti, is increased and therefore able to selectively produce more ethylene trimers, indicating a change in the oligomerisation pathway.

Currently, the most widely accepted proposed mechanism of ethylene polymerisation is the Cossee-Arlman mechanism, which explains the chain propagation by linear insertion of the ethylene monomer into an existing alkyl group or polymer, bonded to a Cr active site. The termination of the chain occurs *via* β-H-elimination leaving a vinyl end group in the released hydrocarbon product. As a result of the mentioned ethylene insertion mechanism, the products are expected to follow a statistical hydrocarbon distribution, known as the Schulz-Flory (SF) distribution, with only even-membered hydrocarbon chains due to the presence of ethylene as the only monomer. However, the high 1-hexene spike produced with the non-titanated catalyst can be attributed to the complex structure of the catalyst, with different types of active sites and a complex mechanism of oligomerisation, which cannot be explained

solely by the Cossee-Arlman mechanism of statistical chain growth.

From the results of our study, it is found that two types of distinct oligomerisation mechanisms occur simultaneously with the extent between each other depending on the precise catalyst compositions and hence the electronic environment of the different active sites. Besides the Cossee-Arlman mechanism of linear insertion, in the case of alkane oligomers and PE, alkene species are predominately being produced *via* a metallacyclic mechanism ***(Scheme 4.1)***. Two ethylene molecules are able to coordinate to the vacant coordination sphere of the Cr active site and form a chromacyclopentane ring. Two processes can occur at this stage, either *β*-H-transfer and release of 1-butene, or coordination and insertion of another ethylene monomer to form chromacycloheptane ring. This process can continue even further and form bigger chromacyclic rings, where the release of olefin *via β*-H-transfer occurs when the probability of insertion of a new monomer becomes lower than the probability of *β*-H-transfer. The stability of the chromacyclic ring is highly influenced by the structure of Cr active sites. As revealed in the *operando* UV-Vis-NIR DRS spectra, titanation of the catalyst changes the structure of the Cr oligomerisation sites by forming Si-O-Ti-O-Cr linkages, as testified by the red shifts of $O \rightarrow Cr^{6+}$ CT bands and introduces free surface titanol groups, which increase the acidity of the catalyst surface. Consequently, an increasing Ti loading decreases the stability of the 5-membered chromacyclopentane ring, favouring *β*-H-transfer and the release of 1-butene and therefore reducing the selectivity towards 1-hexene. Alternatively, given the DFT studies of Robinson *et al.*[54] and the work of Emrich *et al.*,[55] the high 1-butene selectivity in the case of the titanated catalysts can be explained by the Cossee-Arlman mechanism over the oligomerisation sites with a very low *α*, while 1-hexene is still being produced over trimerisation sites *via* the metallacyclic mechanism.

Ethylene trimerisation catalysts have been reported for chromium-based homo-

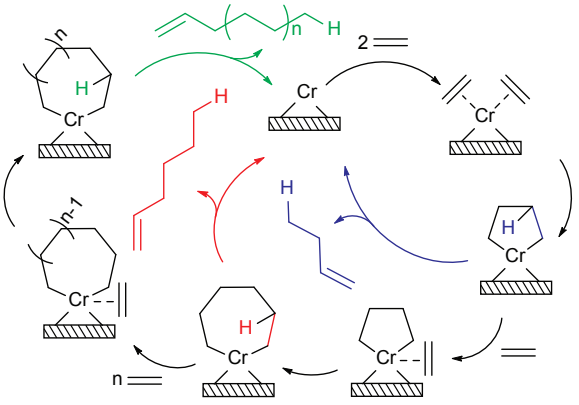

[SCHEME 4.1]
Metallacyclic mechanism for selective ethylene oligomerisation.

geneous systems, basically consisting of multidentate ligands reacted with chromium salts and activated with aluminium alkyl co-catalyst, some of them being commercialised.[56–59] The isotopic labelling and regiochemistry studies of Agapie *et al.*[60,61] on such catalytic systems strongly support the metallacyclic mechanism of the selective ethylene trimerisation and tetramerisation, which might occur through the Cr^{+}/Cr^{3+} and Cr^{2+}/Cr^{4+} redox cycles as shown by the X-ray absorption spectroscopy (XAS) and electron paramagnetic resonance (EPR).[62–64] Similarly, the metallacyclic mechanism was proposed for the silica-supported chromium catalyst discussed in this ***Chapter***, although it has to be noted that a heterogeneous catalyst is more difficult to define due to the heterogeneity of different surface chromium sites. The advantage of the catalyst material examined in this ***Thesis*** is its multifuncionality, *i.e.* the selective oligomerisation capabilities of some of the chromium sites and co-/polymerisation activity of other sites, within a single Phillips catalyst.

4.4 CONCLUSIONS

The oligomerisation properties of a TEAl-modified Phillips-type ethylene polymerisation catalyst were tested in a specially developed *operando* setup allowing the relation of data gathered by UV-Vis-NIR diffuse reflectance spectroscopy, mass spectrometry and gas chromatography techniques. This combination of methods allowed a real-time study of working catalysts and reaction products. The incorporation of titanium inside the Cr/SiO_2 Phillips-type catalysts by the formation of Cr-O-Ti-O-Si linkages alters the electronic environment of Cr ions and changes the oligomerisation capabilities of the catalyst. Consequently, different distributions of the *in-situ* produced ethylene oligomers were revealed, highly dependent on the architecture of the catalyst. Paraffinic oligomers show an exponential decay explained by the Cossee-Arlman linear insertion mechanism. On the contrary, olefinic oligomers in the case of the non-titanated Cr/SiO_2 catalyst exhibit a much more complex distribution, with a higher selectivity towards 1-hexene than what is expected from the linear insertion mechanism. The high ethylene trimerisation activity is a consequence of the metallacyclic oligomerisation mechanism. The addition of Ti modifies the trimerisation Cr sites and creates new oligomerisation sites, which favour β-H-transfer in the chromacyclopentane intermediate and release of the 1-butene product, therefore decreasing the selectivity towards 1-hexene. These results open new possibilities for both academic and industrial research of the Phillips polymerisation system, as they show that by a proper selection of the catalyst structure it is possible to change the distribution of the *in-situ* produced oligomers and therefore change the amount of α-olefins that are able to co-polymerise with ethylene to form the desired grade of PE.

4.5 ACKNOWLEDGMENTS

Gerrit van Hauwermeiren and Julien Decrom (Total Research and Technology, Feluy) are acknowledged for preparation of the catalyst materials. Ad Mens (Utrecht University) is acknowledged for the construction of the experimental setup.

4.6 REFERENCES

[1] M. P. McDaniel, *Adv. Catal.* **2010**, *53*, 123–606.

[2] E. Groppo, C. Lamberti, S. Bordiga, G. Spoto, A. Zecchina, *Chem. Rev.* **2005**, *105*, 115–184.

[3] B. M. Weckhuysen, R. A. Schoonheydt, *Catal. Today* **1999**, *51*, 215–221.

[4] R. Cheng, Z. Liu, L. Zhong, X. He, P. Qiu, M. Terano, M. S. Eisen, S. L. Scott, B. Liu, *Adv. Polym. Sci.* **2013**, *257*, 135–202.

[5] J. P. Hogan, R. L. Banks, US2825721, **1958**.

[6] J. P. Hogan, R. L. Banks, US2951816, **1960**.

[7] R. Merryfield, M. P. McDaniel, G. Parks, *J. Catal.* **1982**, *77*, 348–359.

[8] B. Liu, P. Šindelář, Y. Fang, K. Hasebe, M. Terano, *J. Mol. Catal. A Chem.* **2005**, *238*, 142–150.

[9] B. M. Weckhuysen, L. M. De Ridder, R. A. Schoonheydt, *J. Phys. Chem.* **1993**, *97*, 4756–4763.

[10] B. M. Weckhuysen, L. M. De Ridder, P. J. Grobet, R. A. Schoonheydt, *J. Phys. Chem.* **1995**, *99*, 320–326.

[11] B. M. Weckhuysen, A. A. Verberckmoes, A. R. de Baets, R. A. Schoonheydt, *J. Catal.* **1997**, 166, 160–171.

[12] L. Zhong, M.-Y. Lee, Z. Liu, Y.-J. Wanglee, B. Liu, S. L. Scott, *J. Catal.* **2012**, *293*, 1–12.

[13] C. A. Demmelmaier, R. E. White, J. A. van Bokhoven, S. L. Scott, *J. Catal.* **2009**, *262*, 44–56.

[14] A. Zecchina, E. Groppo, A. Damin, C. Prestipino, in *Top. Organomet. Chem.* (Eds.: C. Copéret, B. Chaudret), Springer, Berlin, **2005**, vol. 16, pp. 1–35.

[15] B. M. Weckhuysen, A. A. Verberckmoes, A. L. Buttiens, R. A. Schoonheydt, *J. Phys. Chem.* **1994**, *98*, 579–584.

[16] B. M. Weckhuysen, I. E. Wachs, R. A. Schoonheydt, *Chem. Rev.* **1996**, *96*, 3327–3350.

[17] D. S. McGuinness, N. W. Davies, J. Horne, I. Ivanov, *Organometallics* **2010**, *29*, 6111–6116.

[18] E. Groppo, C. Lamberti, S. Bordiga, G. Spoto, A. Zecchina, *J. Catal.* **2006**, *240*, 172–181.

[19] E. Groppo, J. Estephane, C. Lamberti, G. Spoto, A. Zecchina, *Catal. Today* **2007**, *126*, 228–234.

[20] a) M. P. Conley, M. F. Delley, G. Siddiqi, G. Lapadula, S. Norsic, V. Monteil, O. V. Safonova, C. Copéret, *Angew. Chem. Int. Ed.* **2014**, *53*, 1872–1876. (b) M. P. Conley, M. F. Delley, G. Siddiqi, G. Lapadula, S. Norsic, V. Monteil, O. V. Safonova, C. Copéret, *Angew. Chem. Int. Ed.* **2015**, *53*, 6670–6670.

[21] M. F. Delley, M. P. Conley, C. Copéret, *Catal. Lett.* **2014**, *144*, 805–808.

[22] S. L. Scott, J. Amor Nait Ajjou, *Chem. Eng. Sci.* **2001**, *56*, 4155–4168.

[23] A. Fong, Y. Yuan, S. L. Ivry, S. L. Scott, B. Peters, *ACS Catal.* **2015**, *5*, 3360–3374.

[24] R. E. Dietz, US3887494, **1975**.

[25] G. Debras, J.-P. Dath, EP0882743 B1, **1998**.

[26] T. J. Pullukat, D. Plaines, M. Shida, US3780011, **1973**.

[27] J. P. Hogan, D. R. Witt, US3622521, **1971**.

[28] B. Horvath, US3625864, **1971**.

[29] T. J. Pullukat, R. E. Hoff, M. Shida, *J. Polym. Sci. Polym. Chem. Ed.* **1980**, *18*, 2857–2866.

[30] L. L. Böhm, *Angew. Chem. Int. Ed.* **2003**, *42*, 5010–5030.

[31] G. Wilke, *Angew. Chem. Int. Ed.* **2003**, *42*, 5000–5008.

[32] H. H. Brintzinger, D. Fischer, R. Mulhaupt, B. Rieger, R. M. Waymouth, R. Mülhaupt, B. Rieger, R. M. Waymouth, *Angew. Chem. Int. Ed.* **1995**, *34*, 1143–1170.

[33] D. L. Myers, J. H. Lunsford, *J. Catal.* **1986**, *99*, 140–148.

[34] B. M. Weckhuysen, H. J. Spooren, R. A. Schoonheydt, *Zeolites* **1994**, *14*, 450–457.

[35] G. Ghiotti, E. Garrone, A. Zecchina, *J. Mol. Catal.* **1988**, *46*, 61–77.

[36] D. D. Beck, J. H. Lunsford, *J. Catal.* **1981**, *68*, 121–131.

[37] B. M. Weckhuysen, R. A. Schoonheydt, F. E. Mabbs, D. Collison, *J. Chem. Soc. Faraday Trans.* **1996**, *92*, 2431.

[38] J.-M. Jehng, I. E. Wachs, B. M. Weckhuysen, R. A. Schoonheydt, *J. Chem. Soc. Faraday Trans.* **1995**, *91*, 953–961.

[39] M. F. Delley, F. Núñez-Zarur, M. P. Conley, A. Comas-Vives, G. Siddiqi, S. Norsic, V. Monteil, O. V. Safonova, C. Copéret, *Proc. Natl. Acad. Sci. U. S. A.* **2014**, *111*, 11624–11629.

[40] D. Cicmil, J. Meeuwissen, A. Vantomme, J. Wang, I. K. Ravenhorst, H. E. van der Bij, A. Muñoz-Murillo, B. M. Weckhuysen, *Angew. Chem. Int. Ed.* **2015**, *54*, 13073–13079; **Chapter 2**

[41] W. Xia, B. Liu, Y. Fang, K. Hasebe, M. Terano, *J. Mol. Catal. A Chem.*, **2006**, *256*, 301–308.

[42] "Platts Global Ethylene Price Index, www.platts.com/news-feature/2015/petrochemicals/pgpi/ethylene, (accessed June **2015**).

[43] E. Groppo, K. Seenivasan, C. Barzan, *Catal. Sci. Technol.* **2013**, *3*, 858–878.

[44] C. Lamberti, A. Zecchina, E. Groppo, S. Bordiga, *Chem. Soc. Rev.* **2010**, *39*, 4951–5001.

[45] A. Damin, F. Bonino, S. Bordiga, E. Groppo, C. Lamberti, A. Zecchina, *ChemPhysChem* **2006**, *7*, 342–344.

[46] W. Xia, B. Liu, Y. Fang, T. Fujitani, T. Taniike, M. Terano, *Appl. Catal. A Gen.*, **2010**, *389*, 186–194.

[47] F. C. Jentoft, *Adv. Catal.* **2009**, *52*, 129–211.

[48] R. A. Schoonheydt, *Chem. Soc. Rev.* **2010**, *39*, 5051–5066.

[49] B. M. Weckhuysen, R. A. Schoonheydt, *Catal. Today* **1999**, *51*, 223–232.

[50] S. Petit, J. Madejova, A. Decarreau, F. Martin, *Clays Clay Miner.* **1999**, *47*, 103–108.

[51] M. Watari, *Appl. Spectrosc. Rev.* **2013**, *49*, 462–491.

[52] C. E. Housecroft, A. G. Sharpe, *Inorganic Chemistry*, Pearson Education Limited, Harlow, 2nd ed., **2005**, pp. 555–588.

[53] P. S. Kalsi, *Spectroscopy of Organic Compounds*, New Age International (P) Ltd. Publishers, New Delhi, 6th ed., **2007**, pp. 11–14.

[54] R. Robinson, D. S. Mcguinness, B. F. Yates, *ACS Catal.*, **2013**, *3*, 3006–3015.

[55] R. Emrich, O. Heinemann, P. W. Jolly, C. Krüger, G. P. J. Verhovnik, *Organometallics*, **1997**, *16*, 1511–1513.

[56] W. K. Reagen, EP0417477 A2, **1990**.

[57] J. R. Briggs, US4668838, **1987**.

[58] F.-J. Wu, US5550305, **1996**.

[59] J. T. Dixon, P. Wasserscheid, D. S. McGuinness, F. M. Hess, H. Maumela, D. H. Morgan, A. Bollmann, EP2075242 A1, **2007**.

[60] T. Agapie, S. J. Schofer, J. A. Labinger, J. E. Bercaw, *J. Am. Chem. Soc.*, **2004**, *126*, 1304–1305.

[61] T. Agapie, J. A. Labinger and J. E. Bercaw, *J. Am. Chem. Soc.*, **2007**, *129*, 14281–14295.

[62] L. H. Do, J. A. Labinger, J. E. Bercaw, *ACS Catal.*, **2013**, *3*, 4–7.

[63] I. Y. Skobelev, V. N. Panchenko, O. Y. Lyakin, K. P. Bryliakov, V. A. Zakharov and E. P. Talsi, *Organometallics*, **2010**, *29*, 2943–2950.

[64] J. Rabeah, M. Bauer, W. Baumann, A. E. C. Mcconnell, W. F. Gabrielli, P. B. Webb, D. Selent and A. Bru, *ACS Catal.*, **2013**, *3*, 95–102.

[65] P. D. Smith, D. D. Klendworth, M. P. McDaniel, *J. Catal.* **1987**, *105*, 187–198.

UNIVERSITEIT UTRECHT ACADEMIEGEBOUW
Utrecht, The Netherlands

V

Summary and Future Perspectives

Polyethylene (PE) presents a large class of polymers with an exponentially growing consumption worldwide. Although possessing a relatively simple chemical formula of the repeating CH_x units, the chain length, the type and length of the branching, and density, offer a wide scope of possible PE grades, each suitable for different types of commercial application. Since the 1950s, several types of ethylene polymerisation catalysts and polymerisation processes have been developed. Linear low density polyethylene (LLDPE) is one of the most versatile types of PE, being used for the production of thin films, bags, toys, containers, pipes, covers and flexible tubing. The production of LLDPE involves the co-polymerisation of ethylene with α-olefins using Phillips, Ziegler-Natta or metallocene-type catalysts in gas, slurry or solution phase processes. In this ***Dissertation***, the triethylaluminium (TEAl)-induced *in-situ* ethylene oligomerisation properties of $Cr/Ti/SiO_2$ Phillips-type catalysts have been studied in order to offer an alternative route for the incorporation of short-chain branching inside the PE, without the need of an additional α-olefin feed, multiple reactors or catalysts. This was achieved through the integration of multiple analytical techniques and the development of new *operando* setups. The presented findings open a new era of Phillips-type polymerisation catalysis, while the developed methods offer a unique approach to study other catalytic systems in great detail.

5.1 SUMMARY

The motivation for the work studied in this ***Dissertation*** is based on a serendipitous finding at an industrial polymerisation plant, where PE was being produced using Ziegler-Natta and Phillips-type catalysts. During one run on a chromium polymerisation line with the $Cr/Ti/SiO_2$ catalyst, the *in-situ* generation of ethylene co-monomers was suspected as it was required to reduce the usual amount of 1-hexene feed in order to achieve the same amount of branching inside the PE. This effect was caused by the contamination of chromium polymerisation lines with TEAl from the lines that were running Ziegler-Natta-type catalysts.

In that respect, a new TEAl-modified surface-titanated $Cr/Ti/SiO_2$ catalyst was developed and analysed both at the macroscopic and microscopic scales as described in ***Chapter 2***. Firstly, the catalyst was tested in slurry-phase ethylene polymerisation experiments in a 4 *L* semi-batch reactor. Its performance was compared to the $Cr/Ti/SiO_2$ catalyst, which was not modified with TEAl, but used in a reaction with externally added 1-hexene co-monomer in order to introduce the butyl branching. ^{13}C NMR experiments confirmed the *in-situ* generation of co-monomer by the detection of mainly butyl branches in the PE. Further GPC-IR analysis of the PE resin showed that the TEAl-modified catalyst produced PE with more interesting molecular weight distribution (MWD) and short-chain branching distribution (SCBD) as the desired reverse incorporation of co-monomer into longer PE chains was promoted when co-monomer was generated *in-situ* with the TEAl-modified $Cr/Ti/SiO_2$ catalyst, com-

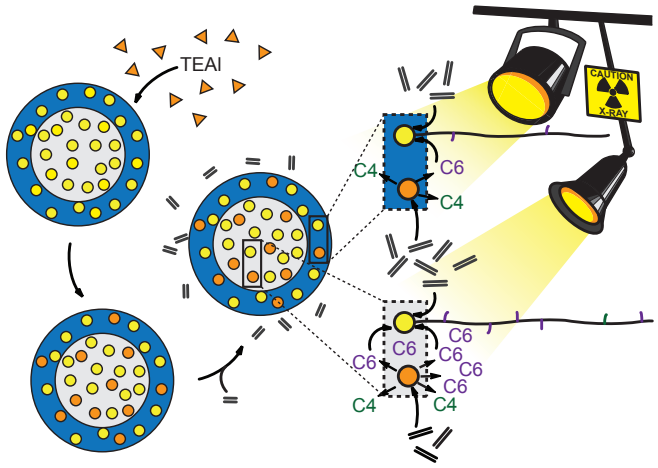

[FIGURE 5.1]
STXM proved to be an indispensable micro-spectroscopy method able to discriminate between the active sites producing low molecular weight linear chain and high molecular weight short-chain branched polyethylene within a single TEAl-modified Phillips catalyst particle.

pared to the polymerisation reactions with externally added co-monomer and Cr/Ti/SiO_2 catalyst, which is not modified with TEAl. The catalyst was further characterised with various bulk techniques, *i.e.* DRIFTS, UV-Vis-NIR DRS, EPR and XRD, and microscopic techniques, *i.e.* SEM-EDX and STXM, in order to achieve a complete picture of the pristine Cr/Ti/SiO_2 catalyst, the catalyst after modification with TEAl and the catalyst-PE product after the polymerisation of ethylene. STXM provided for the first time microscopic insight into the Phillips Cr/Ti/SiO_2 catalyst particle and the spatial distribution of its constituting elements including the low abundant Cr. Ultimately, the study revealed that the catalyst was able to produce two different types of PE. Low molecular weight linear-chain PE with less branching was produced in the Ti-rich catalyst particle shell, compared to the Ti-scarce areas inside the catalyst particle core, where high molecular weight short-chain branched PE was produced ***(Figure 5.1)***. The presence of Ti inside the catalyst particle shell not only inhibits the incorporation of co-monomer but also inhibits the *in-situ* generation of co-monomer. Therefore, shorter linear PE chains are created in the Ti-abundant shell while on the Ti-scarce TEAl-modified Cr sites co-monomer is *in-situ* produced and subsequently incorporated on the polymerisation sites producing longer chains leading to the reverse co-monomer incorporation. It was shown that the catalyst particle structure directly influences the polymer composition by confirming the macroscale findings on a microscopic level.

In ***Chapter 3***, the TEAl-modified and TEAl-unmodified Cr/SiO_2 and Cr/Ti/SiO_2 Phillips-type ethylene polymerisation catalysts were further analysed with diffuse re-

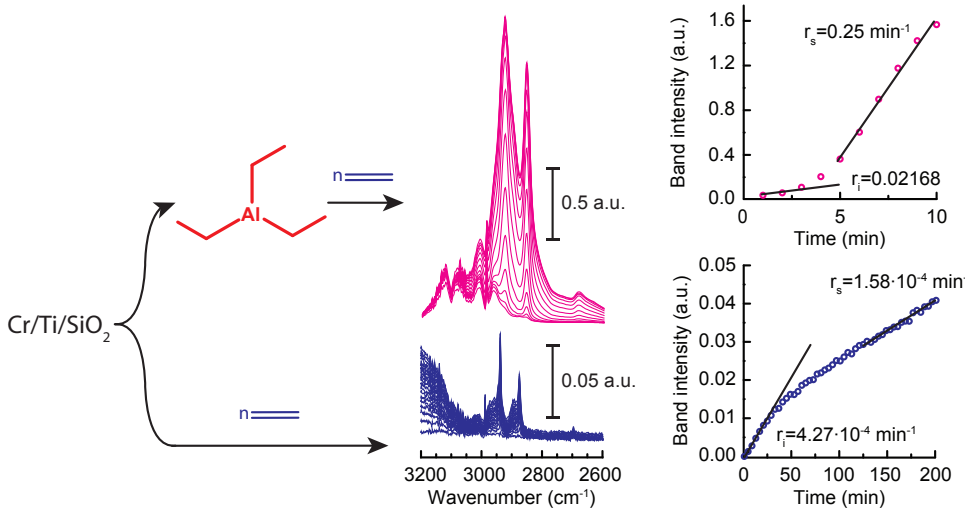

[FIGURE 5.2]
The TEAl-modified Cr/Ti/SiO_2 catalyst (magenta) exhibits significantly higher polymerisation activity than the original catalyst, which was not pre-treated with TEAl (blue).

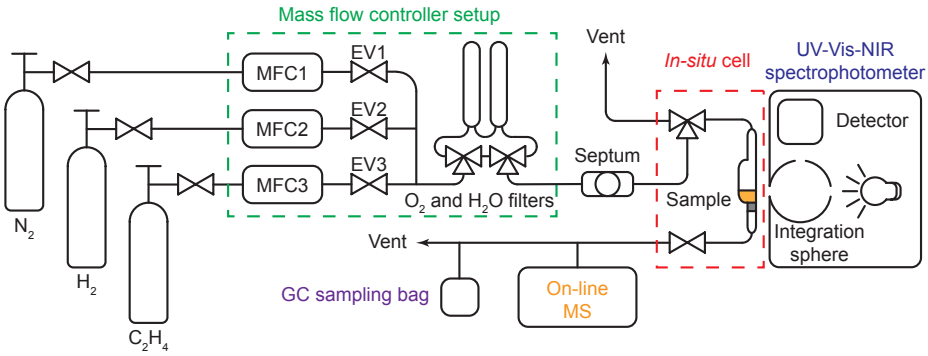

[FIGURE 5.3]
UV-Vis-NIR diffuse reflectance spectroscopy, mass spectrometry and gas chromatography setup developed for the testing of solid catalysts and products obtained in the gas phase in reactions at 1 *bar* and temperatures in the range from RT to 473 *K*. The *operando* setup includes changeable gas reactant sources, mass flow controller setup (green), septum for the injection of co-catalyst, 4 cm^3 air-tight quartz reactor (red), Varian Cary 500 spectrophotometer (blue), OmniStar mass spectrometer (orange) and gas sampling bag for the GC(-MS) analysis of gas phase (magenta). All lines and the reactor are traced and heated to the desired reaction temperature monitored by a couple of thermocouples.

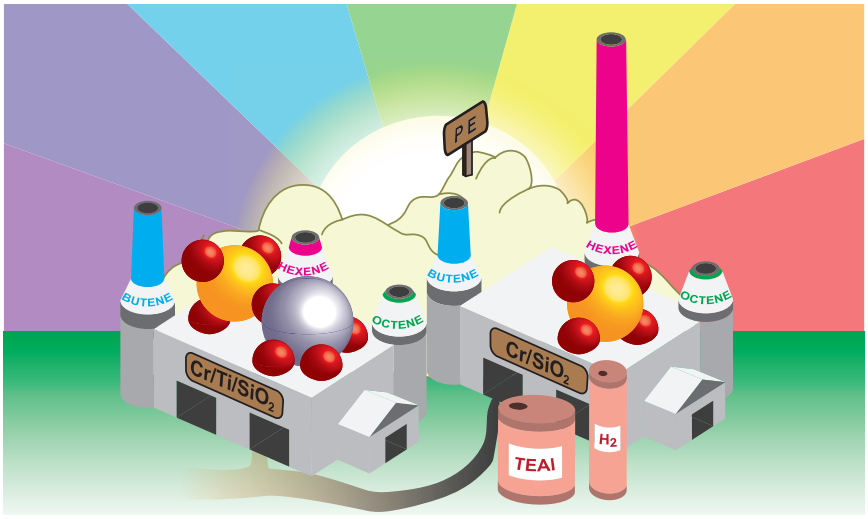

[FIGURE 5.4]
The yield and the distribution of the *in-situ* produced LAOs shows a high dependency on the catalyst structure and polymerisation conditions. The formation of Cr-O-Ti-O-Si linkages favours the *β*-H-transfer, while decreasing the selectivity towards 1-hexene.

flectance infrared Fourier-transform spectroscopy (DRIFTS) in a specially designed setup, which allowed the analysis of the vibrational modes of the catalyst and PE product with a minimal sample preparation under *operando* conditions. Several different catalyst compositions, containing 0, 2 and 4 *wt.%* of total Ti loading, were tested in order to investigate the influence of the degree of titanation and modification with TEAl. The analysis of the hydroxyl group stretching region of the Cr/SiO_2 and $Cr/Ti/SiO_2$ catalysts allows us to discuss in depth the origin of the 3610 cm^{-1} band. It was concluded that this band can be assigned to the stretching vibration of bridged titanol group in contrast to the earlier proposed bridged silanol group interacting with a chromium centre,[1] as it is present only in the catalyst and support materials containing titanium.

Time-resolved DRIFT spectra and related kinetic analysis of the data showed a promotional effect on the shortening of the induction time and the increase of the polymerisation rate with increasing titanium loading inside the catalyst, attributed to the increase of the support acidity. The catalyst modified with TEAl prior to the polymerisation of ethylene exhibited a significant increase of the polymerisation activity ***(Figure 5.2)***. However, the process of *in-situ* ethylene oligomerisation could not be confirmed with DRIFTS under the selected experimental conditions.

The focus was further kept on the TEAl-modified $Cr/Ti/SiO_2$ catalysts as the new *operando* setup has been developed ***(Figure 5.3)***, which allowed the investigation of the working catalysts by UV-Vis-NIR diffuse reflectance spectroscopy (DRS), while the gas phase was continuously monitored by on-line mass spectrometry (MS) and in the end analysed by gas chromatography (GC). The results presented in ***Chapter 4*** offered not only the insight on the changes of the electronic properties of Cr in the UV-Vis-NIR spectra and the detection of the forming PE, but also gave the possibility to detected the *in-situ* produced light linear α-olefins (LAOs) and to elucidate the influence of the degree of titanation of the catalyst, activation temperature and hydrogen added to the reactant mixture on the selective oligomerisation ***(Figure 5.4)***. Non-titanated Cr/SiO_2 Phillips-type catalyst shows a higher activity towards ethylene oligomerisation with a higher selectivity to 1-hexene. The 1-hexene spike causes the deviation from the distribution expected from the linear insertion mechanism attributing the high ethylene trimerisation activity to the metallacyclic ethylene oligomerisation mechanism. The titanation of the catalyst causes the formation of Cr-O-Ti-O-Si linkages and creation of more reducible Cr^{6+} species than in the non-titanated catalyst, leading to the faster development of the polymerisation rate. On the other hand, titanation also decreases the oligomerisation activity while the newly created oligomerisation active sites favour β-H-transfer in the chromacyclopentane intermediate increasing the selectivity towards 1-butene. The addition of hydrogen

to the ethylene reactant mixture increases the overall oligomer yield, especially of the saturated oligomers. As a chain-transfer agent, hydrogen is involved at the early stages of the polymerisation in the termination of the chain growth, increasing the concentration of saturated oligomers. Higher activation temperature increases the oligomer yield due to the creation of more reactive Cr sites with liberated coordination sphere through the dehydroxilation of the catalyst surface.

5.2 FUTURE PERSPECTIVES

From this ***Thesis*** a number of scientific questions and ideas emerge. The production of PE with reverse co-monomer incorporation without any externally added co-monomer *via* the *in-situ* oligomerisation of ethylene, opens the possibility for the industrial production of this specific type of LLDPE using a single catalyst. The practical advantages are numerous. First of all, the elimination of a separate co-monomer feed decreases the price of raw materials. The costs of the purification, transport and chances of reactor poisoning are thus also decreased. The catalyst can be utilised within the existing Phillips polymerisation lines while the whole process in order to produce PE with reverse SCBD can be performed within a single-reactor system in contrast to dual-reactor systems ***(Figure 5.5)***. Furthermore, the compatibility issues of the catalysts used in tandem catalysis could be also avoided.

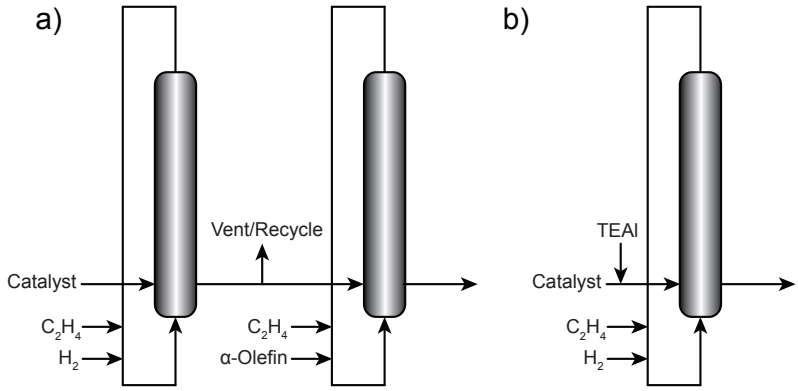

[FIGURE 5.5]
a) Dual-reactor system for the production of PE with reverse co-monomer incorporation. In the first reactor, low molecular weight PE is being produced in the absence of an α-olefin co-monomer and continuously transferred to the second reactor where higher molecular weight PE is being produced with short-chain branching coming from the co-polymerisation with externally added α-olefin co-monomer. **b)** Single reactor alternative for the production of PE with reverse co-monomer incorporation using the TEAl-modified Cr/Ti/SiO_2 catalyst described in this ***Thesis***. In this case, the co-monomer is produced inside the reactor. Adapted from Soares and McKenna.[2]

In order to optimise the polymerisation and oligomerisation activity and selectivity of the *in-situ* produced olefins, the structure of the presented catalyst can be modified. For example, the influence of a different size of the titanated shell may have an effect on the relative amounts of short-chain branched PE and PE with less branching. Another interesting study could be the investigation of the more homogeneous titanation of the catalyst particle by using co-gel silica-titania as the support material. Furthermore, the range of possible co-catalyst materials, not only limited to aluminium alkyls, is rather vast and would certainly require future attention. For example, hydrosilanes proved to be a highly effective co-catalyst in the production of LLDPE by co-monomer free polymerisation of ethylene.[3-5]

Additional work on the mechanistic elucidation of the *in-situ* oligomerisation process and the role of hydrogen would include the isotopic labelling experiments with the $^{13}C_2H_4$, C_2D_4 and D_2 as reactants, especially helpful for the infrared studies in order to avoid the overlap of the alkyl groups of different compounds.

Ultimately, the characterisation methods and setups developed for the research of this catalytic system can be applicable for other studies involving solid catalysts, especially in the case of very sensitive materials when a highly controlled reaction atmosphere or when the minimal sample manipulation is required. Further improvement of the setup could include the design of a new type of reactors in order to expand its applicability to both high and low ethylene pressure reactions.

5.3 REFERENCES

[1] M. P. Conley, M. F. Delley, G. Siddiqi, G. Lapadula, S. Norsic, V. Monteil, O. V. Safonova, C. Copéret, *Angew. Chem. Int. Ed.* **2014**, *53*, 1872–1876.

[2] J. B. P. Soares, T. F. L. McKenna, *Polyolefin Reaction Engineering*, Wiley-VCH, Weinheim, **2012**, pp. 17–27.

[3] S. J. Martin, E. A. Benham, M.P. McDaniel, B. W. Gerhold, US4988657, **1991**.

[4] M. P. McDaniel, *Adv. Catal.* **2010**, *53*, 123–606.

[5] C. Barzan, D. Gianolio, E. Groppo, C. Lamberti, V. Monteil, E. A. Quadrelli, S. Bordiga, *Chem. Eur. J.* **2013**, *19*, 17277–17282.

RIJN EN ZON WINDMOLEN
Utrecht, The Netherlands

VI

Nederlandse Samenvatting

Polyethyleen (PE) is één van de belangrijkste klassen polymeren met een exponentieel groeiende markt wereldwijd. De diversiteit in het gebruik van polyethyleen is ondanks de relatief simpele chemische formule te herleiden naar parameters als ketenlengte, het soort en de lengte van de vertakkingen en de dichtheid. Sinds de jaren 1950 zijn er verschillende katalysatoren en processen ontwikkeld voor de productie van PE. Een belangrijke klasse polyethyleen is het lineaire lage dichtheid polyethyleen (LLDPE). Dit is een veelzijdig polymeer met verscheidene toepassingen zoals filmen, tassen, speelgoed, boxen, buizen en flexibele leidingen. De productie van LLDPE omvat de co-polymerisatie van ethyleen met α-olefines met behulp van een Phillips, Ziegler-Natta of metalloceen-type katalysator in gas-, slurry- of oplossingsfaseprocessen. Het werk dat is beschreven in dit proefschrift bestudeerd triethylaluminium (TEAl) als promotor voor de *in-situ* oligomersatie van ethyleen met behulp van een $Cr/Ti/SO_2$ Phillips-type-katalysator, met als doel het vinden van een alternatieve route voor het vormen van korte-keten vertakkingen in PE zonder dat daar extra α-olefines, meerdere reactoren of katalysatoren voor nodig zijn. Dit werd bereikt door de integratie van meerdere analysetechnieken en de ontwikkeling van nieuwe *operando*-opstellingen. Dit proefschrift biedt nieuw inzicht in de Phillips polymerisatie-katalysator terwijl tegelijkertijd methodes zijn ontwikkeld welke ook voor de studie van andere katalysatorsystemen uitermate geschikt zijn.

6.1 SAMENVATTING

Het werk dat in dit ***Proefschrift*** wordt beschreven is gebaseerd op een toevallige ontdekking bij een polymerisatie fabriek waar PE werd geproduceerd met behulp van Ziegler-Natta en Phillips-type-katalysatoren. Tijdens een reactie in een chroom-polymerisatielijn met een $Cr/Ti/SiO_2$ katalysator bleek dat ethyleen co-monomeren *in-situ* werden gevormd. Dit kon worden afgeleid uit het feit dat de gevormde PE met een zekere hoeveelheid vertakkingen alleen gevormd kan worden als de aanwezige 1-hexaan door ethyleen gereduceerd wordt. Deze chromium lijn bleek vervuild te zijn met TEAl dat gebruikt wordt bij processen met Ziegler-Natta- katalysatoren.

Op basis hiervan werd een nieuwe met TEAl behandelde $Cr/Ti/SiO_2$ katalysator met titanium in de buitenste laag van de katalysatordeeltjes ontwikkeld. De katalysator is geanalyseerd op macroscopisch en microscopische schaal, zoals staat beschreven in ***Hoofstuk 2***. In eerste instantie werd de katalysator getest in een slurry-ethyleenpolymerisatiereactie in een 4 *L* semi-batch reactor. Waarna deze resultaten werden vergeleken met die van de $Cr/Ti/SiO_2$ katalysator die niet was behandeld met TEAl, in een reactie waar 1-hexaan als co-monomeer was toegevoegd om butylketens te introduceren. De *in-situ* vorming van het co-monomeer werd bevestigd door ^{13}C NMR waar butyl-vertakkingen in het PE werden waargenomen. Uit analyse van de producten met GPC-IR bleek dat de katalysator die behandeld was met TEAl, PE vormde met een interessant molecuulgewicht, polydispersiteit (MWD) en verdeling van de korte-vertakkingen (SCBD). Dit komt doordat de gewenste opname van het

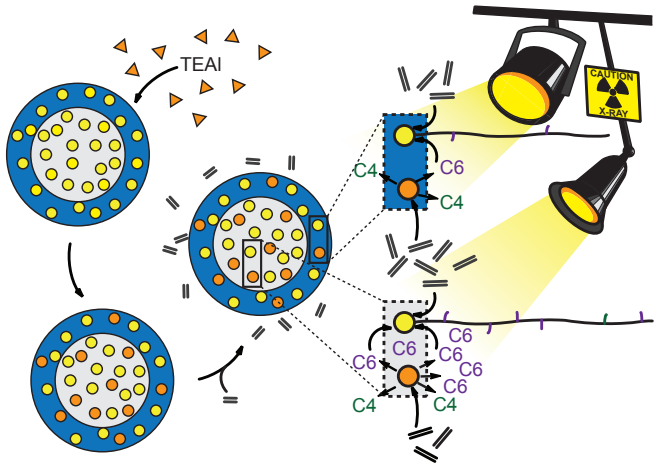

[FIGUUR 6.1]
STXM is een onmisbare micro-spectroscopische techniek om onderscheid te maken tussen de actieve plaats waar lineaire polyethyleenketens met een laag molecuul gewicht, en de actieve plaats waar korte vertakte polyethyleenketens met een hoog molecuulgewicht worden gevormd binnen één enkel katalysatordeeltje van de met TEAl behandelde Phillips katalysator.

co-monomeer in de langere PE ketens werd bevorderd wanneer de co-monomeren *in-situ* werden gevormd in de met TEAl behandelde Cr/Ti/SiO_2 katalysator. Om een goed beeld te krijgen van wat er zich afspeelt in het katalysatormateriaal zijn zowel de Cr/Ti/SiO_2 katalysator voor en na behandeling met TEAl als het katalysator-PE mengsel na reactie geanalyseerd met behulp van diverse bulk-karakterisatietechnieken, met name DRIFTS, UV-Vis-NIR DRS, EPR en XRD, en microscopietechnieken, met name SEM-EDX en STXM. Dit is de eerste keer dat STXM is gebruikt voor het bestuderen van de Phillips Cr/Ti/SiO_2 katalysator en de ruimtelijke spreiding van de verschillende elementen hierin, waaronder de lage concentraties Cr in een katalysatordeeltje. Uiteindelijk bleek dat de katalysator in staat was om twee verschillende soorten PE te produceren. Lichte-lineaire PE ketens met weinig vertakkingen werden gevormd in de schil van de katalysatordeeltjes waar veel Ti aanwezig was, terwijl in de Ti-arme kern van de katalysatordeeltjes juist PE met een hoog molecuulgewicht en veel vertakkingen werd gevormd ***(Figuur 6.1)***. De in de schil aanwezige Ti blokkeert zowel de *in-situ* productie van het co-monomeer als de opname van het co-monomeer in het PE. Dit resulteert in de vormig van kortere lineaire PE ketens in de schil terwijl in de Ti-arme kern Cr-TEAl complexen juist in staat zijn om het co-monomeer *in-situ* te produceren en vervolgens in te bouwen in de groeiende keten met als gevolg langere PE-ketens wat lijdt tot *reverse co-monomer incorporation*. Doordat de waarnemingen die op macroscopisch niveau zijn gedaan konden worden bevestigd met microscopische technieken is bewezen dat de structuur van de katalysatordeeltjes direct van invloed is op de samenstelling van het polymeer.

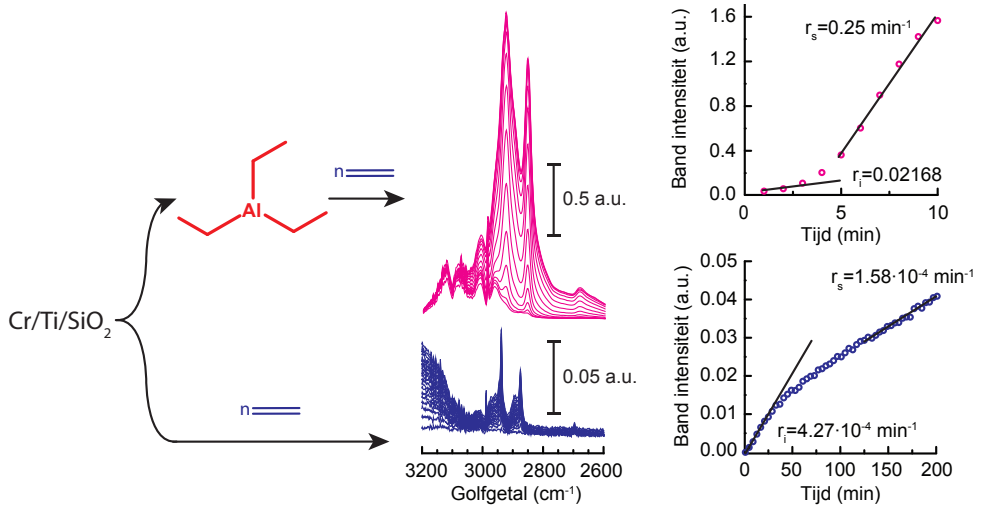

[FIGUUR 6.2]
De met TEAl behandelde Cr/Ti/SiO_2 katalysator (magenta) laat een veel hogere activiteit zien dan dezelfde katalysator zonder TEAl behandeling (blauw).

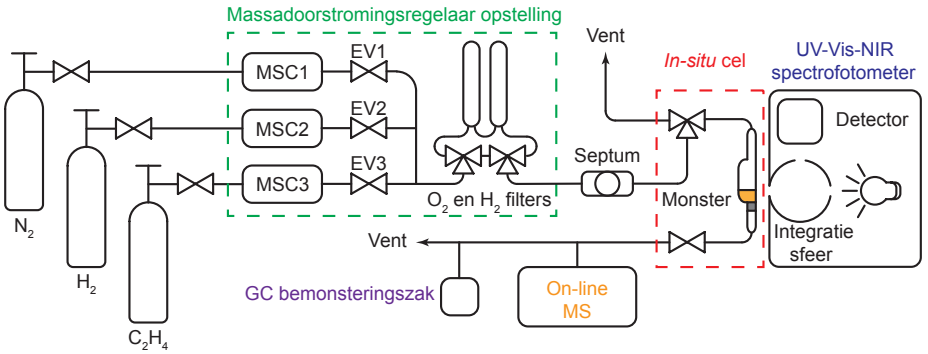

[FIGUUR 6.3]
UV-Vis-NIR verstrooide difuus reflectie spectroscopie, massaspectroscopie en gas chromatografie opstelling die is ontwikkeld voor het testen van vaste katalysatoren en producten die gevormd worden in de gasfase in reacties van 1 *bar* met temperaturen tussen kamertemperatuur en 473 *K*. De *operando*-opstelling bevat verwisselbare reactiegassen, een massadoorstromingsregelaar (groen), een poort voor het toevoegen van de co-katalysator, een 4 cm^3 luchtdichte kwartsreactor (rood), een Varian Cary 500 spectrofotometer (blauw), een Omnistar massaspectrometer (oranje) en een gasbemonsteringszak voor de GC(-MS) analyse van de gasfase (magenta). Alle leidingen en de reactor kunnen worden verwarmd tot de reactietemperatuur en worden gecontroleerd *via* thermoelementen.

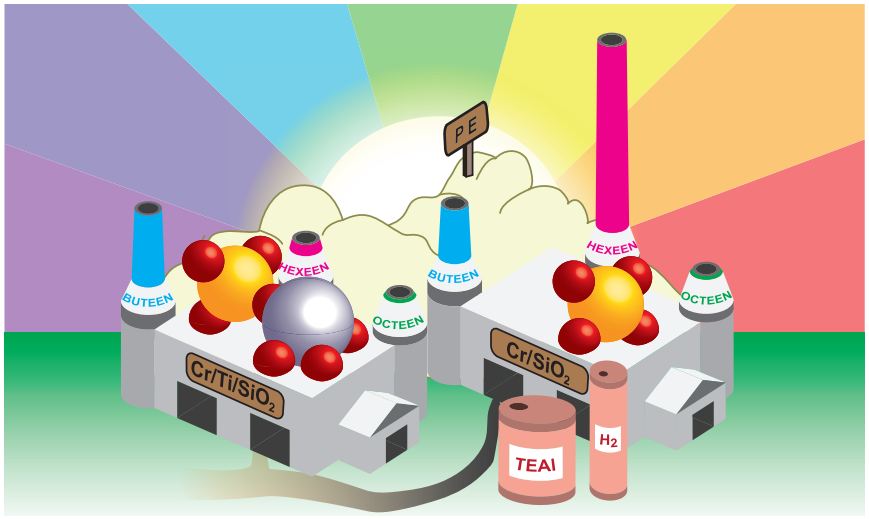

[FIGUUR 6.4]
De opbrengst en distributie van de in-situ gevormde LAO's is afhankelijk van de katalysatorstructuur en de reactiecondities. De vorming van Cr-O-Ti-O-Si verbindingen resulteert in een β-H-overdracht waardoor de selectiviteit naar 1-hexeen afneemt.

In ***Hoofdstuk 3*** worden de TEAl en TEAl-gemodificeerde Cr/SiO_2 en $Cr/Ti/SiO_2$ Philips ethyleen polymerisatie katalysatoren verder geanalyseerd met behulp van diffuus reflectie Fouriertransformatie infraroodspectroscopie (DRIFTS) in een speciaal daarvoor ontwikkelde opstelling. Hierdoor konden de vibratiemodes van de katalysator en het gevormde PE worden geanalyseerd met minimale bewerking van het materiaal en onder operando omstandigheden. Diverse katalysatorsamenstellingen, *i.e.* met 0, 2 en 4 *wt.%* Ti belading, zijn getest om de invloed van de behandeling met TEAl en de hoeveelheid Ti te onderzoeken.

De betekenis van de 3610 cm^{-1} band is onderzocht door middel van de analyse van de hydroxyl strek regio van de Cr/SiO_2 en $Cr/Ti/SiO_2$ katalysatoren. Deze band kan worden toegeschreven aan de strek vibratie van een gebrugde titanol groep welke een interactie vertoond met een chroom atoom in tegenstelling tot een gebrugde silanol groep, hetgeen eerder is voorgesteld in de literatuur.[1] Deze band is namelijk enkel zichtbaar bij katalysatoren en dragermaterialen welke titanium bevatten.

Uit tijdsafhankelijke DRIFTS spectra en kinetiek analyses bleek dat het verhogen van de Ti-concentratie in de katalysator resulteert in het verkorten van de inductietijd en een toename van de polymerisatiesnelheid. Dit kan worden toegeschreven aan een verhoging van de zuurheid van het dragermateriaal. Wanneer de katalysator werd behandeld met TEAl voorafgaand aan de polymerisatie van ethyleen lijdt dit tot een significante toename van de polymerisatieactiviteit ***(Figuur 6.2)***. Het was onder de gekozen reactiecondities echter niet mogelijk om de *in-situ* oligomerisatie van ethyleen te bevestigen met behulp van DRIFTS.

Een nieuwe *operando*-opstelling werd ontwikkeld waardoor het mogelijk was om met UV-Vis-NIR diffuus reflectie spectroscopie (DRS) te kijken naar een werkende katalysator terwijl de samenstelling van de gasfase continu geanalyseerd wordt *via* massaspectroscopie (MS) en aan het eind van de reactie met gaschromatografie (GC). Hiermee werd gefocust op de $Cr/Ti/SiO_2$ katalysator die behandeld is met TEAl. De resultaten, die worden beschreven in ***Hoofdstuk 4***, geven inzicht in de electronische eigenschappen van het Cr en de vorming van PE in de UV-Vis-NIR spectra maar laten bovendien zien dat het mogelijk is om de *in-situ* gevormde lineaire α-olefines (LAOs) te detecteren. Dit maakte het mogelijk om de invloed van de Ti-concentratie in de katalysator, de activatietemperatuur, en de hoeveelheid waterstof in het reactiemengsel op de oligomerisatieselectiviteit te testen ***(Figuur 6.4)***. De Cr/SiO_2 Phillips-katalysator zonder Ti is actiever voor de ethyleen-oligomerisatie en heeft een hogere selectiviteit voor 1-hexaan, vermoedelijk wordt deze hoge activiteit voor de trimerisatie van ethyleen veroorzaakt door een metallocyclisch ethyleenoligomerisatiemechanisme. Dit resulteert in een hogere 1-hexaanconcentratie in het reactiemengsel dan normaal is voor een lineair invoegingsmechanisme. In de aanwezigheid

van Ti worden Cr-O-Ti-O-Si verbindingen gevormd en zijn meer reduceerbare Cr^{6+} centra aanwezig dan in de katalysator zonder Ti, waardoor de polymerisatiesnelheid toeneemt. Verder lijdt de aanwezigheid van Ti ook tot een afname in de oligomerisatiesnelheid terwijl de aanwezige oligomerisatieplaatsen bovendien de β-H overdracht in het chromocyclopentaanintermediar bevorderen wat resulteert in een hogere selectiviteit naar 1-buteen. Wanneer waterstof aan het ethyleenreactiemengsel wordt toegevoegd gaat de totale opbrengst van oligomeren en met name van de verzadigde oligomeren omhoog. In een vroeg stadium van de polymerisatiereactie stopt waterstof de groei van het gevormde polymeer wat resulteert in een hoge concentratie verzadigde oligomeren. Een hogere activatietemperatuur leidt ook tot een hogere concentratie oligomeren doordat er meer reactieve Cr met vrije coordinatieplaatsen wordt gevormd *via* de dehydroxilatie van het katalysatoroppervlak.

6.2 TOEKOMSTPERSPECTIEF

Dit proefschrift roept ook een aantal vragen en ideeën op. De productie van PE met behulp van de *reverse co-monomer incorporation* zonder apart toegevoegde co-monomeren *via* de *in-situ* oligomerisatie van ethyleen, opent de weg voor de productie van dit specifieke LLDPE met behulp van maar één katalysator. Dit levert praktische voordelen op. In de eerste plaats hoeft er nu geen aparte co-monomeer meer toe-

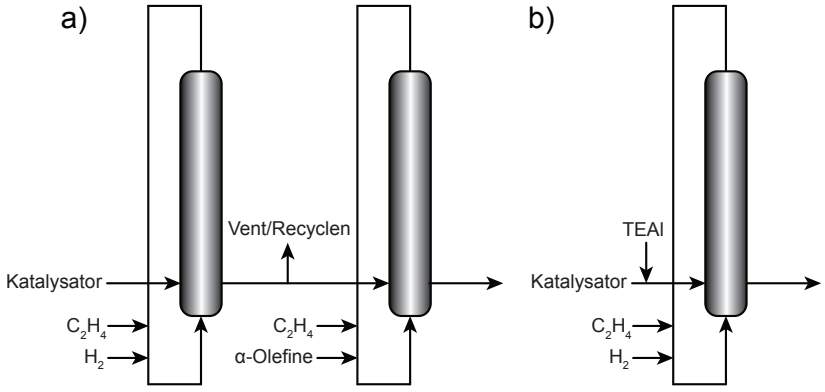

[FIGUUR 6.5]
a) Een dubbel reactorsysteem voor de productie van PE met *reverse co-monomer incorporation*. In de eerste reactor wordt PE met een laag molecuulgewicht gevormd zonder *α*-olefine co-monomeer. Dit wordt *via* een continu proces doorgevoerd naar de tweede reactor waar PE met een hoog molecuulgewicht en korte vertakkingen wordt gevormd *via* copolymerisatie met daar toegevoegde *α*-olefine co-monomeren. **b)** Alternatief met één reactor voor de productie van PE met *reverse co-monomer incorporation* met een met TEAl behandelde $Cr/Ti/SiO_2$ katalysator zoals wordt beschreven in dit proefschrift. In dit geval wordt de cokatalysator *in-situ* gevormd. Aangepast van Soares en McKenna.[2]

gevoegd te worden wat de prijs van de reactanten drukt. De kosten voor het zuiveren, transport en het risico op vergiftiging van de reactor nemen daardoor ook af. De katalysator kan worden gebruikt in bestaande Phillips polymerisatie infrastructuur terwijl het hele proces om PE te produceren *via* SCBD kan worden uitgevoerd in één enkel reactorsysteem in plaats van een dubbel reactorsysteem ***(Figuur 6.5)***. Problemen met de comptabiliteit van de katalysatoren die worden gebruikt voor tandem katalyse kunnen dan bovendien worden voorkomen.

Om de activiteit en selectiviteit van de polymerisatie- en oligomerisatiereactie voor de *in-situ* geproduceerde oligomeren te optimaliseren moet de structuur van de katalysator worden aangepast. Zo is bijvoorbeeld de dikte van de getitaneerde schil mogelijk van invloed op de relatieve hoeveelheden PE met korte zijketens en PE met weinig tot geen vertakkingen. Verder kan het interessant zijn om te onderzoeken wat de invloed is van een meer homogene verdeling van de titanium in de katalysatordeeltjes, bijvoorbeeld in een co-gel silica-titania dragermateriaal. Bovendien zijn er behalve aluminiumalkylen nog een breed scala aan mogelijke co-katalysatormaterialen dat zeker onderzocht moet worden. Een goed voorbeeld hiervan zijn hydrosilanen, waarvan bekend is dat ze dienen als co-katalysator in de productie van LLDPE *via* een polymerisatie van ethyleen zonder monomeren.[3-5]

Verdere opheldering van het mechanisme van de *in-situ* oligomerisatie en de rol van waterstof hierin is mogelijk door middel van isotoopverrijkingsexperimenten met $^{13}C_2H_4$, C_2D_4 en D_2 als reactanten. Dit is in het bijzonder van nut bij de infraroodstudies omdat het overlap van de banden afkomstig van de verschillende alkylgroepen zal voorkomen.

Uiteindelijk zullen de karakterisatiemethoden en opstellingen die zijn ontwikkeld voor het onderzoek aan dit katalysatorsysteem kunnen worden toegepast bij het bestuderen van andere vaste katalysatormaterialen, in het bijzonder bij zeer gevoelige materialen waar het hebben van controle over de gasfase van belang is of wanneer hanteren van het monster niet nodig is. De opstelling zelf zou nog verder verbeterd kunnen worden door het ontwerpen van een nieuw type reactor dat bruikbaar is bij zowel hoge als lage druk reacties.

6.3 REFERENTIES

[1] M. P. Conley, M. F. Delley, G. Siddiqi, G. Lapadula, S. Norsic, V. Monteil, O. V. Safonova, C. Copéret, *Angew. Chem. Int. Ed.* **2014**, *53*, 1872–1876.

[2] J. B. P. Soares, T. F. L. McKenna, *Polyolefin Reaction Engineering*, Wiley-VCH, Weinheim, **2012**, pp. 17–27.

[3] S. J. Martin, E. A. Benham, M.P. McDaniel, B. W. Gerhold, US4988657, **1991**.

[4] M. P. McDaniel, *Adv. Catal.* **2010**, *53*, 123–606.

[5] C. Barzan, D. Gianolio, E. Groppo, C. Lamberti, V. Monteil, E. A. Quadrelli, S. Bordiga, *Chem. Eur. J.* **2013**, *19*, 17277–17282.

HISTORIC MAP OF UTRECHT 1652
www.mappery.com

List of Abbreviations

1-C4	1-butene
1-C6	1-hexene
1-C8	1-octene
2-C6	2-hexene
3-C6	3-hexene
AFM	atomic force microscopy
BET	Brunauer-Emmet-Teller
BHT	2,6-di-*tert*-butyl-4-methylphenol
BJH	Barrett-Joyner-Halenda
c-2-C4	*cis*-2-butene
CLS	Canadian Light Source
CT	charge transfer
DFT	density functional theory
DRIFTS	diffuse reflectance infrared Fourier-transform spectroscopy
DRS	diffuse reflectance spectroscopy
e	electron
EPMA	electron probe microanalysis
EPR	electron paramagnetic resonance
Et	ethyl
FID	flame ionisation detector
FT-IR	Fourier-transform infrared
GC	gas chromatography
GC-MS	gas chromatography–mass spectrometry
GPC-IR	gel permeation chromatography – infrared
HDB	hexadeuterobenzene
HDPE	high density polyethylene
HMDS	hexamethyldisiloxane
IR	infrared
LA-MS	laser ablation–mass spectrometry
LAO	linear alpha olefin
LDI-MS	laser desorption/ionisation–mass spectrometry
LDPE	low density polyethylene
LLDPE	linear low density polyethylene

M	metal
MCT	mercury-cadmium-telluride
MDPE	medium density polyethylene
MWD	molecular weight distribution
MS	mass spectrometry
n-C4	*n*-butane
n-C6	*n*-hexane
n-C8	*n*-octane
NIR	near infrared
NMR	nuclear magnetic resonance
Oh	octahedral symmetry
PE	polyethylene
PIXE	proton-induced X-ray emission
R	alkyl group
RBS	Rutherford backscattering spectrometry
RT	room temperature
SCBD	short-chain branching distribution
SEM-EDX	scanning electron microscopy – energy dispersive X-ray
SF	Schulz-Flory
SIMS	secondary ion mass spectrometry
ssNMR	solid-state nuclear magnetic resonance
STXM	scanning transmission X-ray microscopy
t-2-C4	*trans*-2-butene
TC	total carbon
TCB	trichlorobenzene
Td	tetrahedral symmetry
TEAl	triethylaluminium
TEM	transmission electron microscopy
TGA	termogravimetric analysis
TIBAl	triisobutylaluminium
TIP	titanium isopropoxide
TPD-MS	temperature programmed desorption–mass spectrometry
TPR	temperature programmed reduction
UU	Utrecht University
UV-Vis-NIR	ultraviolet-visible-near infrared
XAS	X-ray absorption spectroscopy
XRD	X-ray diffraction
XRF	X-ray fluorescence

Publications, Conferences & Awards

PUBLICATIONS

Chapter II

D. Cicmil, J. Meeuwissen, A. Vantomme, J. Wang, I. K. van Ravenhorst, H. E. van der Bij, A. Muñoz-Murillo and B. M. Weckhuysen, "Polyethylene with Reverse Co-monomer Incorporation: From an Industrial Serendipitous Discovery to Fundamental Understanding", *Angew. Chem. Int. Ed.* **2015**, *54*, 13073–13079.

Chapter III

D. Cicmil, J. Meeuwissen, A. Vantomme and B. M. Weckhuysen, "Real-time Analysis of a Working Cr/Ti/SiO_2 Ethylene Polymerisation Catalyst with *In-situ* DRIFT Spectroscopy", *in preparation.*

Chapter IV

D. Cicmil, I. K. van Ravenhorst, J. Meeuwissen, A. Vantomme and B. M. Weckhuysen, "Structure-Performance Relationships of Cr/Ti/SiO_2 Catalysts Modified with TEAl for Oligomerisation of Ethylene: Tuning the Selectivity towards 1-Hexene", *Catal. Sci. Technol.* **2015**, *DOI: 10.1039/c5cy01512j.*

Other

H. E. van der Bij, D. Cicmil, J. Wang, F. Meirer, F. M. F. de Groot and B. M. Weckhuysen, "Aluminum-phosphate Binder Formation in Zeolites as Probed with X-ray Absorption Microscopy", *J. Am. Chem. Soc.* **2014**, *136*, 17774–17787.

D. Cicmil, S. Anastasova, A. Kavanagh, D. Diamond, U. Mattinen, J. Bobacka, A. Lewenstam, A. Radu, "Ionic Liquid-based, Liquid-junction-free Reference Electrode", *Electroanalysis* **2011**, *23*, 1881–1890.

CONFERENCES

The Netherlands' Catalysis and Chemistry Conference

D. Cicmil, J. Meeuwissen, A. Vantomme, I.K. van Ravenhorst and B.M. Weckhuysen, "The Influence of Ti inside the Phillips Polymerisation Catalyst on the Selective Ethylene Oligomerisation"

Noordwijkerhout, The Netherlands, March 8, **2015** [**poster**]

D. Cicmil, J. Meeuwissen and B.M. Weckhuysen, "STXM Imaging of the Ethylene Polymerisation Cr/SiO_2 Catalyst"

Noordwijkerhout, The Netherlands, March 11, **2014** [**oral**]

Total's Catalysis of Polymerisation Days

D. Cicmil, J. Meeuwissen, A. Vantomme and B.M. Weckhuysen, "Identification of Ethylene Oligomerisation Active Sites"

Lille, France, November 14, **2014** [**oral**]

European Association for Chemical and Molecular Sciences Congress

D. Cicmil, J. Meeuwissen and B.M. Weckhuysen, "Chemical Imaging of the Phillips Catalyst with Soft X-ray Microscopy"

Istanbul, Turkey, September 1, **2014** [**oral**]

AWARDS

The VIRAN award for the best poster presented during the 16th Netherlands' Catalysis and Chemistry Conference, with the poster entitled "The Influence of Ti inside the Phillips Polymerisation Catalyst on the Selective Oligomerisation of Ethylene".

Noordwijkerhout, The Netherlands, March 8, **2015**

Acknowledgments

What we call the beginning is often the end
And to make an end is to make a beginning.
The end is where we start from.

Little Gidding
T. S. Eliot

Since the beginning of the mankind, we have thrived to solve problems. In order to catch fish, break stone, melt metal ore; we had to think and develop suitable techniques and methods. In the universe of all knowledge, the light of reason and science started as a candle light, quickly growing and elucidating bigger and darker parts of the universe. Still, the more we know and the more powerful our torches are, as we unravel layer by layer of the darkness surrounding us, we still cannot see the ultimate end. The force of the unknown is driving us further and further, just as a flywheel, inspiring us to jump into darkness. This can be done alone, as proven by many brilliant minds throughout history. However, nowadays, we can achieve this only through a union of people with skills complementing each other.

In that respect, I would like to thank first my supervisor, **Bert Weckhuysen**, for giving me the opportunity to dive into the pool of PhD research and to explore and use very advanced characterisation techniques, often rather limitedly available in other research groups. I am honoured for the chance to elucidate some of the mysteries about the Phillips catalyst on the same topic in which you obtained your own doctorate 20 years ago! But furthermore, to meet, spend time, party and work together with many people, who made my PhD years in Utrecht unforgettable. From you I have learnt how to get the maximum out of my work and further present the results in the best way, which has led to many creative presentations, figures and a poster award. You have made our collaboration with Total run as smooth as possible. Thank you also for very prompt replies to my e-mails, no matter how busy your schedule. I have learned to work independently and also to appreciate working in a team. I wish you and your family all the best in the future, and I am sure our paths will cross again. The scientific world is small.

Many thanks to my industrial partners from Total Petrochemicals, **Jurjen**, **Aurélien**, **Jean-Michel** and **Olivier**, for fruitful discussions and brainstorming during our meetings. I have learnt a lot about the industrial aspects of the research. We have proved that the Industry-Academia synergy is what guides this world towards a better future. **Jurjen**, thanks for being my main contact during the first three years of my PhD. With your brilliant mind I don't need to wish you any luck at Shell. **Aurélien**, without your knowledge in olefin polymerisation catalysis our collaboration wouldn't have been as fruitful as it is. I hope that your next collaboration with Utrecht will be even more productive. Think about skiing one winter in Serbia, there are more possibilities than in Montenegro. **Jean-Michel**, your in-depth involvement with so many research groups amazes me. Thank you for annoying my French colleagues by making the *Catalysis of Polymerisation Days* in English, giving me the opportunity to present my work and find out about other research you are carrying out with other universities. **Gerrit**, thank you for all the samples and teaching me about ethylene polymerisation using bench reactors. Your support really helped this project.

The huge conglomerate of the Inorganic Chemistry and Catalysis group would not be able to run smoothly if it was not for the support staff. Dear **Dymph**, **Monique** and **Iris**, although no one in the group really knows the exact number of people working in the group, your planning and organisational skills are keeping everything in order. **Ad M** and **Ad vdE**, thank you not only for your help regarding my setups, but also for teaching me how to make things myself, which has saved many of the beam times. Without **Rien**, my catalysts would not be safe inside the glove box so that it can be "photographed" by **Marjan** under the SEM microscope. **Fouad**, thank you for the vibrational-IT-football expertise, and for the constant confusion by your comprehension of what is up/down, third/fourth floor, in the DDW building. I hope that all of you are going to have an easier work day now, with the recent additions to your team. **Oscar**, **Pascal**, **Herrick** and **Jan Willem**, I wish you had joined the group earlier so that I could have bothered you more. No doubt, with the growth rate of our group, you will be really busy.

The diverse range of topics studied in the ICC group, would not exist without the academic staff of the group. **Krijn**, **Petra**, **Frank**, **Pieter**, **Javi**, **Jovana**, **Rosa**, **Monica**, **Florian**, **Peter N** and **Gareth**, thank you for broadening my knowledge in other fields.

As a researcher in the ICC group, I had the possibility to use many advanced synchrotron techniques, one of them being STXM. Several beam times at the Canadian Light Source in Saskatoon and work with **Chithra**, **Jian**, **Jay** and **Yingshen** proved to be fruitful not only for me, but also for my other colleagues. Long beam time shifts were made shorter and (in principle) less stressful with **Hendrik**, **Sam**, **Ramon**, **Korneel**, **Mustafa** and **Christa**.

I would also like to thank the other co-authors and colleagues, who were not mentioned earlier, involved with the work used for my publications. **Ara**, you did a great job with the EPR measurements and data processing! [happy Google translate voice intonation]. **Mario**, good luck with the development of Blueprint, it is definitely very useful and I am sure I will have to use it in future. **Hans** and **Peter M**, thank you for the ultramicrotomy of my samples. **Ilse**, it was my honour to give a speech during your MSc graduation ceremony and in that way to conclude my supervision of your master project. Your perseverance and motivation, even when the experiments were not going well, kept the project on track. In that sense, you were the only person in the group who could really understand how tricky the handling of the Phillips catalyst was. It was my pleasure, and I wish you good luck now with your own PhD project.

As I said earlier, no one really knows the exact number of people going through our group. I will try to mention every PhD student, Postdoc fellow and staff member I have met since my start: **Abhishek**, **Ad vdE**, **Ad M**, **Angeloclaudio**, **Ana**, **Andy**, **Anne Mette**, **Anne-Eva**, **Annelie**, **Anton**, **Antonio**, **Ara**, **Arjan**, **Arjen**, **Baira**, **Bart**, **Beatriz**, **Bert**, **Boyang**, **Carlo**, **Carlos**, **Cédric**, **Charlotte**, **Christa**, **Christoph**, **Clare**, **Daniël**, **Davide**, **Diego**, **Dilek**, **Donglong**, **Dymph**, **Eelco**, **Egor**, **Elena**, **Emke**, **Emma**, **Evelien**, **Fang**, **Fernando**, **Fiona**, **Florian**, **Fouad**, **Frank dG**, **Frank H**, **Gang**, **Gareth**, **Gonzalo**, **Hans**, **Harry**, **Hebatalla**, **Hendrik**, **Herrick**, **Hirsa**, **Homer**, **Ilona**, **Ilse**, **Inés Uno**, **Inés Dos**, **Inez**, **Inge**, **Iris**, **Iván**, **Jan**, **Jan Philipp**, **Jan Willem**, **Jamal**, **Javi**, **Jelle**, **Jesper**, **Jeroen**, **Jessi**, **Jinbao**, **Jochem**, **Joe**, **Joe Z**, **Joel**, **Joris**, **Jose**, **Jovana**, **JX**, **Karin**, **Katarína**, **Katinka**, **Khaled**, **Korneel**, **Krijn**, **Leila**, **Lennart**, **Lisette**, **Luis**, **Mahnaz**, **Manuel**, **Marianna**, **Mario**, **Marjan**, **Marleen**, **Marjolein**, **Mark**, **Martin**, **Matthew**, **Matti**, **Michal**, **Miguel**, **Monica**, **Monique**, **Mozzafar**, **Mustafa**, **Nazila**, **Nynke**, **Oscar**, **Özgün**, **Pascal**, **Pasi**, **Patric**, **Pengfei**, **Peter B**, **Peter H**, **Peter M**, **Peter N**, **Peter dP**, **Peter S**, **Petra**, **Pieter B**, **Pieter M**, **Qingyun**, **Rafael**, **Ramon**, **Reshmi**, **Rien**, **Rob**, **Robin**, **Rogier**, **Rolf**, **Rosa**, **Roy**, **Ru-Pan**, **Sam**, **Sandra**, **Sang-Ho**, **Sankar**, **Selvedin**, **Siswati**, **Sophie**, **Stanislav**, **Stefan**, **Suresh**, **Suwarno**, **Suzanne**, **Tamara**, **Tao**, **Thomas E**, **Thomas vH**, **Thomas H**, **Thomas G**, **Ties**, **Tom D**, **Tom vD**, **Upakul**, **Wenhao**, **Wouter L**, **Ying**, **Yuen**, **Zafer** and **Zoki**. It would be too much to acknowledge each of you personally, therefore I would like to thank you all for the collaboration, borrels, coffee breaks, work discussions, talks, conferences, very interesting Debye lunch lectures, DO days, Debye spring schools, labuitjes, dinners, parties, nights out and sports events. We have all learned a lot from each other, even many negative things, but that's all a part of finding out what the world is. I will try to keep in touch with as many of you I can, and I am hoping to continue working with you in some way in the future. The network that our group let us build is priceless.

I have lived in three countries, Serbia, Montenegro and Ireland, before moving to the Netherlands. Utrecht will always have a special place in my heart, and will be the city I will always look forward to coming back to. During my first "two and a bit"-years in Utrecht, I have lived in many different houses. Starting first with **Joe** and then **Zoki** at Catherijnekade, then moving with **Zoki** to join **Eli** at Milosdreef and afterwards joining **Paulina** and **Sylwia** at Leliestraat. Thank you all for being such pleasant, caring and fun housemates. Last two years I have spent in the most awesome flat in Adelaarstraat. **Antonio**, take care of it, I am sure you will enjoy a lot!

I am happy to have had the opportunity to show my appreciation to the ICC group by organising one of the **labuitjes** together with **Ad vdE**, **Elena**, **Javi**, **Jelle** and **Wouter L**. The experience of fitting the day activity and dinner into a quite strict budget made me feel like a real magician. Abracadabra! Furthermore, I was in the **Long Island Iced Tea borrel** committee for a couple of years. With **Joe**, I took the LIIT baton from **Hendrik** and **Ilona**, to the (un)forgettable borrel at the Ornsteingebouw coffee area in 2013. We have really mastered our Excel skills by creating the Ultimate Multicocktail Planner and Calculator™. In 2014, **JX** also joined the organisers, before handling the baton to **Ara**, **Jeroen** and **Peter B** in 2015. As an usual LIIT borrel, this one was also (un)forgettable as I received... an award for the best costume!

The timing of the LIIT borrel at the beginning of each year was perfect as I could allow myself a few drinks before the start of the sport season. As most of you have noticed by the improvised drying racks around the department, many of our colleagues were not just very good scientists but also very active sportsmen. **Joe** was our triathlon catalyst, and together with **Rob** and **I**, one of the co-founders of **Team MiRoJo**. Our ordinary day was rather simple, but tough. Eat, sleep, train, work, train, repeat. We even thought about the environment and finances of the ICC group by cycling on our road bikes to many conferences and schools, one of them being as far as Germany. Besides the triathlon, we also did running competitions and cycling tours, and involved even more people including some of the staff members. **Joe**, **Rob**, **Qingyun**, **Annelie**, **Monica**, **Fernando**, **Javi**, **Ana**, **Inés Uno**, **Fiona**, **Silvia**, **Ramon**, **Tamara**, I wish you jellyfish-free warm waters and many miles under your feet and wheels. **JX**, my stationary cycling buddy, I hope you will recover soon and pass my greetings to **Amber** during the next spinning class. I couldn't have finished my writing without the **Hellas Triathlon Club**. Jongens and meisjes, thank you for taking my mind away from my thesis.

I am not the best football player but I do what I am told. It was my great honour to get the chance to join **Multiple Scoregasms** after many years of supporting the **20**, **21** and **22 Seconds of Fun**. It was a real joy playing at the NIOK football tournament, Debye sports day, Ascension Day tournament and Olympos league together

with **Zoran**, **Gareth**, **Roy**, **Joe**, **Javi**, **Carlo**, **Sam**, **Fouad**, **Antonio**, **Wenhao**, **Tomáš**, **Martin**, **David F**, **Khaled**, **Martin**, **Tom D**, **Wouter N**, **Thomas E** and **Michele**. Some of the tactics proved to be really good, such as the "rooster" formation, while the headless chicken tactics should be definitely avoided. I would like to suggest to our professors to include the following question in the interview for hiring new people: Do you play football?

Moving away from Serbia meant that I had to leave many dear people behind. I am really happy that the distance didn't mean anything to you, that we all stayed in touch and see each other whenever we get a chance. My childhood friends from Smederevo, whom I have known for 23 years, **Đole**, **Mira**, **Taki**, **Uki**, **Kida**, **Peca**, **Laza**, **Maja Z**, **Jelena Đ**, **Beba**, I am looking forward to many joyous events with you. Много значи што увек могу да рачунам на вас, што сте увек били моја подршка. Кад год бих дошао за Смедерево, ми бисмо само наставили где смо стали као да сам све време био ту. Желим вам све најлепше и увек рачунајте на мене! My secondary school friends, **Ivana**, **Milena**, **Sanja**, **Marta G**, **Mica I/P**, and the rest from the **IV/4** class good luck in Australia, the US, Croatia and Serbia. **Maja M**, thank you for tricking me into enrolling in the studies at Faculty of Physical Chemistry and being my unofficial mentor. **Mica**, **Slavka**, **Viki**, **Milan B**, **Vlada R**, **Vlada J**, **Džoni**, **Jasmina**, **Jana**, **Nevena**, **Ruža**, **Tijana**, thank you for reminding me how fun our Uni days were whenever we meet. When's our next kafana? Mountaineering and orienteering club **Rudar Geolog**, it is amazing to see how long friendships can last and that after so many years when you meet each other, you are still like kids, even though some of you already have grandchildren. Special thanks to my closest support **Marta** and **Jovana M**, and all of the other youth members of the club.

My **Big Fat Serbian Family**... Моја велика мрсна српска породицо, веома сам срећан што вас имам и много ми је жао што не могу увек бити уз вас. Чак и кад сам у Србији, не могу вас све видети, али сте увек у мом срцу. **Сања**, **Поп**, **Марија**, **Михајло**, **Наталија**, **Далиборка** и **Радмила** са дечицом, **Маша**, **Јеца**, **Његош**, мали **Павле** и **Јована**, **Рашко**, **Биља**, **Ана**, **Јована В**, **Дуле**, **Ђоле О**, **Дада** и индијанци, **Деки**, мали **Јоца**, деда **Јоца**, **Срђан**, **Сања Ц**, **Гина**, **Вера**, **Нада**, **Санда**, **Ненад**, **Дане**, **Бека**, **Ика**, **Маја**, придружени чланови **Марко**, **Млађа**, **Пикси**, **Лаки**, **Дејан**, **Тихомир**, **Коста**, и најновији кум **Ђоле**. Пропустио сам ненамерно многе драге тетке, тече, стричеве, стрине, бабе, деде, ујаке, ујне, кумове, породичне пријатеље и рођаке, **Цицмиле**, **Обрадовиће**, **Дрекиће** и **Гаргенте**. Много нас је (хвала Богу), тешко је све набројати... Тако и треба, надам се да ће бити све теже и теже. **Бојана**, хвала ти што ме волиш и бринеш о мени као брату, и што не мора да бринем пуно о мом бати јер знам да је у добрим рукама. Већ си део наше породица, а надам се ускоро и званично.

Thanks to my parent's piece of land at the Adriatic cost, I have spent cumulatively about two years of my life in Montenegro. Starting from the tents, gas lamps, tin food and longdrops, we have now developed the **Holm Oak Villa** with our own hands. I am quite grateful to it as it bonded my family and for being a special and magical place, which connected me with many cousins from the Obradovićs branch and friends whom I would never have met otherwise. **Buđa**, **Šile**, **Kopta**, **Vića**, **Peja**, **Švaba**, **Sanja V**, **Naca**, **Milica**, **Dina**, **Sara**, **Kika**, **Maša**, **Bere**...

Serbian diaspora is quite huge. I am really proud to share my roots with strong, brave and smart people, which you all are. **Nevena**, **Jelena B**, **Cane**, **Danijela**, **Stefan Nemanja**, **Jelena O**, **Aleks** and **Tijana Ž**, thank you for the events, drinks and hospitality in the Netherlands. **Bambi**, I am sorry for letting you down so many times. Your positivity and spirit cannot be explained with any words of praise. I hope I'll have more chances to see the little sweetheart **Momo** before she grows up. **Milan K**, thanks for the support and Skype talks from Bern. You haven't convinced me yet to come to work and live in Switzerland.

Aca, thank you for being my mentor in Dublin. Without the internship at DCU, I doubt I would be at this stage now. Good luck in England, I am hoping to see you, **Tanja** and **Mila** soon. If you see **Paja M** and **Lei**, pass on my greetings.

Slavka, my Uni partner in science and travelling. Thank you for the time in Ireland, France, Belgium and the Netherlands during our bachelor studies in Belgrade. I will never forget our press passes, which we used to enter museums. Thank you for your hospitality in Austria and the support during the Vienna mud race. Good luck with the last steps in your PhD, you are almost there! Being such a courageous girl that you are, there is no obstacle you cannot overcome.

Arthur and **Jackie**, thank you for your care and cheering for me many times around Europe, dinners in Utrecht and weekends in Newcastle, which seem like they are becoming a tradition! It means a lot that you were there for me many times when my parents couldn't be.

Hendrik, we can definitely say that you can't really know a person unless you spend night shifts with him on a beam time. And we had so many beam times in that jolly little place of Saskatune in the middle of nowhere. It was a pleasure listening to the classical music with you, in a small warm hutch, with *Aurora borealis* shimmering above our heads. Thanks for all the fun during our PhD days.

Sam, I'm sorry for my shortest night out during the St Patrick's Day in year... wish I could remember. Thank you for many STXM beam trips. Your extended knowledge aboot Saskatoon and your enthusiasm aboot X-ray spectroscopy are really inspiring.

Gareth, the youngest ass. professor in Utrecht, right? You might be a good and promising scientist but you are a terrible karaoke singer. And some of the goals you

missed... I would have even scored! At least you've got passion. Thanks for the chat, support, fun and nights out together, I'm hoping to have many more now that my favourite Irish is coming back.

Fiona, thank you for being such a nice and easy going person. It was always fun hanging around with you and trying not to have my ass kicked during many triathlon competitions. Your accent always makes me homesick for the time I spent in Ireland.

Amber, without your enthusiasm and coaching during the spinning and kick-bag sessions, my Ironman adventure would have been a lot more difficult. You are *the* person I would like to have next to me if I ever get into a fight. I am looking forward to the opportunity of training more with you. Maybe for my next Ironman?

Sophie, thank you for the long talks during the coffee breaks, long talks at Schiermonnikoog and even longer talks during the preparation for the NIOK exam. On the other hand, your advice before I even started formatting my thesis really saved me a lot of time. I am really amazed by the quality of your PhD work knowing that you had a family to take care of and a real job to think about.

Stefan, I think I've seen you more during the nights out than at the department. It was my pleasures attending the wedding of **Mariette** and you, the awesome party afterwards and the New Year celebration at Tivoli.

Annelie, thank you for the swimming tips and being there for many triathlon competitions. Trying to beat you at 100 m will be my next goal. Many thanks also for the Dutch translation of the summary of my thesis, I hope you enjoyed it a bit.

Thomas E, I have never met more organised person than you. Thank you and **Maren** for the hospitality in Aachen, Pub Quiz, nights out and many dinners and poker nights at your house. You have invented some really cool dance moves. Have you considered joining a theatre? I think you would be a great Snow White.

Javi, your resourcefulness in science really inspired me and with no doubt you will have a bright future in industry. You and **Sandra** know how to organise really good parties! It was my pleasure meeting both of you and now I am looking forward to meeting, **Elisa**, the newest member of your family.

Carlo, you were one of the first people who approached me when I arrived in Utrecht and I was really surprised how much you already knew about me. Thank you for all the advice, coffee breaks and drinks we had together. I must admit that I really miss being annoyed by you asking for my Origin and Adobe PS skills.

Roy, thanks for everything you did for the whole group, for your enthusiasm in organising Winterberg ski trips, Ascension day football tournaments and many company visits. Many PhDs should really look up to you. I wish you all the best in your last stage of your PhD and future career.

Gang, I'm sorry for missing some of the social events you have organised, but it is

because you organised a lot! Anyway, you need to practise your aiming skills before I could join for Laser tag. I am looking forward to another travel with you like the one to Copenhagen.

Hirsa and **David**, your generosity and hospitality cannot be explained. I've even celebrated two of my birthdays at your home! You really made me feel like a proper Colombian. It was always difficult to leave your house without a couple of last shots. I can't wait to see you and your girls again.

Ara, both working and going out with you were never boring. Thank you for your help with my project, you were one of the most capable postdocs I've ever known. I could always count on you. As I discussed with **David**, we are extremely happy that you are a scientist and not a coat seller... Otherwise, all people in Utrecht would be wearing your coats!

Ana, I simply don't know how such a big heart can be hidden inside a little girl like you. Your support, faith and care made a huge difference especially in my last year, and your friendship one of the most valuable memories from Utrecht. It is my honour to know you.

Qingyun, thank you for being my real friend and helping me many times in Utrecht and now from the other side of the world. I have learnt a lot about Chinese culture (and Chinese pop stars) from you and found too many similarities with Serbian, especially regarding love and respect you have for your family and friends. As an extremely fun girl, our night shifts at Soleil in Paris passed really quickly. Thank you also for being our universal weight unit. You would definitely tell me now to lose some QQs. I can't wait to see you again!

Rob... A great scientist, great triathlete, great man and a great friend! Thank you for being there whenever I would hit the wall. Spending time with you, whether it was for leisure or sports, was always enjoyable. Well, maybe not always sports, as both of us are very competitive. Still, there are a lot of kilometres to cover until you become an Ironman. Thank you, bro, for everything you did and will do for me in future. I'm looking forward to our next sports event and seeing your parents and brothers.

JX, thank you for keeping an eye on my schedule, coffee breaks, long talks about everything, ranging from juicy gossip to work related matters. You are a great support and even greater friend! I wish other people could have only a fraction of your good heart, kindness and commitment to the group. Sometimes you were a really annoying desk mate, but nevertheless, I'm going to miss you. Thank you for your help during my final stressful months, you really made my life easier. Good luck with your thesis, you know you can count on me!

Zafer, my dear friend, you are the most generous person I have ever met. Knowing that you are there for me, any time of the day, made me feel like you are my safe

haven, and your house like my own house. I needed that so many times. Thank you also for the help with my thesis, discussions about work and even some experiments. Dinners, drinks, nights out, talks, coffee breaks, travels and chance to meet **Müge**, **Ali**[2] and Turkish community I will never forget. Stay strong and please know that I will be always there for you.

My dearest professor and friend, **Jovana**, драга Зеко, хвала ти за сву подршку, искреност и најмудрије савете који су ми помогли да изгурам докторат. Твоје пријатељство ми много значи док ће ми твоја изузетна снага, креативност и истрајност бити вечита инспирација и узор. Заслужујеш све најлепше! Бићу увек ту за тебе и надам се **Милин** омиљени ујка.

Мој куме, **Ђоле**, ми смо доказ да другарство не познаје границе. Колико дуго се знамо? Ни не памтим више, али кад год се видимо кући, у граду, у фарбари, чак и кад "нема ништа ново", никад није досадно. Хвала ти посебно што си био уз мене последњих година, што си ме чекао на аеродрому, висио на Скајпу... Сада смо и пред Богом породица, јер сте ми **Маја** и ти указали част да будем кум на вашем венчању. Никад нисам сумњао у вас, моје срце је са вама. Обоје заслужујете само најбоље, моја сестро и куме, а најбоље нас тек очекује!

Zoki, цимеру, другарчино, брате, за најдраже људе је просто немогуће исказати речи хвале и захвалности које заслужују. Твоја пажња и љубав према породици и друговима, саосећајност са другима, брилијантност у науци, шаху, фудбалу, чине те изузетним човеком. Прошли смо кроз много тога заједно, рвећи се са докторатом и носталгијом за породицом и пријатељима. Хвала ти за сву подршку. Много ми је жао што те нисам знао боље током наших основних студија, али биће времена да надокнадимо пропуштено, сада и са **Марином** и **Алексом**, твојом дивном породицом. Част ми је што си ми паранимфа, и још већа част што си ме такође позвао да будем уз тебе! У то никад није било ни мало сумње, тако је морало бити!

Мој brate **Josife**, I don't know how to say it without making it sound like a cliché... but thank you for everything. If I'd like to write down all the things we went through together, work, travels, dinners, difficult trainings and parties, I'd probably need an additional chapter, of which many parts would be censored. That's the true friendship! To have someone who understands me, who will share the happiest moments but also someone who will be there as a pillar and a ray of light when it becomes dark. If it wasn't for you, I would have never started triathlon and ultimately crossed the Ironman finish line while holding your hand, exactly how we are now finishing our doctorates. Thank you for being adopted Serb, the angel on one and the devil on my other shoulder, my paranimf, my best friend and my true brother. We have a lot of adventures ahead of us, memories to be made and pages to be written.

My nans, моје баке, **Јело** и **Бојо**, хвала вам за вашу љубав и бригу, и бесане ноћи бринући да ли је мој авион слетео или да ли је вожња колима прошла у реду. Хвала вам што сте бринуле о мени и пружиле савршено детињство. Бака **Јело**, хвала ти што си одржала обећање и што ћеш моћи да окачиш моју диплому на зид. Надам се да ће ти дати снаге да будеш још дуго, дуго, дуго, уз твоје унуке и праунуке, јер те и даље требамо. Бака **Бојо**, хвала што си ме сачекала да се опростимо пре него што си отишла на дуги пут. Знам да си мој анђео чувар и да помно пазиш на мене са неба заједно са **Нином**, **Стевом** и **Гојком**.

My brother, **Пајо**, за неке људе схватиш колико ти недостају тек кад их напустиш. Кад се сетим колико се ме само нервирао док смо били деца... Сада бих све дао да можеш да ми идеш на живце сваки дан. Током последњих година много пута нисам хтео да причам са тобом, не зато што сам заборавио, већ само зато што ми је тешко што нисам ту са тобом. Ти си мој ослонац без обзира на то колико си хиљада километара далеко, јер знам да си бесконачно близу у мом срцу. Хвала ти, мали мили бато, за сву подршку и искрену љубав, за све песме које си за мене наручивао и за сваку сузу који си пустио. Волим те бескрајно...

And finally, my parents, моји родитељи, **Мама** и **Тата**, ово није мој успех. Ово је ваш успех! Без вашег одрицања, несебичне љубави и неограничене подршке, ја не бих био овде. Моја срећа вам је увек била на првом месту. Хвала вам на вашој снази и мудрости, јер сте ме научили љубави према породици и пријатељима, науци, спорту, док је ваша креативност и слобода коју сте ми омогућили током одрастања пресликана у мојој сопственој креативности, самосталности а понекад и у сулудим идејама. Увек сте мислили на мене, чак и кад је значило да ћете морати да ме пустите да одем. Бити добар човек, који верује у људе и који је спреман устати против неправде и у одбрану других, је универзална врлина коју сте ме научили и коју су препознали и цене сви људи које сам упознао, без обзира из ког дела света долазе. Поносан сам на вас због свега и много, много, много вас волим...

Мама, Тата, ова књигу свим срцем посвећујем вама.

Mum, Dad, this book I dedicate to you with all of my heart.